Imaging the effects of 1 Hz Repetitive Transcranial Magnetic Stimulation during motor behaviour

Lucy Lee

Thesis submitted for the degree of Doctor of Philosophy, October 2004

Wellcome Department of Imaging Neuroscience
Institute of Neurology

University College London

Abstract

Repetitive Transcranial Magnetic Stimulation (rTMS) can be used to induce temporary alterations in the excitability of the brain in healthy subjects. For some motor behaviour it has been possible to impair or improve performance following rTMS, but for most simple tasks performance is unaltered. This suggests that the motor system is able to compensate, to some extent, for the changes in excitability induced by rTMS. Potentially this makes rTMS a useful tool for studying reorganisation in the healthy motor system, and may provide insights into adaptive mechanisms after injury such as ischaemic stroke. The work presented in this thesis examines rTMS-induced changes in regional excitability following 1Hz rTMS to the primary motor cortex, and potential compensatory mechanisms during various motor tasks.

The results of three functional neuroimaging experiments reveal significant changes in movement-related responses and coupling with the motor system following rTMS. The results of a behavioural experiment suggest that the increases in movement-related responses in the right premotor cortex have a functional role in maintaining motor performance following 1Hz rTMS to left primary motor cortex. Analyses of effective connectivity suggest that the influence of the right premotor cortex in maintaining motor performance after rTMS is mediated via increased transcallosal connections from right to left premotor cortex, as opposed to non-homologous connections from right premotor to left motor cortex.

Increased activity in motor areas not normally engaged in task performance may contribute to compensatory mechanisms during altered cortical excitability. Analyses of effective connectivity suggest that operational remapping of motor networks may also occur, and this may also contribute to compensatory mechanisms for rTMS-induced reductions in cortical excitability. Mapping these patterns of reorganisation in the motor system may provide a useful method to study acute compensatory plasticity of the human brain and may help to understand how the brain reacts to more permanent lesions. Establishing the functional relevance of increased activity in areas not normally engaged in task performance using TMS may play a key role in rehabilitation and provide a mechanistic understanding of compensatory mechanisms in stroke patients.

Table of Contents

Figures

Tables

Abbreviations

AMT	Active Motor Threshold
BA	Brodmann Area
BOLD	Blood Oxygen Level Dependent
CMA	Cingulate Motor Area
DCM	Dynamic Causal Modelling
EEG	Electroencephalography
EMG	Electromyography
EPI	Echo Planar Imaging
FDG	Flouro-2-deoxy-D- glucose
FDI	First Dorsal Interosseus muscle
fMRI	Functional Magnetic Resonance Imaging
GABA	Gamma-aminobutyric acid
GLM	General Linear Model
HRF	Haemodynamic Response Function
ICI	Intracortical Inhibition
ICF	Intracortical Facilitation
ISI	Interstimulus Interval
LLSR	Long Latency Stretch Reflex
M1	Primary Motor Area
MEP	Motor Evoked Potential
MRI	Magnetic Resonance Imaging
MT	Motor Threshold
PET	Positron Emission Tomography
PMd	Dorsolateral Premotor cortex
PMv	Ventrolateral Premotor cortex
PPI	Psychophysiological Interaction
rCBF	Regional Cerebral Blood Flow
rCMR-glc	Regional Cerebral Metabolic Rate - glucose
RMT	Resting Motor Threshold
rTMS	Repetitive Transcranial Magnetic Stimulation
SMA	Supplementary Motor Area

SEP	Somatosensory Evoked Potential
SP	Silent Period
SPECT	Single Photon Emission Computerized Tomography
TMS	Transcranial Magnetic Stimulation
SPM	Statistical Parametric Mapping
VAC	vertical plane extending from the anterior commisure, perpendicular to the anterior commisure-posterior commisure line
VPC	vertical plane extending from the posterior commisure, perpendicular to the anterior commisure-posterior commisure line

Acknowledgments

I would like to thank Karl Friston and John Rothwell for their support and guidance over the past three years.

Additional thanks are due to Hartwig Siebner and Richard Frackowiak for many hours of discussion, supervision and teaching, and the staff of the Functional Imaging Laboratory and Sobell Department of Motor Neuroscience and Movement Disorders for their help with the experiments and the equipment.

None of this would have been possible without the support and glial cell functions provided by William Lee, especially in the final weeks.

This work was funded by The Wellcome Trust

Chapter 1

Introduction

Repetitive Transcranial Magnetic Stimulation (rTMS) can be used to induce temporary alterations in the excitability of the brain in healthy subjects. For some motor behaviour it has been possible to impair or improve performance following rTMS, but for most simple tasks performance is unaltered. This suggests that the motor system is able to compensate, to some extent, for the changes in excitability induced by rTMS. Potentially this makes rTMS a useful tool for studying reorganisation in the healthy motor system, and may provide insights into adaptive mechanisms after injury such as ischaemic stroke.

The aim of the work presented in this thesis is to explore how rTMS changes regional excitability and how the motor system compensates for these changes.

Compensation for abnormal excitability may be achieved through plasticity, defined as *"Any enduring change in cortical properties either morphological or functional" (Donoghue et al., 1996).* The motor system of adult humans displays these properties of plasticity from the synaptic level, to cortical representations of motor output and within the networks of cortical areas sub-serving motor behaviour.

Synaptic plasticity refers to a change in the efficacy of synapses between two neurones. "Hebbian" or associative synaptic plasticity (Hebb, 1949) is used to describe modulation of the strength of a synapse that is dependent on the temporal correlation of pre and post synaptic firing. Evidence for the presence of such mechanisms in the motor cortex, and its functional role, is outlined in Section 1.1.1 describing the anatomy of the human motor system.

Plasticity of **cortical motor representations** describes the modification of the somatotopic organisation of the primary motor cortex seen in response to lesions (Liepert et al., 2000), amputation (Cohen et al., 1991), surgery (Duffau, 2001), training (Classen et al., 1998) and altered cortical excitability (Ziemann et al., 2002). The anatomical and synaptic substrates of these plastic changes are described

below. Changes in motor cortical representations following manipulation of cortical excitability in healthy subjects are examined in Chapters 3, 5 and 6 of this thesis, and discussed further in Chapter 7.

Plasticity of the **motor system** at the level of networks of motor areas may be achieved through degeneracy (Price and Friston, 2002). The concept of "degeneracy" was introduced by Edelman and colleagues (Tononi et al., 1999;Edelman and Gally, 2001) and refers to the ability of biological systems that are structurally different to perform the same function. Degeneracy is a many-to-one structure function mapping and in this context it implies that more than one set of cortical structures can support the same function. It has therefore emerged as an important feature of functional brain architectures; providing an important substrate for functional recovery after focal lesions (Price and Friston, 2002). Within the motor system degeneracy may provide a framework for understanding compensatory mechanisms in both patients (Johansen-Berg et al., 2002b;Werhahn et al., 2003;Fridman et al., 2004) and healthy subjects (Strens et al., 2003). Further evidence for degeneracy in the motor system of healthy subjects is presented in Chapter 4, and discussed further in Chapter 7.

1.1 The Motor System

The experiments presented in this thesis describe the effects of transcranial magnetic stimulation to the motor system, as revealed by functional neuroimaging and measures of motor behaviour. In order to establish a framework for interpreting and understanding the results of these experiments, a brief overview of the anatomical and functional characteristics of the areas comprising the human motor system is provided, particularly those features that are relevant to synaptic and representational plasticity.

Roland and Zilles proposed a definition of cortical motor areas as those areas having projections to spinal motor neurons, containing a representation of the somatomotor apparatus and always being active during the planning and execution of voluntary movements, but rarely being active in other circumstances (Roland and Zilles, 1996). The cortical areas comprising the motor system include the agranular frontal cortex (Brodmann Areas 4 and 6) and cingulate motor areas (BA24). This

basic division represents an oversimplification and may include up to ten further subdivisions, made on the basis of functional and microscopic characteristics (Roland and Zilles, 1996;Rizzolatti et al., 1998;Geyer et al., 2000a). The premotor cortices are involved in initiating and planning voluntary movement; the primary motor cortex generates commands for specific muscles or muscle groups, which are communicated via the corticospinal tract. The subcortical motor system comprises the basal ganglia, thalamus, cerebellum and corticospinal tract. The basal ganglia, thalamus and cerebellum relay sensory information and have a role in fine-tuning movements. There are few empirical data regarding the connectivity of the motor areas in humans; therefore connections shown in Figure 1.1 are inferred from homologies with non-human primates where human data are unavailable.

1.1.1 Cortical Motor Areas

The **primary motor cortex** (M1) is a subdivision of the agranular frontal cortex described by Brodmann (Brodmann, 1903) as Areas 4 and 6. Area 4 is characterised by the lack of granule cells in layer IV and distinguished from the premotor cortex (Area 6) by the presence of giant pyramidal cells (Betz cells) in layer V (Meyer, 1987). In humans, Area 4 can be subdivided into Area 4a (anterior) and 4p (posterior) on the basis of neurotransmitter binding patterns (Geyer et al., 1996). The primary motor cortex extends from the fundus of the central sulcus to the vertex of the precentral gyrus, and from the Sylvian fissure to the mesial wall of the frontal lobe. With increasing distance laterally, the rostral border of Area 4 moves towards the anterior wall of the central sulcus (Geyer et al., 2000a).

Betz cells and other layer V pyramidal cells give rise to excitatory cortical and spinal projections and have numerous local collateral branches (Ghosh and Porter, 1988), with horizontal connection systems within M1 extending over 1cm (Huntley and Jones, 1991;Hess and Donoghue, 1994). The strength of these excitatory glutamatergic horizontal pathways (Hess et al., 1994) is probably influenced by GABA-ergic inhibitory interneurons (Hess and Donoghue, 1994;Donoghue, 1995;Hess et al., 1996). In M1 these local inhibitory connections consist of stellate or basket cells located in layers III to V, with horizontal myelinated axons that synapse on pyramidal cells (Jones, 1983;Meyer, 1987).

There is increasing evidence that these extensive horizontal connections provide a basis for cortical representation plasticity. Unmasking of excitatory horizontal connections by reducing GABA-ergic inhibition leads to changes in cortical representations in rats (Jacobs and Donoghue, 1991) and humans (Ziemann et al., 1998a;Ziemann et al., 1998b). Further evidence supporting this hypothesis is provided by findings in animals (Huntley, 1997) and humans (Ziemann et al., 2002), that reorganisation of cortical maps is confined to cortical areas with strong horizontal connections, and does not occur between areas that are not connected, such as face / whisker and hand / forelimb. These findings establish a role for synaptic plasticity seen in horizontal pathways in M1, which are capable of long-term depression (Hess and Donoghue, 1996) and long-term potentiation when paired with stimulation of extrinsic inputs (Hess et al., 1996) that may include cortico-cortical and thalamocortical pathways.

In addition to extensive horizontal local cortico-cortical connections the primary motor cortex receives afferent sensory input pertaining to the activity of muscles via the thalamus and primary somatosensory cortex (Ghosh et al., 1987). Additional afferent inputs come from the premotor cortices (ventrolateral premotor cortex, caudal dorsolateral premotor cortex and supplementary motor area), cingulate motor area and Area 5 of the parietal cortex (Muakkassa and Strick, 1979;Ghosh et al., 1987;Tokuno and Tanji, 1993) in a roughly somatotopic arrangement. In addition there are transcallosal afferents from the contralateral M1 (Sloper and Powell, 1979), and sparse transcallosal inputs from the contralateral premotor areas (Rouiller et al., 1994). These connections, derived from macaque data, are assumed to be present in humans. The output projections of M1 layer V pyramidal cells consist predominantly of direct, prominent connections to the spinal cord via the corticospinal tract (see below).

Initial experiments during surgery in humans (Penfield and Rasmussen, 1950) demonstrated that electrical stimulation of the cortical surface led to movement of the limbs. The representation of body parts appeared to be arranged in an orderly fashion with the leg located medially and the face laterally (close to the Sylvian fissure). More recent data from intracortical microstimulation shows that broad subdivisions of body parts exist (face, upper limb, lower limb, trunk) and that within these areas these are multiple distributed, overlapping representations of body

parts (see Sanes and Schieber (2001) for a review). This pattern is not surprising given that studies of corticospinal projection neurones in the macaque suggest that outputs from large areas of primary motor cortex converge onto single spinal motor neurons, while at the same time outputs from any single neuron synapse with multiple spinal neuron pools (Shinoda et al., 1981).

Low spatial resolution data from early functional neuroimaging experiments in humans using positron emission tomography (PET) (Colebatch et al., 1991;Grafton et al., 1991) provided initial evidence from human subjects that representations of proximal and distal arm movements overlap. Sanes et al. (1995) and Rao et al. (1995) used the higher spatial resolution of functional magnetic resonance imaging (fMRI) to demonstrate the presence of overlapping and distributed activity during movement of the fingers, wrist and arm (Sanes et al., 1995;Rao et al., 1995).

The primary motor cortex has a central role in the execution and control of voluntary movement. Work in non-human primates suggests that the activity of cells in M1 code for the direction of limb movement through the construction of a population vector, such that the activity of directionally tuned cells in M1 is proportional to the angle between the actual direction of movement and the preferred direction of the cell (Georgopoulos et al., 1982;Georgopoulos et al., 1986). Subsequent experiments suggest that the motor cortex represents movements in terms of the direction and velocity of the required movement, not on the basis of individual muscles (Alexander and Crutcher, 1990;Ashe and Georgopoulos, 1994;Kakei et al., 1999). Experiments in human subjects suggests that this internal model or mapping between the intended movement and muscle activation is plastic and can be re-learnt, for example if subjects are required to make movements in an artificial force-field (Shadmehr and Mussa-Ivaldi, 1994). The primary motor cortex also appears to be heavily involved in various aspects of motor skill learning: changes in cortical representations and neuron discharge properties are seen during skill acquisition in non-human primates (see Sanes and Donohuge (2000) for a review). In humans, changes in motor representations (Pascual-Leone et al., 1994a) and discharge properties of cortical neurones (Classen et al., 1998) can be seen during motor learning.

Figure 1.1

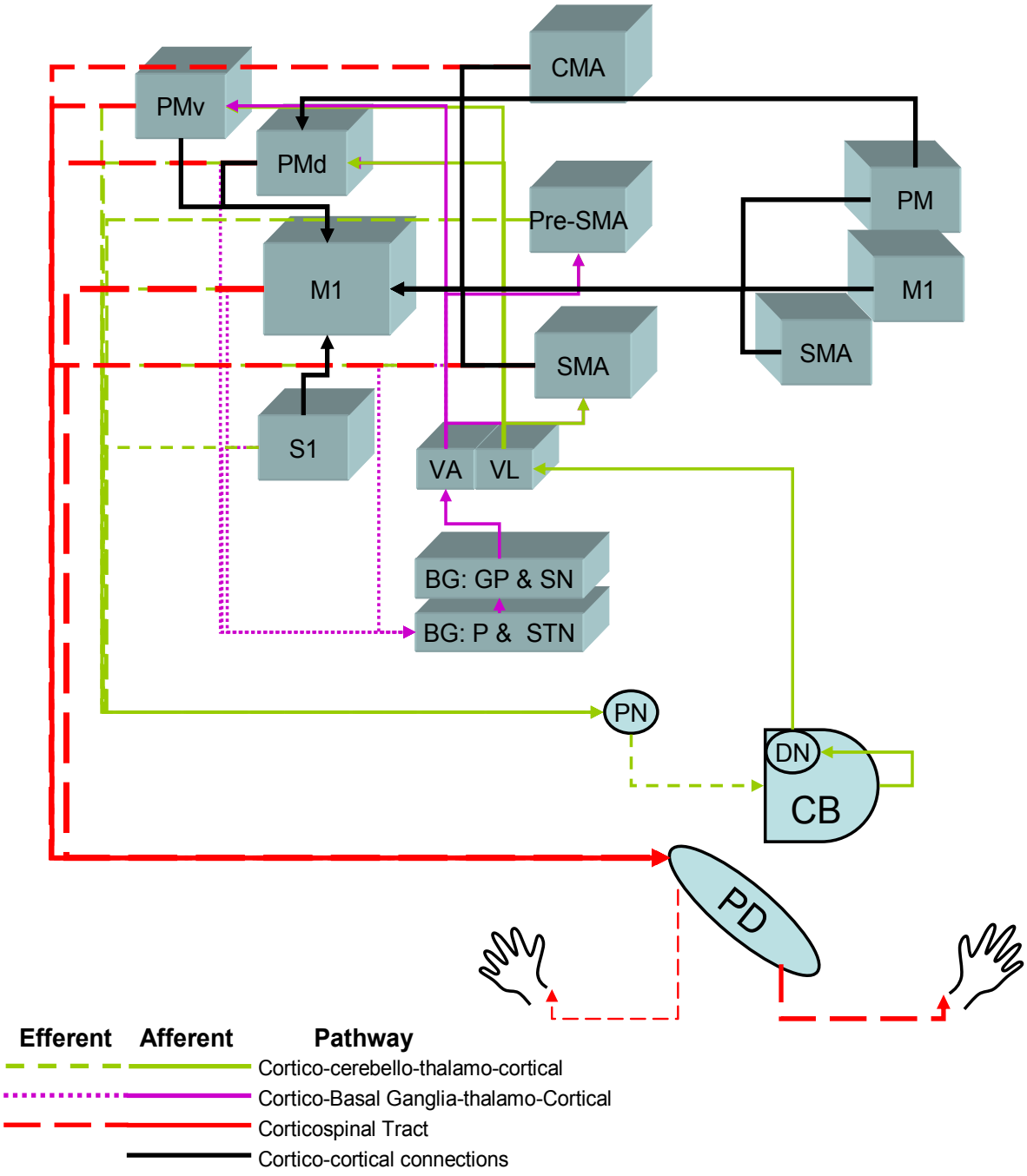

Figure 1.1: Anatomical connections of the motor system based of literature presented in Chapter 1. **M1**: Primary motor cortex, **S1**: Primary somatosensory cortex, **PMd**: Dorsolateral premotor cortex, **PMv**: Ventrolateral premotor cortex, **SMA**: Supplementary motor area, **CMA**: Cingulate motor area, **VA**: Ventral anterior nucleus of thalamus, **VL**: Ventral lateral nucleus of thalamus, **BG**: Basal ganglia, **GP**: Globus pallidus, **SN**: Substantia nigra, **STN**: Subthlamic nucleus, **P**: Putamen, **PN**: Pontine nucleus, **DN**: Dentate nucleus, **CB**: Cerebellum, **PD**: Pyramidal decussation

The **premotor cortices** modulate motor output in two ways: first by connections to the primary motor cortex and second, via projections to the spinal cord (Dum and Strick, 1991).

The **lateral premotor cortex** consists of those parts of BA6 that are located on the lateral surface of the cortex. The rostral border of BA4 forms the caudal extent of the lateral premotor cortex (BA6). The rostral border of BA6 is not defined by any anatomical landmarks. In the macaque the lateral premotor cortex can divided into at least four further regions (Geyer et al., 2000a) on the basis of cytoarchitecture, connectivity and function. In humans there are at least two subdivisions: dorsal and ventral; the results of imaging studies suggest that there may be further subdivisions within these (Picard and Strick, 2001).

The **dorsolateral premotor cortex** (PMd) is located within the rostral precentral gyrus and caudal superior frontal gyrus (Rizzolatti et al., 1998). In the macaque there are clear differences in the connectivity of the rostral and caudal parts of the PMd (Rizzolatti et al., 1998). This may also be the case in humans and may explain the rostro-caudal gradient in activations seen with different motor tasks (Picard and Strick, 2001). The PMd appears to be involved in action planning, response selection, movement preparation and visual guidance of motor responses, especially when the actions are cued by arbitrary associations (Wise et al., 1996). Within the PMd cognitive aspects of motor behaviour appear to be processed more rostrally, especially when the task is nonroutine (Passingham, 1997) whereas the caudal PMd appears to be engaged by simpler and automatic motor tasks (Jueptner et al., 1997).

The **ventrolateral premotor cortex** (PMv) is located ventral to the frontal eye fields and caudal to BA44/45, but the extent of this area in humans is not well established (Grezes and Decety, 2001). In the macaque this area receives extensive input from the parietal cortex, and has been implicated in visuomotor transformations during grasping and object-cued movements, and action observation (Rizzolatti et al., 1998). Imaging studies in humans have yet to yield conclusive evidence for the role of PMv in action observation or object manipulation tasks (Picard and Strick, 2001;Grezes and Decety, 2001).

The **medial premotor cortices** consist of those parts of BA6 located on the mesial surface of the cortex and BA24, located within the cingulate sulcus.

The **supplementary motor area** (SMA) (mesial BA6) is subdivided into at least two further anatomically distinct regions: the SMA proper and the pre-SMA (Zilles et al., 1995). Macroscopically, the border of M1 and SMA proper roughly corresponds to the VPC line, and the border between SMA proper and pre-SMA to the VAC line (Vorobiev et al., 1998). The SMA-proper appears to contain a somatotopic representation (Fink et al., 1997) and appears to be implicated in simple motor tasks (those with basic temporal and spatial organisation, or that are highly practised) (Picard and Strick, 1996), externally triggered movements, motor preparation and learnt sequences (Passingham, 1996;Deiber et al., 1999;Picard and Strick, 2001). The pre-SMA appears to be more involved in cognitive aspects of motor control, such as processing of movement cues, rather than response selection (Picard and Strick, 2001).

The **cingulate motor areas** (CMA) consist of three subdivisions of BA 24, located within the cingulate sulcus, that may correspond to cingulate motor areas in the macaque (Picard and Strick, 1996). From a small number of human imaging studies it appears that caudal CMA may contain somatotopic representations and may be involved in simple motor tasks (Picard and Strick, 1996) whereas rostral CMA may be involved in more complex actions, such as conditional associations between cues and movements (Paus et al., 1993).

1.1.2 Subcortical Motor Systems

The **corticospinal tract** is the major output of the motor cortices, enabling the cerebral cortex to excite muscles. It is formed from the axons of layer V pyramidal cells which project via the internal capsule to the medullary pyramids. 70-90% of these projections decussate, forming the lateral column of the contralateral spinal cord; the remaining 10-30% form the ipsilateral ventral column (Nathan et al., 1990). Descending corticospinal projections terminate in the spinal cord, synapsing either on interneurons, or directly on motorneurons. Direct monosynaptic projections are most commonly from axons originating in the hand area, and may therefore have a role in dextrous movements of distal muscles (Muir and Lemon, 1983) A significant

proportion of corticospinal neurons (~50% in monkeys (Dum and Strick, 1991), 60% in humans (Jane et al., 1967)) originate from the SMA, cingulate motor areas and premotor areas.

The **basal ganglia** (striatum, subthalamic nucleus, globus pallidus and substantia nigra) are interconnected subcortical structures. Layer V neurones from the somatosensory and motor cortices project to the putamen (part of the striatum) (Jones et al., 1977); the subthalamic nucleus receives input from M1, SMA and PMd (Parent and Hazrati, 1995a;Parent and Hazrati, 1995b). The striatum and subthalamic nucleus project to the globus pallidus and substantia nigra, which in turn project to the thalamus and the brain stem. The thalamus and basal ganglia therefore form part of a cortico-basal ganglia-thalamo-cortical loop. Damage to the basal ganglia results in abnormalities of movement (e.g. bradykinesia, tremor) and muscle tone (Crossman, 2000).

The **thalamus** is a collection of nuclei that act as a relay; transmitting information from the basal ganglia, cerebellum (Holsapple et al., 1991) and ascending somatosensory spinal cord (Lemon and van der Burg, 1979) to the cortex, as well as between cortical areas (Sherman and Guillery, 2002). The ventral lateral nucleus receives input from the cerebellum (contralateral dentate nucleus) and projects to cortical motor areas (Matelli and Luppino, 1996). The ventral anterior nucleus also projects to cortical motor areas, but receives input from the basal ganglia (Jones, 1987).

The **cerebellum** has a three-layered cortex, surrounding a white-matter core within which are the cerebellar nuclei. The cerebellum receives inputs from the spinocerebellar tracts conveying movement-related sensory information from muscle spindles, tendon organs, joint and cutaneous receptors and spinal interneurons. The cerebellum also receives topographically organised inputs from the contralateral cerebral cortex via the pontine cerebellar nuclei. The majority of these cortico-pontine tracts originate in the sensorimotor areas, such as primary motor and sensory cortices, SMA and premotor cortex (Allen and Tsukahara, 1974). Purkinjie cells from the cerebellar cortex project to the cerebellar nuclei (Voogd and

Glickstein, 1998), which influence movement via excitatory projections to the spinal cord and, via the ventrolateral thalamus (Asanuma et al., 1983), to the primary, supplementary and premotor cortices (Matelli et al., 1989;Matelli and Luppino, 1996). Recent work (Kelly and Strick, 2003) demonstrates the presence of distinct cerebello-thalamocortical circuits for motor processing in non-human primates comprising cerebellar lobules IV-VI, distinct regions of the dentate nucleus and ventrolateral thalamus and M1. Cerebellar damage causes deficits of coordinated movement such as ataxia, tremor, nystagmus and poor balance, underlying the role of the cerebellum in fine-tuning motor behaviour. The cerebellum has also been strongly implicated in many aspects of motor learning (Raymond et al., 1996;Doyon et al., 2003). Work in non-human primates demonstrates that the cerebellum also receives inputs from and projects to prefrontal and parietal cortices (Dum et al., 2002;Kelly and Strick, 2003;Dum and Strick, 2003;Clower et al., 2004); strongly suggesting a role in cognitive and visuospatial functions. Work by Desmond et al. suggests that the human cerebellum may also contain distinct subdivisions for motor and non-motor processes (Desmond et al., 1997).

1.2 Transcranial magnetic stimulation and functional neuroimaging

Transcranial Magnetic Stimulation (TMS) is a method of non-invasively stimulating the human brain in awake, behaving humans (Barker et al., 1985). It is a valuable tool for investigating many aspects of brain function. It can be used to examine cortical excitability; connectivity and functional organisation (see Chapter 2). Repetitive Transcranial Magnetic Stimulation (rTMS) causes immediate and lasting changes in cortical excitability at the site of stimulation and at distant sites (Ferbert et al., 1992;Siebner and Rothwell, 2003). The effects of stimulating the motor and premotor cortices with 1Hz rTMS are reviewed in Chapter 2. Despite widespread changes in cortical and corticospinal excitability 1Hz rTMS has very limited effects on basic motor behaviour, suggesting that the motor system is able to compensate, to some extent, for temporary alterations in excitability. Potentially this makes rTMS

a useful tool for studying plastic reorganisation in the healthy motor system, and may provide insights into adaptive mechanisms after injury such as ischemic stroke. Given the results of lesion experiments in animals (Liu and Rouiller, 1999;Frost et al., 2003), and imaging studies of stroke in humans (Chollet et al., 1991;Weiller et al., 1992;Cramer et al., 1997;Cao et al., 1998;Seitz et al., 1998;Cuadrado et al., 1999;Johansen-Berg et al., 2002a;Ward et al., 2003a;Ward et al., 2003b), compensatory changes in response to rTMS may involve a wide range of cortical and subcortical motor areas that are conditional on the motor task under investigation. It will therefore be necessary to measure changes in activity across the whole brain during motor behaviour in order to provide a complete picture of compensatory plasticity.

TMS can be used to obtain direct measures of excitability from primary motor cortex and to examine changes in the responsiveness of the primary motor cortex to inputs from distant motor areas. It is not possible to assess the excitability of sub-cortical structures, neither is it possible examine the effects of changes in the excitability of primary motor cortex on other areas. In addition, measures of cortical excitability obtained with TMS are significantly altered during muscle activation (Mazzocchio et al., 1994;Ridding et al., 1995). This makes it difficult to obtain an accurate picture of changes in excitability in the motor system during movement. Functional neuroimaging is a well established method of measuring changes in synaptic activity across the whole brain during a wide range of conditions. Functional neuroimaging provides an indirect measure of synaptic activity; it does not provide information about excitability, but it can be used to characterise functional specialisation (changes in task-related activity in specific anatomical locations) and functional integration (changes in the degree of influence or coupling between anatomical locations with respect to experimental manipulations) (see Chapter 2). These two methods can be combined to examine changes in movement-related activity in the motor system following changes in the excitability of the primary motor cortex induced by rTMS.

Functional neuroimaging has been combined with TMS by previous investigators. These experiments have used a range of imaging techniques (PET, fMRI, EEG) to look at the effects of single and repetitive stimuli on the synaptic activity in the

resting brain, both in terms of functional segregation and integration. This work is reviewed in Chapter 2. The effects of rTMS on synaptic activity during movement have not previously been investigated using functional neuroimaging. The aim of the experimental work presented in this thesis is to examine the changes in movement-related responses and movement-related coupling within the motor system during periods of abnormal cortical excitability induced by 1Hz rTMS, and to explore the functional relevance of these changes using measures of motor behaviour.

1.3 Summary of experimental work

Chapter 2 describes the experimental techniques used in this thesis and reviews the effects of 1Hz rTMS on the excitability of the primary motor and somatosensory cortices. Chapters 3 and 5 describe two functional imaging experiments examining the effects of 1Hz rTMS on two types of movement related activity: freely selected finger movements and paced, cued finger tapping, measured with Positron Emission Tomography (PET). Chapter 4 examines the functional significance of changes in movement related activity following 1Hz rTMS, using a choice reaction time task. Chapter 6 examines the effects of 1Hz rTMS on motor representations and movement-related coupling during finger tapping measured using functional magnetic resonance imaging (fMRI) and dynamic causal modelling (DCM).

Chapter 2

Methods: Transcranial Magnetic Stimulation and Functional Neuroimaging

This chapter describes the methods used in the experiments presented in this thesis. All the experiments use 1 Hz repetitive transcranial magnetic stimulation (rTMS); therefore the first section of this chapter gives an overview of the principles of TMS and the methods of measuring and modulating cortical excitability with TMS. The effects of 1 Hz rTMS on the excitability of the sensorimotor system are also reviewed.

The second section of this chapter describes the two neuroimaging techniques used in this thesis: positron emission tomography (PET) and functional magnetic resonance imaging (fMRI). It outlines of the principles of these techniques and summarises the neuroimaging data analysis methods used in this thesis.

2.1 Transcranial Magnetic Stimulation

2.1.1 Basic Mechanisms of TMS

TMS was first used to stimulate the human brain by Barker et al. (Barker et al., 1985). The technique uses Faraday's principle of electromagnetic induction: a coil of wire (the TMS coil) is placed against the scalp and a large, rapidly changing electrical current is passed through it. This creates a magnetic field which passes relatively unimpeded through the scalp and skull. The magnetic field lasts about 1ms with a fast rise and slow tail. This induces an electrical current in the conducting tissues of the brain (Jalinous, 1991) that is proportional to the rate of change of the field and is therefore greatest at the start of the pulse (~200 μs). This induced current can change the resting membrane potential of neurons and may lead to an action potential if the current is large enough (Rothwell et al., 1999). The amplitude and rate of change of current in the TMS coil determines the size of the current induced in the cortex (Walsh and Rushworth, 1999;Cowey and Walsh, 2001).

The currents induced by TMS flow parallel to the surface of the brain (Tofts, 1990) in the opposite direction to the electrical current in the stimulating coil. Because neurones are activated more effectively by longitudinal than transverse currents TMS preferentially stimulates neuronal elements that are oriented horizontally within the cortex, running parallel to the longitudinal axis of TMS coil (Amassian et al., 1992). Therefore small alterations in the orientation of the TMS coil on the scalp can alter the efficacy of stimulation and result in excitation of different populations of cortical neurons (Amassian et al., 1992). The nerve fibre is stimulated by the spatial differential of the electric field along the axis of the axon i.e. the more steeply the voltage falls off with distance down an axon, the more likely stimulation is to occur. If the axon is parallel to the electrical field there is no change in voltage with distance along the length; however if the axon bends out of the parallel orientation, for example over the lip of the central sulcus, then the spatial derivative is high and likelihood of stimulation is increased (Maccabee et al., 1993). Preferential stimulation of intrinsic hand muscles can be achieved by delivering currents that flow perpendicular to the central sulcus, from posterior to anterior, exciting horizontal fibre systems aligned in this direction (Mills et al., 1992).

The latency of electromyographic (EMG) responses measured in upper limb muscles after TMS suggests that TMS excites the pyramidal cells whose axons form the descending corticospinal tracts transsynaptically (Rothwell, 1997). A single TMS pulse produces repetitive activity in the cortex, leading to a series of descending volleys in the corticospinal tract. These are described as indirect or ‘I’ waves, as compared to the direct or ‘D’ waves elicited by direct electrical stimulation of the motor cortex (Patton and Amassian, 1954;Amassian et al., 1987). EMG responses to TMS (motor evoked potentials: MEPs) result from the summation of I wave volleys and are therefore susceptible to variations in the excitability of the intervening synapses (Kiers et al., 1993).

The geometry and size of the TMS coil determines the area of cortex in which currents are induced (for a review see Terao and Ugawa (2002). Using a figure-of-eight or double cone coil and strong stimulus intensities it may be possible to stimulate tissue at a distance of 3-4cm from the surface of the coil (Terao et al., 2000), however most stimulation occurs within 2-3cm from the coil. The interaction between the curvature of the cortex and the rapid reduction in the strength of the

magnetic field with increasing distance from the surface of the TMS coil gives a spatial resolution of TMS of approximately 1cm (Brasil-Neto et al., 1992;Wassermann et al., 1992) i.e. differential effects of stimulation can be discerned with coil movements of 1cm but the effects of individual stimuli are more widespread. Given that the strength of the magnetic field produced during a TMS pulse decreases progressively with increasing distance from the centre of the coil and therefore effective direct stimulation occurs in a limited area of cortex close to the centre of the coil (Roth et al., 1991;Barker, 1999), any effects of TMS seen outside this area are thought to be mediated by cortico-cortical and cortico-subcortical connections.

2.1.2 TMS techniques used to study the motor system

Single or paired pulses of TMS can be used to obtain electrophysiological information about the excitability of the motor cortex. Trains of repetitive transcranial magnetic stimuli (rTMS) of differing frequencies, intensities and duration can be used to modulate the excitability of the cortex. It is well established that rTMS to M1 can change the excitability of the motor system depending on the frequency of stimulation. Low frequency rTMS (less than or equal to 1Hz) tends to reduce the excitability of the stimulated area and high frequency rTMS (5Hz or greater) tends to increase excitability (Pascual-Leone et al., 1994b;Maeda et al., 2000b). These changes in excitability can outlast stimulation for at least several minutes (Pascual-Leone et al., 1998).

TMS can also be used to disrupt ongoing cortical activity during a cognitive or motor task, either as single stimuli or very short (less than 500ms) trains of rTMS. This technique, sometimes referred to as a ‘virtual lesion’ approach, it is thought to act via the immediate effect of TMS increasing neuronal noise at the site of stimulation disrupting organised cortical activity (Walsh and Rushworth, 1999).

The effects of TMS on the excitability of the motor system can be assessed directly by measuring motor evoked potentials (MEPs) or indirectly by functional neuroimaging (e.g. positron emission tomography (PET), functional magnetic resonance imaging (fMRI), electroencephalography (EEG)) and measures of motor

behaviour (e.g. force generation, movement velocity, movement accuracy, reaction times, response accuracy, sequence learning). Each of these methods has strengths and weaknesses. Electrophysiological techniques provide a direct, objective measure of cortical and / or corticospinal excitability. Section 2.1.3 describes the methods available for assessing the excitability of the motor system, and reviews the findings of studies where these techniques have been used to examine the effects of 1Hz rTMS. It is only possible to obtain direct measures of excitability from primary motor cortex and to examine changes in the responsiveness of the primary motor cortex to inputs from distant motor areas. It is not possible to assess the excitability of sub-cortical structures using TMS; neither is it possible to examine the effects of changes in the excitability of M1 on the excitability of other areas. Functional neuroimaging enables the characterisation of TMS effects on synaptic activity throughout the brain, both at rest and during task performance, but it does not provide a direct measure of excitability. The role of functional neuroimaging in evaluating the distributed effects of 1Hz rTMS is discussed in Section 2.1.6. Importantly, neither directly measured changes in cortical excitability nor changes in synaptic activity measured with functional neuroimaging necessarily translate into changes in motor task performance. The use of functional indicators of brain activity, such as changes in reaction times, performance accuracy and rate of learning can provide this information. However, there are several potential problems with the interpretation of changes or lack of changes in such outcome measures. These are also discussed with respect to studies using 1Hz rTMS in Section 2.1.7.

2.1.3 Measuring the excitability of the motor cortex and corticospinal tract with TMS

TMS can be used in a variety of ways to measure the excitability of the motor cortex and corticospinal tract. As described above, all TMS effects are thought to be generated transsynaptically; therefore any TMS measure reflects the responsiveness of the stimulated area to an input i.e. the efficacy with which the synapses respond to an input.

The motor threshold (MT) refers to the lowest intensity of TMS that can elicit a motor evoked potential of approximately 50 μV. The MT is thought to reflect neuronal membrane excitability because it is increased by drugs that alter

membrane conductance (Ziemann et al., 1996;Chen et al., 1997b). It can be measured in resting or activated muscles (AMT and RMT respectively) and tends to be greater for larger and more proximal muscles (Chen et al., 1998). Although the motor threshold depends on the excitability of corticospinal axons, it is also sensitive to the membrane potential of cortical and spinal motorneurons: the nearer they are to threshold, the lower the TMS threshold. This explains why the AMT is lower than the RMT for any given muscle. The RMT represents the intensity of stimulation required to activate cortico-spinal neurones, and therefore it is assumed that stimulation at or above the RMT will also activate cortico-cortical connections (Rothwell, 1997). In this thesis the RMT will be used to define the threshold of stimulation delivered in the studies described below. Subthreshold stimulation refers to stimulation given below RMT, whereas suprathreshold describes stimuli at intensities at or above RMT i.e. causing muscle twitches.

The amplitude of the motor evoked potential (MEP) elicited from a peripheral muscle represents a measure of the excitability of the cortex, sub-cortex and spinal tract. An MEP recruitment curve describes the rate of increase in MEP amplitude with increasing stimulus intensity. It provides a measure of the excitability of a larger area of cortex than the MT (Hallett et al., 1999).

The silent period (SP) describes a short cessation of muscle activity when a single pulse of TMS is delivered during voluntary muscle contraction. The duration of the late phase of the SP provides a measure of the excitability of cortical inhibitory interneurons (presumably GABAb-ergic) (Fuhr et al., 1991;Chen et al., 1999).

2.1.3.1 Local effects of TMS on synaptic efficacy

The most rapid modulation of synaptic efficacy by TMS occurs within milliseconds of stimulation. Local cortical excitability can be investigated using pairs of TMS pulses delivered from 1-200ms apart. The most frequently used paired-pulse paradigm (Kujirai et al., 1993) gives a subthreshold conditioning stimulus to condition the MEP amplitude elicited by a subsequent suprathreshold test stimulus. At inter-stimulus intervals (ISIs) of 1-5ms the amplitude of the test MEP is inhibited (intracortical inhibition: ICI), and at longer ISIs (8-30ms) the response is facilitated (intracortical facilitation: ICF). These phenomena appear to occur in the cortex (Kujirai et al.,

1993;Nakamura et al., 1997;Di Lazzaro et al., 1998;Di Lazzaro et al., 1999b). GABA agonists and glutamatergic antagonists increase ICI and decrease ICF whereas drugs that alter membrane conductance have no effect (Ziemann et al., 1996;Liepert et al., 1997;Ziemann et al., 1998c).

2.1.3.2 Local effects of 1Hz rTMS

The effects of low-frequency (1Hz or less) rTMS to the sensorimotor hand area on cortical excitability have been investigated with a variety of methods. These studies reveal a complex pattern of interactions among different sets of cortical neurones. 1Hz rTMS modulates the excitability of corticospinal projections from the site of stimulation, indexed by reduced amplitude of MEPs (Wassermann et al., 1996;Chen et al., 1997a;Maeda et al., 2000b;Touge et al., 2001;Romero et al., 2002;Tsuji and Rothwell, 2002) and reduced slope of MEP recruitment curves (Muellbacher et al., 2000;Gangitano et al., 2002) in relaxed hand muscles. 1Hz rTMS has also been shown to increase resting motor threshold for intrinsic hand muscles (Muellbacher et al., 2000;Fitzgerald et al., 2002).

In addition to a reduced corticospinal output and an attenuated response to sensory input (see below), intracortical neuronal processing within the sensorimotor hand area is modified by 1 Hz rTMS. Using the paired-pulse paradigm of Kujirai et al. (Kujirai et al., 1993), it has been shown that 1Hz rTMS decreases facilitatory interactions between intracortical circuits at the site of stimulation (Romero et al., 2002).

1Hz rTMS reduces the amplitude of the Long Latency Stretch Reflex (LLSR) (Tsuji and Rothwell, 2002). This may reflect decreased excitability of corticospinal projections or reduced sensitivity of the primary motor hand area to sensory afferents i.e. cortico-cortical inputs. Enomoto et al. report a decrease in the peripherally evoked SEP after rTMS to M1 (Enomoto et al., 2001). Knecht et al. report decreased performance on a tactile discrimination task following 1Hz rTMS to primary somatosensory cortex (Knecht et al., 2003). Satow et al. investigated thresholds for detecting tactile stimuli, and found that 0.9Hz rTMS to S1 was followed by increased tactile thresholds, but no change in SEP amplitude or performance on a two point discrimination task (Satow et al., 2003). These studies suggest that 1Hz rTMS reduces the responsiveness of the somatosensory system

to ‘natural’ or external inputs, and that this leads to impairments in performance of some sensory behaviour.

2.1.4 Intra-hemispheric effects of TMS

Using a variation of the paired-pulse techniques described above Civardi et al. demonstrated that, at an ISI of 6ms, stimulation of the premotor cortex (3-5cm anterior to the motor hand area) with sub- and suprathreshold conditioning stimuli lead to inhibition and facilitation of responses from the ipsilateral motor hot-spot respectively (Civardi et al., 2001).

Modulating the excitability of the premotor cortex with rTMS can induce more enduring changes in the excitability of the ipsilateral M1. 1 Hz rTMS to M1 and PMd reduces the amplitude of MEPs elicited from M1 (Chen et al., 1997a;Gerschlager et al., 2001). The direction of distributed changes in cortical excitability appears to be frequency-dependent and the direction of effects on MEP amplitude appears to be similar for M1 and PMd stimulation. However, other measures of corticocortical excitability such as paired-pulse excitability may not follow such a straightforward relationship. For example, subthreshold 1Hz rTMS to PMd increases ICF at 7ms for up to one hour (Munchau et al., 2002) whereas subthreshold 1Hz rTMS to M1 decreases ICF (Romero et al., 2002).

When two sessions of 1Hz rTMS are delivered to the premotor cortex on consecutive days the effects on motor excitability have a longer duration (Baumer et al., 2003), suggesting that the distributed effects of premotor stimulation are not restricted to an immediate modulation of motor excitability.

2.1.5 Inter-hemispheric effects of TMS

Cracco et al. first demonstrated TMS-evoked transcallosal responses (Cracco et al., 1989). Ferbert et al. showed that conditioning stimuli delivered to the motor cortex of one hemisphere caused inhibition of MEPs elicited from the contralateral motor cortex 5-6ms later (Ferbert et al., 1992). Mochizuki et al (2004) used lower intensity conditioning stimuli to demonstrate inhibition of test MEPs and SEPs 150ms after stimulation of the contralateral motor and ventral premotor cortex (Mochizuki et al., 2004). Other studies (Meyer et al., 1995;Meyer et al., 1998) have also

demonstrated the presence of inhibitory interactions between homologous primary motor areas by inducing silent periods in active muscles ipsilateral to the site of stimulation. Ugawa et al (1993) and Hanajima et al (2001) (Ugawa et al., 1993;Hanajima et al., 2001) report the presence of subtle facilitatory interactions between the motor cortices at short interstimulus intervals (4-5ms) followed by late inhibition. These studies confirm that stimulation of the primary motor cortex has immediate effects on synaptic efficacy in distributed brain areas, the most readily measured of which being the contralateral motor cortex.

In addition to these immediate effects, rTMS delivered to the primary motor cortex can alter the excitability of the contralateral motor cortex, and the magnitude of interhemispheric effects, for longer periods of time. An initial study by Wassermann et al. suggested that 1Hz rTMS at a suprathreshold intensity resulted in reduced excitability of the contralateral motor cortex, as measured by a reduction in the slope of the MEP recruitment curve (Wassermann et al., 1998). Recent studies have shown opposing effects of 1Hz rTMS on the excitability of the stimulated and contralateral hemispheres. Suprathreshold 1Hz rTMS decreased MEP amplitude in the stimulated hemisphere while decreasing intracortical inhibition (Plewnia et al., 2003) and increasing the slope of MEP recruitment curves (Schambra et al., 2003) in the contralateral hemisphere. Gilio *et al.* (Gilio et al., 2003) found increased MEP amplitudes in the contralateral hemisphere and a reduction of the early phase of paired-pulse inhibition from the stimulated (conditioned) to the non-stimulated (test) hemisphere. Using a series of control experiments, these authors concluded that these effects were predominantly mediated by cortico-cortical circuits rather than spinal mechanisms or afferent feedback. rTMS to the primary motor cortex results in a range of lasting changes in the excitability of distributed brain areas (measured in the contralateral motor cortex); the direction of changes differs between the local and distributed effects. The exact mechanisms of interhemispheric effects of TMS are incompletely understood but rTMS to the primary motor cortex undoubtedly results in a range of lasting changes in the excitability of distributed brain areas mediated via direct corticocortical (Di Lazzaro et al., 1999a) or cortico-subcortical-cortico pathways (Gerloff et al., 1998a).

2.1.6 Measuring the effects of TMS on synaptic activity

The electrophysiological techniques outlined above only monitor excitability changes in the primary motor cortex or changes in the responsiveness of the primary motor cortex to inputs from distant motor areas. Functional neuroimaging enables the visualisation of TMS effects on synaptic activity throughout the brain, both at rest and during task performance. However, it does not provide a direct measure of excitability. Imaging techniques such as positron emission tomography (PET) and the blood oxygen level dependent (BOLD) signal acquired in functional magnetic resonance imaging (fMRI) provide indirect measures of neuronal activity. These techniques rely on the coupling between increased synaptic activity and increased oxygen and glucose consumption (rCMR-glc, measured with [^{18}F] FDG-PET); and subsequent increases in cerebral blood flow (CBF) (measured with $H_2{}^{15}O$ PET and BOLD fMRI). The two techniques used in the experiments presented in this thesis are described in more detail in Section 2.2.

It is important to establish a 'proof of principle', demonstrating that it is possible to detect local effects of TMS at subthreshold intensities. Subthreshold TMS alters the responsiveness of the cortex to subsequent stimuli; therefore it should be possible to detect changes in synaptic activity using imaging techniques. The use of suprathreshold TMS in the motor system is more problematic because, by definition, suprathreshold stimuli will cause movement and therefore re-afferent feedback will contribute to any changes seen at the site of stimulation. Recording EEG activity over the whole cortex Ilmoniemi *et al.* showed that single subthreshold TMS pulses elicited an immediate increase in local activity, spreading to adjacent ipsilateral motor and premotor areas within 3-10 ms, and to the homologous contralateral M1 within 20ms (Ilmoniemi et al., 1997). Using $H_2{}^{15}O$ PET Siebner *et al.* found frequency dependent changes in regional cerebral blood flow (rCBF) restricted the site of stimulation (M1) during short trains of subthreshold stimulation (1-5Hz rTMS) (Siebner et al., 2001). Takano et al. report increases in rCBF at the site of stimulation (M1) following short trains of subthreshold 5Hz rTMS (Takano et al., 2004). The magnitude of the rCBF changes correlated with changes in paired-pulse excitability, suggesting that rCBF is sensitive to changes in excitability measured using direct techniques. Given that it is possible to measure local effects

of TMS with functional imaging techniques, it is now possible to examine distributed effects.

2.1.6.1 Effects of 1Hz rTMS measured with imaging techniques

In addition to the immediate effects of TMS, the studies reviewed in Sections 2.1.4 and 2.1.5 indicate that rTMS delivered to the primary and pre- motor cortices can alter the excitability of distributed brain areas. In one of the earliest PET imaging experiments to examine the effects of rTMS Fox et al. observed increases rCBF in left M1 (site of stimulation) during suprathreshold 1Hz rTMS that slowly decreased in magnitude after cessation of stimulation (Fox et al., 1997). Positive correlations with the rCBF changes at the site of stimulation were seen in the ipsilateral sensory and premotor areas and contralateral SMA. Negative correlations were seen in the contralateral M1. These changes may reflect direct effects of rTMS or effects of repeated hand movements induced by suprathreshold stimuli. This explanation is supported by the findings of Strafella and Paus who showed that increases in rCBF at the site of stimulation (M1), ipsilateral premotor cortex and contralateral M1 measured with $H_2{}^{15}O$ PET were correlated with changes in MEP amplitude during paired-pulse TMS (Strafella and Paus, 2001). Examining the effects of intensity (sub- to suprathreshold) with 1Hz rTMS Speer et al report increases in rCBF (measured with $H_2{}^{15}O$ PET) at site of stimulation (M1), contralateral cerebellum and in bilateral sub-cortical structures (Speer et al., 2003). The data presented in this paper suggest a non-linear relationship between intensity and rCBF at the site of stimulation: subthreshold stimulation appears not to evoke a significant increase in rCBF; whereas suprathreshold stimulation does. Okabe et al used SPECT to investigate changes in rCBF during subthreshold 1Hz rTMS (Okabe et al., 2003). They failed to see any changes in rCBF at the site of stimulation, but reported increased synaptic activity in the ipsilateral cerebellum and decreased synaptic activity in the contralateral M1, SMA, premotor and parietal regions. In common with Speer et al this study also reports decreases in rCBF in the contralateral prefrontal and parietal cortices.

Chouinard et al. examined the effects of subthreshold 1Hz rTMS to M1 and premotor cortex (Chouinard et al., 2003). In each experiment the change in

amplitude of MEPs evoked during PET scans were correlated with changes in rCBF. Following 1Hz rTMS to M1 positive correlations with decreased MEP amplitude were seen in the contralateral M1, ipsilateral cerebellum, cingulate motor area and subcortical structures. A simple comparison of rCBF before and after rTMS demonstrated a trend toward increased rCBF at the site of stimulation and the ipsilateral premotor cortex. Following subthreshold 1Hz rTMS to left premotor cortex widespread positive correlations with decreased MEP amplitude were seen bilaterally in the ventral premotor areas, cingulate motor areas, subcortical structures and a range of prefrontal and parietal regions. The authors infer that areas showing parallel changes in rCBF with MEP amplitude are likely to be anatomically connected to site of stimulation (based on the macaque literature). It is also of note that 1Hz rTMS to primary and premotor cortex had similar effects on MEP amplitudes, but that there was minimal overlap in the location observed changes in rCBF.

These two methods of measuring changes in activity and excitability provide complementary information. Changes in excitability or synaptic efficacy determined using direct measures i.e. electrophysiological techniques do not have a straightforward relationship with measures of synaptic activity, measured with functional imaging. Moreover, what neither method provides is any information about the functional relevance of these alterations in synaptic activity and efficacy. For this it is necessary to use measures of motor performance.

2.1.7 Changes in functional measures of motor behaviour

TMS can be used to disrupt or enhance motor performance in two modes: an acute disruptive mode (single-pulse or short trains of high-frequency rTMS) or a conditioning mode (prolonged trains of rTMS). Day et al first demonstrated that stimulation of the primary motor system following an auditory cue to move delayed reaction times for wrist flexion by up to 150ms, without affecting the pattern of muscle activity during the subsequent movement (Day et al., 1989).

Acute disruptive effects of premotor TMS have been studied in a series of experiments using simple and choice reaction tasks (Schluter et al., 1998),

revealing an asymmetry in premotor contribution to task performance: TMS to left premotor cortex at short, but not long, cue-stimulus intervals increased reaction times for right and left handed responses in a choice reaction time task; whereas TMS to right premotor cortex only increased reaction times for left handed responses. During simple reaction time tasks, TMS did not affect reaction times. The effects of TMS on motor performance depend on the timing and location of TMS and the type of task being performed. The disruptive effect of TMS may also occur by affecting task related activity a connected area. Meyer and Voss showed that appropriately timed suprathreshold stimuli to the primary motor hand area can delay ballistic hand movements performed with the ipsilateral hand (Meyer and Voss, 2000).

TMS delivered during motor behaviour may fail to show any effect of task performance. The area stimulated may not be uniquely involved in a particular aspect of the task being tested or other areas may compensate for the TMS induced disruption. Alternatively, the stimulated area may be crucial for task performance but stimulation parameters are inadequate to produce a substantial perturbation (e.g. intensity too weak, sub-optimal coil orientation) or the timing of the stimulus is incorrect i.e. the area is stimulated at a time when it is not participating in the task. These factors complicate the interpretation of null results.

Prolonged trains of rTMS can be used to alter motor behaviour by inducing lasting changes in the responsiveness of the stimulated cortex and connected areas. Lasting modulation of motor performance by rTMS conditioning also requires stimulation of an area involved in task performance. However, modulating the excitability of the primary motor cortex, known from imaging and primate experiments to be active across a huge range of motor tasks, has met with limited success in altering task performance. Despite the well documented effects of 1Hz rTMS on the excitability of corticomotor projections (Section 2.1.3-5) no impairment of manual motor control by 1Hz rTMS has been convincingly demonstrated during simple motor tasks e.g. paced fist clench (Pascual-Leone et al., 1998), finger tapping (Wassermann et al., 1996;Chen et al., 1997a), maintenance of tonic contraction (Strens et al., 2002) peak force and acceleration during finger pinch (Muellbacher et al., 2000). 1Hz rTMS to the premotor cortex also fails to impair

finger tapping and generation of freely selected movement sequences (Siebner et al., 2003).

Recent work has revealed effects of rTMS on more demanding motor behaviour. Subthreshold 1Hz rTMS to M1 decreased finger tapping rates when subjects were asked to tap as fast as possible with their right (dominant) hand and in tapping rates for both hands when tapping at subjects' fastest comfortable pace (Jancke et al., 2003). Subthreshold 1Hz rTMS to left motor and premotor cortices increased reaction times in a 'masked prime' task (Schlaghecken et al., 2003). In both studies, the authors infer that the tasks used were harder than those reported in previous work; leading to deficits in motor performance. This suggests that the motor system may be able to compensate, to some extent, for changes in cortical excitability during simple tasks, but not during more demanding behaviour. This concept of compensatory changes in response to alterations in motor excitability in discussed in more detail in Chapter 7.

Suprathreshold 1Hz rTMS impairs early consolidation of motor learning using a simple ballistic movement task (Muellbacher et al., 2002;Baraduc et al., 2004). An additional motor learning experiment showed that the same rTMS protocol did not disrupt learning of a dynamic force field (Baraduc et al., 2004). These to studies serve to emphasise that the effects of rTMS conditioning on motor behaviour can be extremely task specific.

1Hz rTMS appears to have opposite effects on the excitability of the stimulated and non-stimulated primary motor cortex which leads to differences in the effect on motor performance, specifically, an improvement in performance of a sequential key-pressing task with the hand ipsilateral to the stimulated hemisphere, and no change in performance with the hand contralateral to the site of stimulation (Kobayashi et al., 2004). The authors postulate that this may be due to a 'release' from the transcallosal inhibition imposed by the stimulated hemisphere. Differential effects of ipsilateral and contralateral TMS pulses can also be seen during motor learning (Butefisch et al., 2004). Subjects were required to make repetitive thumb movements in the opposite direction to movements induced by TMS. Single pulses of subthreshold TMS were delivered to the primary motor cortex contralateral or ipsilateral to the moving hand during training. TMS pulses delivered contralateral to the moving hand, synchronously with the movements significantly enhanced the

motor memory developed by the training period whereas TMS pulses delivered to the primary motor cortex ipsilateral to the moving hand lead to a failure to encode the motor memory seen with training alone. The authors suggest that synchronous TMS pulses delivered to contralateral M1 may enhance training by enhancing Hebbian plasticity; whereas TMS delivered to the ipsilateral M1 may enhance interhemispheric inhibition, thus decreasing the potential for training induced plasticity.

Chapter 5 examines differences in local and transcallosal effects of 1Hz rTMS on movement-related activity.

2.1.8 Safety of 1Hz rTMS

Single pulse TMS techniques have an excellent safety record in healthy subjects. The major safety concern when using rTMS is the possibility of inducing seizures. Several cases of rTMS induced seizures have been reported, and these have lead to the establishment of conservative stimulation guidelines (Wassermann, 1998). An important part of the safety procedures when using rTMS is careful screening of subjects to exclude those with a history of head injury, neurosurgery, neuropsychiatric disorders, use of medications that lower seizure thresholds and a personal or family history of epilepsy. The use of 1Hz rTMS at threshold or subthreshold intensities has not been associated with seizures in healthy adults. The stimulation protocols used in studies reported in this thesis all fall within the guidelines published by Wassermann (Wassermann, 1998).

A number of studies have specifically investigated the effects of 1Hz rTMS. Wassermann et al. reported no effects of suprathreshold 1Hz rTMS on immediate and delayed memory, verbal fluency, prolactin levels or standard 16 channel EEG recordings (Wassermann et al., 1996). Mottaghy et al. 2003 compared diffusion weighted MR images before and after subthreshold 1Hz rTMS (Mottaghy et al., 2003). They report a small decrease in diffusion coefficient at the site of stimulation that normalised within five minutes. The authors suggest that this finding is suggestive of a temporary impairment in the sodium-potassium pump function. Liebetanz et al. 2003 delivered suprathreshold 1Hz rTMS to rats for five days (Liebetanz et al., 2003). In vivo magnetic resonance spectroscopy and post-mortem histology failed to detect any changes in cerebral metabolites and no abnormal

histological findings were reported. The authors stress that this does not exclude the possibility of acute changes, but their findings offer further support for the safety of 1Hz rTMS.

2.2 Functional Neuroimaging

This section is divided into four sub-sections: the neurovascular origins of functional imaging data, principles of PET, principles of fMRI and data analysis techniques.

2.2.1 Neurovascular coupling and neuroimaging signals

Haemodynamic functional neuroimaging methods such as PET and fMRI provide indirect measures of neuronal activity. They are predicated on the coupling between increased synaptic activity and increased oxygen and glucose consumption; and subsequent increases in cerebral blood flow (CBF) (Raichle, 1998). Although a relationship between neuronal activity, metabolic rate and blood flow undoubtedly exists, the specific details are far from established. Neuronal activity is metabolically demanding. Increases in neuronal activity cause an increase in oxygen and glucose consumption (Hyder et al., 1997) which can be measured in humans with PET using a variety of isotopes (Frackowiak et al., 1980a;Frackowiak et al., 1980b;Fox et al., 1988). This increase in metabolic activity appears to be mediated at least in part by a transient increase in glycolysis triggered by glutamate transport into astrocytes during synaptic activity (Magistretti and Pellerin, 1999;Bonvento et al., 2002). The subsequent increase in blood flow may be triggered by a variety of mechanisms including changes in pH (Kuschinsky and Wahl, 1978), astrocyte function (Bonvento et al., 2002) and nitric oxide release (Dirnagl et al., 1993).

Neuronal activity refers to afferent inputs (pre- and postsynaptic processing) and efferent outputs (spike rate). Over the past few years an increasing number of studies have provided evidence that changes in pre and postsynaptic processing, but not spike rate, contribute to activity-dependent increases in CBF. Evidence from studies using rat cerebellar cortex suggest that increases and decreases in CBF are not proportional to changes in spike activity (see Lauritzen and Gold (Lauritzen and Gold, 2003) for review). Logothetis et al (2001) used simultaneous recordings of spike activity, local field potentials and BOLD signals to show that BOLD signal amplitude correlated better with non-spiking activity (Logothetis et al., 2001). Further work suggests that at very low and high rates of synaptic activity there is a

plateau in the otherwise linear relationship between synaptic activity and CBF (Mathiesen et al., 1998;Norup-Nielsen A. and Lauritzen, 2001).

The mechanism by which 1Hz rTMS which reduces cortical responsiveness or excitability is unclear and may involve reduced efficacy of excitatory inputs or increased activity of inhibitory interneurons. It is therefore important to consider the relationship between CBF and inhibitory activity before examining the effects of 1Hz rTMS on CBF with functional neuroimaging techniques. Activity at inhibitory synapses is metabolically demanding (Ackermann et al., 1984;Nudo and Masterton, 1986). Studies using rat cerebellum have demonstrated that increases in both inhibitory and excitatory synaptic activity lead to increases in CBF. When inhibitory and excitatory pathways were stimulated simultaneously greater increases in CBF were observed than during stimulation of either pathway alone (Caesar et al., 2003). These findings suggest that active synaptic inhibition (increased activity of inhibitory interneurons) results in increased CBF. Decreased excitability of a brain region may also represent deactivation: reduced intrinsic activity or loss of excitatory input from connecting areas. Gold and Lauritzen (2002) have demonstrated that baseline CBF levels are relatively insensitive to decreases in synaptic activity especially when compared to the robust increases in CBF seen with increased excitatory activity (Gold and Lauritzen, 2002). The implication of this finding is that detecting decreases in synaptic activity via decreases in rCBF may be problematic.

2.2.2 Principles of PET

Positron emission tomography uses a variety of radioactively labelled biological probes (e.g. $H_2{}^{15}O$, ^{18}F-FDG, ^{18}F-Dopa) to detect changes in physiological (e.g. blood flow), metabolic (e.g. glucose metabolism) or neurotransmitter processes (e.g. dopamine receptors). The PET studies reported in this thesis use radiolabelled water ($H_2{}^{15}O$) to detect changes in regional cerebral blood flow (rCBF) as an index of synaptic activity. This tracer has a relatively short half-life (approximately 2 min); therefore the isotope was produced in a cyclotron close to the PET scanner and introduced into the human body by intravenous injection. ^{15}O disintegration results in a pair of 511 KeV annihilation photons, which can be detected simultaneously by paired photomultipliers arranged around the subject's head. Detection of two

coincident photons defines a line, which intersects the position of the annihilation event. The intensity of emission indicates the focal concentration of the isotope at any particular position in the head. Data can be reconstructed using correction techniques to obtain a count density that reflects the concentration of the positron emission probe in the tissue. The cumulative signal from each brain region is proportional to the weighted mean blood flow during the scan. These data were acquired over 60 s in order to maximise sensitivity and optimise sampling of radiotracer decay. Because the signal in the resulting PET images is proportional to the integrated synaptic activity over the entire 60s, PET data have a low temporal resolution.

2.2.3 Principles of fMRI

Structural and functional MRI depends on 'spin', a property of atomic nuclei with unpaired protons and neutrons. The nuclei of hydrogen atoms in water have spin, and this is the source of the signal measured in MRI. When placed in an external magnetic field (B_0), nuclei align with (parallel) or against (anti-parallel) the direction of the field. This alignment is not perfect and the axis of the spin will precess around the direction of the magnetic field at a frequency determined by the strength of the magnetic field and the gyromagnetic constant for a particular atomic nucleus ('Larmor frequency'). The alignment of spins anti-parallel to the magnetic field represents a higher energy state than the alignment of spins parallel to the magnetic field; therefore slightly more spins will align parallel with the field, resulting in a small net magnetisation along the direction of the applied field. The net magnetisation can be changed by transferring energy to the protons by applying a radio-frequency (RF) pulse ('excitation'). Excitation of a particular type of nuclei occurs most efficiently when the radio-frequency pulse is delivered at the Larmor frequency. The applied RF pulse generates a weak magnetic field (B_1), around which the net magnetisation now precesses.

After excitation, the spins will return to the low energy state ('relaxation') by emission of radiofrequency energy; this is the signal detected in MRI. Relaxation involves two separate processes: loss of magnetisation in the direction of the B1 field, and increased magnetisation in the direction of the B0 field. These two

processes occur at the same time but with different time constants: termed T1 and T2 respectively. The efficiency with which spin relaxation occurs depends on the interaction between the spins and the surrounding tissues. The T1 and T2 constants describing the relaxation are therefore tissue-specific. Differences in proton density and relaxation rates enable identification of different tissue types: grey matter, white matter, cerebrospinal fluid and blood oxygen level dependent (BOLD) signal in functional MRI.

Deoxygenated haemoglobin is paramagnetic and therefore causes local inhomogeneities in the magnetic field. This reduces the T2*-weighted MRI signal (Ogawa et al., 1990;Turner et al., 1991). Changes in the blood oxygenation level (i.e. the concentration of oxygenated and deoxygenated haemoglobin) lead to changes in the homogeneity of the magnetic field and therefore cause changes in theT2*-weighted or blood oxygen level dependent (BOLD) signal. As described in Section 2.2.1, increased metabolic activity is followed by local increases in blood flow, at about three times the rate necessary to compensate for the increased oxygen utilisation (Fox et al., 1988). This results in a fall in deoxygenated haemoglobin concentration in the capillaries and venules near to the site of increased synaptic activity. Because neural activity is metabolically demanding, changes in the BOLD signal can be used to detect changes in local neuronal activity.

The BOLD response to a transient change in metabolic activity is not instantaneous. Starting 1-2 seconds after the increased metabolic activity, it takes 5-6 seconds to reach a peak and a further 15-30 seconds to return to baseline (Fransson et al., 1998a;Fransson et al., 1998b). The temporal resolution of BOLD fMRI is considerably finer than that of PET, but it is still not on a ‘neuronal’ timescale. The magnitudes of BOLD signal changes seen in fMRI are relatively small and depend on the field strength of the scanner. The spatial resolution of fMRI is determined by the high signal to noise ratio required for reliable signal detection. This can be achieved by balancing the decrease in electronic noise obtained with larger voxel sizes with the reduced physiological signal found at coarser spatial resolutions. In the fMRI experiment presented in Chapter 6 a resolution of 3x3x3mm was used.

2.2.4 Analysis of Functional Neuroimaging Data

All image analysis was performed using Statistical Parametric Mapping software, SPM (Wellcome Department of Imaging Neuroscience, UCL, UK. http://www.fil.ion.ucl.ac.uk/spm). The PET experiments in Chapters 3 and 5 were analysed using SPM99, and the fMRI experiment in Chapter 6 was analysed using SPM2.

2.2.4.1 Preprocessing

The analysis of functional imaging data is based on the assumption that the data acquired from a particular voxel over the course of an experiment are derived from the same anatomical location. In order to ensure that this assumption is not violated the initial step in the data analysis process involves realigning the data to remove the effects of subject movement. Following realignment the data are normalised: transformed into standardised anatomical space and spatially smoothed. Data from individual subjects were pre-processed independently.

Realignment of PET and fMRI data involved estimating six parameters describing a rigid-body affine transformation that minimised the sum-of-squared differences between successive scans. These transformations (estimated relative to the first scan of the time-series) were then applied to the entire data-set, following which the images were re-sampled using spline interpolation (Friston et al., 1995a).

Unwarping: Realignment does not remove all variance within the data caused by movement e.g. EPI data are very susceptible to distortions which result in movement-by-susceptibility interactions which cannot be removed by realignment. Movement parameters can be included as nuisance variables in the statistical model for fMRI data. However, this may be problematic for motor paradigms, as experimental variance can be explained away. To deal with this residual variance, an unwarping procedure (implemented in SPM2) was applied to the fMRI data whereby the rate of change of deformation in the EPI images was estimated. These derivative fields were then applied to the data to remove susceptibility-by-movement interactions (Andersson et al., 2001).

Normalisation: Functional images were normalised to a standardised anatomic space (Talairach and Tournoux, 1988), by matching to a standardised PET or EPI template using linear (twelve parameter affine transformation) and non-linear (discrete cosine basis function) spatial deformations (Friston et al., 1995a). A Bayesian estimation scheme was used to maximise the probability of obtaining the parameters describing the deformations given the data, by maximising the likelihood of the data given the current estimate of the deformations and the prior probability of the deformations.

Coregistration: Structural MR Images from individual subjects were coregistered to the mean functional image using the same procedure as realignment, and normalised to standard anatomical space.

Smoothing: Each image was smoothed with an isotropic Gaussian kernel of 12 mm full-width at half-maximum for PET data and 6mm for fMRI data. This accommodates inter-subject differences in anatomy that remain after normalisation, renders errors in the data more normal (this ensures the validity of inferences based on parametric statistics) and enables the application of Gaussian Field corrections during inference.

2.2.4.2 Anatomical localisation

The anatomic locations presented in this thesis have been identified in two ways. All images are normalised to a standardised anatomic space (Talairach and Tournoux, 1988), using the Montreal Neurological Institute (MNI) template. For brain areas where a probabilistic cytoarchitectonic atlas has been published the probability of the co-ordinates under investigation being in a particular area in more than 3/10 subjects has been used to define the extent of a region (Geyer et al., 1996;Geyer et al., 1999;Geyer et al., 2000b;Grefkes et al., 2001). For those areas where such probabilistic data are not available, the coordinates were displayed on single subject or canonical structural images, and the sulcal and gyral anatomy was identified with the aid of an atlas (Duvernoy, 1999;Schmahmann et al., 2000). Functional locations were then assigned based on the macroscopic anatomic descriptions given in Chapter 1.

2.2.4.3 Statistical analysis of imaging data

The organisation of the brain follows two principles: functional specialisation and functional integration. Functional specialisation implies that anatomically distinct cortical (and sub-cortical) areas are specialised to perform certain aspects of perceptual, cognitive or motor processing. Given a high degree of functional specialisation, no cortical area can perform a meaningful function in isolation. In order to support even a simple perceptual or motor function it is necessary for these anatomically distinct functionally specialised areas to unite, via extrinsic connections between cortical areas. Functional integration describes the pattern of connections established between cortical areas that are unique to a particular function.

Traditionally, the high spatial resolution available with functional neuroimaging data has lent itself to analyses of functional specialisation. However, it is evident from the description above that analyses of neural activity based solely on this principle will provide a limited account of the neuronal substrate of the process under investigation. Therefore, alternative approaches have been developed to investigate task dependent changes in the integration of functionally specific areas. The approaches used in this thesis are described in Section 2.3.2

2.2.4.3.1 Functional Specialisation

The initial analyses of PET and fMRI data described in this thesis used statistical parametric mapping to test hypothesis about regionally specific effects.

Observed neurophysiological responses at each volume element (voxel) in the brain are partitioned into effects of interest, confounds and error. Statistical inferences are made about the size of the effects of interest in relation to the error variance or the other effects using F and T statistics respectively. Because each experiment contains more than one condition of interest, the analysis is performed as a multiple linear regression which is a special case of the General Linear Model (GLM) (Friston et al., 1995b):

$$y = X\beta + e$$

The observed response variable (voxel-specific rCBF or BOLD responses) y is modelled in terms of a linear combination of explanatory variables in the design matrix X plus an independently and identically distributed Gaussian error term e.

The design matrix includes all known variables that may explain the evoked neural responses. Each column of the design matrix (regressor) corresponds to effects of interest (manipulations designed within the experiment) or effects of no interest that may confound the results. The form of the design matrix is predicated on the following assumption: experimental manipulations cause regionally specific neuronal responses. These neuronal responses lead to changes in rCBF which can be detected with PET. Changes in rCBF lead to changes in the BOLD signal which are detected with fMRI. For the PET experiments described in Chapters 3 and 5 the design matrices contained regressors representing the type of activity that subjects performed during the scans, plus an additional regressor representing the mean blood flow per subject. Any changes in rCBF from scan to scan represent the integral of changes in neuronal activity occurring over the 60s during which data were acquired. For the fMRI experiment described in Chapter 6 condition-specific stimulus functions convolved with a haemodynamic response function which is based on the known time course and magnitude of changes in blood volume and deoxyhaemoglobin concentration that determine the BOLD signal (Buxton et al., 1998). fMRI data were also high-pass filtered to remove low-frequency confounds such as scanner drift and aliased biorhythms.

Parameter Estimation: The relative contribution of each column of the design matrix is estimated using ordinary least squares (SPM99). In SPM2 a decorrelation or 'whitening' of the error terms is applied which renders the estimation a maximum likelihood estimation (SPM2). Inferences about the parameter estimates are made using their estimated variance. It is possible to test the null hypothesis that all the parameter estimates are zero using the F statistic to give a SPM {F} map or that a particular linear combination or a "contrast" of the estimates is zero using the T statistic to generate a SPM {T} map.

A mass-univariate approach is used whereby standard univariate statistical tests are applied to each voxel. The results are interpreted as spatially extended process by referring to Gaussian random field theory, a methodological approach that models the probabilistic characteristics of continuous, spatially extended statistical fields (Worsley et al., 1992;Worsley et al., 1996). 'Unlikely' excursions from the GRF for a particular data-set can be interpreted as regionally specific effects within the

data. GRF theory can be used to make corrections for multiple comparisons that depend on the search volume and the smoothness of the normalised residual fields. The GRF correction is based on two main assumptions: (1) The error fields are a reasonable lattice approximation to an underlying random field with a multivariate Gaussian distribution and (2) they are continuous with a differentiable and invertible autocorrelation function. These assumptions can be violated if the data are not sufficiently smooth or the errors are not normally distributed.

The adjustment of p values based on GRF theory depends critically on the class of inference made using SPMs. In the case that no prior anatomical hypothesis exists about the regional specificity of an experimental effect, it is necessary to correct for multiple comparisons across the entire brain. In some cases a more constrained anatomical hypothesis may exist, in which case it is possible to restrict the correction for multiple comparisons to either a single voxel (in which case an uncorrected p-value can be used) or a restricted volume of interest. Unless stated otherwise, activations in this thesis are reported when surviving a threshold of $p<0.05$ corrected for the entire brain or the search volume of interest based on a priori hypotheses.

2.2.4.3.2 Functional Integration

Functional integration describes the pattern of connections established between cortical areas that are unique to a particular function, and this relies on the presence of anatomical connections between distinct functionally specialised areas. Connectivity between cortical areas can be described in a number of ways. Anatomical connectivity is a description of the physical structures connecting two cells or brain regions. Functional and effective connectivity are descriptions of the relationships between patterns of neural activity therefore they involve measurements of neural function. Drawing from the literature describing multiunit microelectrode recording of separable spike trains (Gerstein and Perkel, 1969;Aertsen and Preissl, 1991) *functional connectivity* is defined as the “temporal correlations between spatially remote neurophysiological events” (Friston et al., 1993b), whereas *effective connectivity* is defined as “the influence that one neural system exerts over another either directly or indirectly” (Friston et al., 1993a).

Within the context of functional neuroimaging these definitions of functional and effective connectivity emphasise the difference between descriptions of patterns of neural activity and possible explanations of their origins. Functional connectivity reduces to testing the Null Hypothesis that activities in two regions share no mutual information. In other words, the characterisation of brain activity in terms of functional connectivity is “model free”. In contrast, characterising brain activity in terms of effective connectivity requires a causal or acausal model, in which regions and connections of interest are specified by the researcher, often constrained by a combination of neuroanatomical, neuropsychological and functional neuroimaging data. This is a crucial point when considering the distinction between functional and effective connectivity because it emphasises the shift from a description of what the brain does to a theory of how it does it.

2.2.4.3.2.1 Analyses of Effective Connectivity

In this thesis, effective connectivity amongst brain regions was investigated using psycho-physiological interactions (PPI) and dynamic causal modelling (DCM).

Psycho-physiological Interactions (PPIs) (Friston et al., 1997) aim to explain responses in one cortical area in terms of an interaction between activity in another cortical area (index area) and the influence of an experimental parameter. The analysis is constructed to test for differences in the regression slope of the activity in the index area on the activity in all remaining areas under the different experimental conditions. As these regression slopes are a metric of the coupling between areas, the PPI identifies areas where the degree of coupling with the index region is modulated significantly by the experimental variable. The presence of a significant change in coupling between the index region and other brain areas can be interpreted in two distinct ways: either as a change in the influence of the index area on other brain regions, or as a change in the responsiveness of the index area to inputs from other brain regions (Figure 2.1). A significant PPI cannot be used to disambiguate these interpretations post-hoc. A PPI is used to test an a priori hypothesis about decreased responsiveness or increased influence of the index region. In Chapters 3 and 5 separate PPIs were used to test a priori hypotheses

about the differential effects of 1Hz rTMS on cortical excitability at the site of stimulation, and on the connectivity on the motor areas engaged in the different finger tapping tasks performed during PET scanning.

Figure 2.1

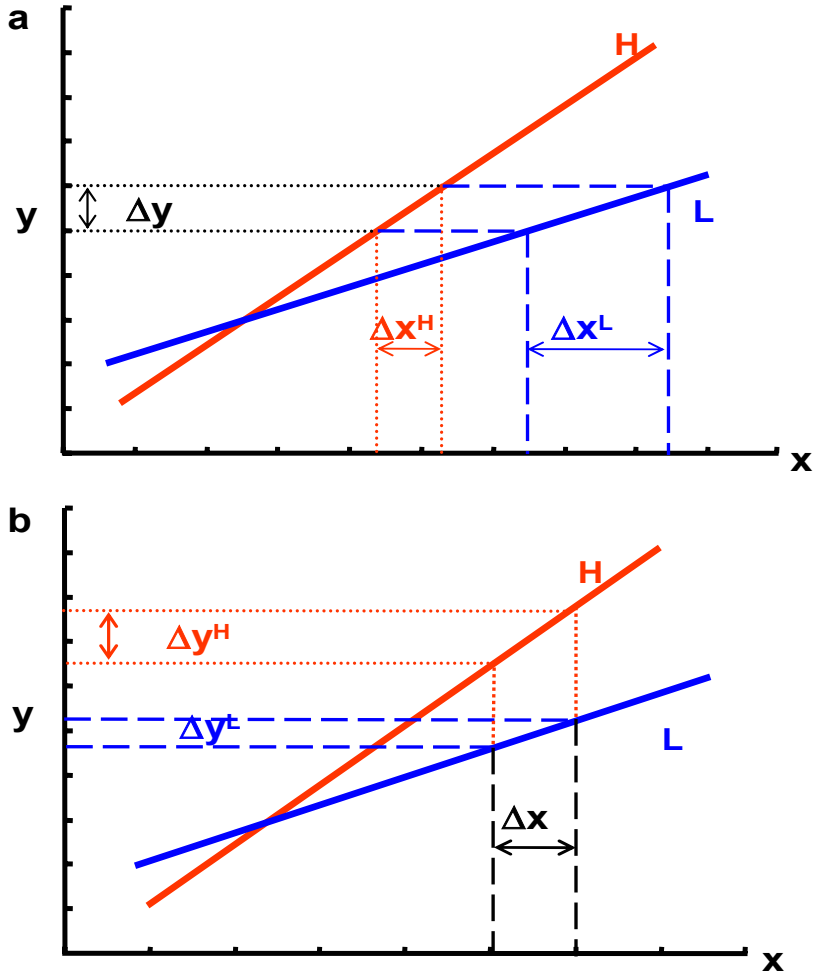

Figure 2.1: Interpretation of PPI analyses. This scheme shows that two mathematically equivalent but biologically complementary hypotheses can be used to motivate the same PPI. In both graphs, *x* represents activity in an index area subtending the physiological variance in the PPI analysis. Conditions H and L represent some psychological or experimental manipulation. In *a* during H, a unit increase in activity in area *y* (Δy) is associated with a small increase in activity in area *x*: Δx^H (dotted red line). During L, Δy is associated with a larger increase in activity in area *x*: Δx^L (dashed blue line). Consequently, this is the change that one would predict if area *a* was thought to be less responsive to activity in area Δy during H. In *b* during H, a unit increase in activity in area *a* (Δx) is associated with a large increase in activity in area *y*: Δy^H (dotted red line). During L, Δx is associated with a smaller change in activity in area *y*: Δy^L (dashed blue line). In short, exactly the same PPI would be predicated if area *y* was thought to be more responsive to Δx during H.

Dynamic Causal Modelling (DCM) is a method of estimating and making inferences about the coupling or efficacy of connections between small numbers of brain areas and how that coupling is influenced by experimental manipulations

(Friston et al., 2003). DCM treats the brain as a dynamic, deterministic input-state-output system where the inputs are conventional stimulus functions describing experimental manipulations, the state variables include parameters describing the regional neuronal activity and the biophysical parameters specifying the haemodynamic response in each region, given the neuronal activity. The outputs are the measured regional BOLD signal. DCM is a causal model because the neurodynamics of any given region are deterministic: changes in neuronal activity in a region 'a' can only be caused by i) direct inputs to that area (if specified), ii) intrinsic activity in the area (via self-connections) and iii) activity in other connected regions. All these connections can be modulated by experimental variables. Unlike PPI analyses, where it is only necessary to specify one seed voxel or index area, in DCM it is necessary to specify the regions that comprise a network of areas. One can also specify how these regions are connected, and where the experimental inputs exert their influence.

DCM relies on the specification of a simple but realistic neuronal model of interacting regions, plus a haemodynamic model of BOLD signal given regional neuronal activity. The neuronal states can be described by equation (1)

$$\dot{z} = F(z, u, \theta) \tag{1}$$

F is a nonlinear function describing the influences among activity in the brain regions included in the model (z), the experimental inputs (u) and the parameters of the model (θ). A bilinear approximation of this equation provides a reparameterisation in terms of the activity in the regions, the connections and the influence of experimental inputs:

$$\begin{aligned} \dot{z} &\approx Az + \Sigma u_j B^j z + Cu \\ &= (A + \Sigma u_j B^j) z + Cu \end{aligned} \tag{2}$$

The matrix A represents the first-order connectivity between the regions (*z*) in the absence of inputs. Constraints on these connections can embed knowledge of anatomical connections, to create a plausible network. The matrix C specifies the direct influence of extrinsic inputs (*u*) on regions (termed sensory or modulatory inputs). The matrix B specifies the changes in intrinsic connections (self connections

or connections between regions) induced by the jth input (u). The parameters of the neuronal state equation are therefore the coupling matrices A, B^j and C. Priors on the coupling parameters ensure that the system remains dissipative and that neuronal activity does not increase exponentially.

The haemodynamic model comprises state variables describing the translation of regional neuronal activity into regional haemodynamic responses. These include a vasodilatory signal (s), normalised flow (f), normalised venous volume (v) and normalised deoxyhaemoglobin content (q) (Friston et al., 2000;Mechelli et al., 2001). Empirically determined priors for the biophysical parameters are based on previous data (Friston et al., 2000).

Combining the neuronal and biophysical states gives a full forward model, whose parameters are estimated using a fully Bayesian approach to derive maximum a posteriori (MAP) estimates. These include the parameters describing the neuronal coupling. The units of these connection parameters are per unit time; a strong connection corresponds to an influence that is expressed quickly with a small time constant.

Chapter 3

Effects of 1Hz rTMS on synaptic activity during right hand movement

3.1 Introduction

Aims of Experiment 1:

1) Establish the use of functional imaging in examining the effects of 1Hz rTMS.
2) Establish the use of functional imaging to investigate changes in movement related activity following 1Hz rTMS.
3) Explore the contribution of analyses of effective connectivity in understanding the effects of rTMS.

The effects of 1Hz rTMS on the excitability of the motor cortex are reviewed in detail in Chapter 2. Previous functional imaging experiments using PET (Fox et al., 1997;Siebner et al., 2001) and fMRI (Bohning et al., 2000) have investigated local and remote effects of 1Hz rTMS on cortical activity. This first experiment extends previous work by using functional imaging and analyses of effective connectivity to investigate the neural correlates of three rTMS related effects on motor cortex activity. First, changes in neural activity at the site of stimulation and at remote cortical and subcortical sites associated with thirty minutes subthreshold stimulation; second, reduced responsiveness of the stimulated site to input from other cortical areas and third, the ability of the motor system to compensate for rTMS induced alterations in cortical excitability.

3.2 Materials and Methods

3.2.1 Subjects

Eight healthy, right-handed volunteers (one female) aged between 20 and 68 (mean age: 37), with no history of neurological disorder or head injury, were recruited from the database of volunteers at the Functional Imaging Laboratory, Institute of Neurology, University College London, UK. Written informed consent was obtained from all participants. The study was approved by the joint ethics committee for the National Hospital for Neurology and Neurosurgery and the Institute of Neurology. The administration of radioactivity was covered under the Motor Studies Licence from the Administration of Radioactive Substances Advisory Committee held at the Functional Imaging Laboratory (RPC528-890 (14364)).

3.2.2 Study design

The study had a 2x2 factorial design, with two levels per factor: "intervention" (real versus sham rTMS) and "task" (movement versus baseline). Figure 3.1 illustrates the study design. Real and sham-rTMS were given on two separate days, at least one week apart. The order of intervention was counterbalanced across subjects. The effects of rTMS were assessed by consecutive PET measurements of regional cerebral blood flow (rCBF) during the first hour after rTMS. Within each scanning session the baseline and movement tasks were alternated. The order of tasks was kept constant within a subject between sessions, but counterbalanced across subjects.

Figure 3.1

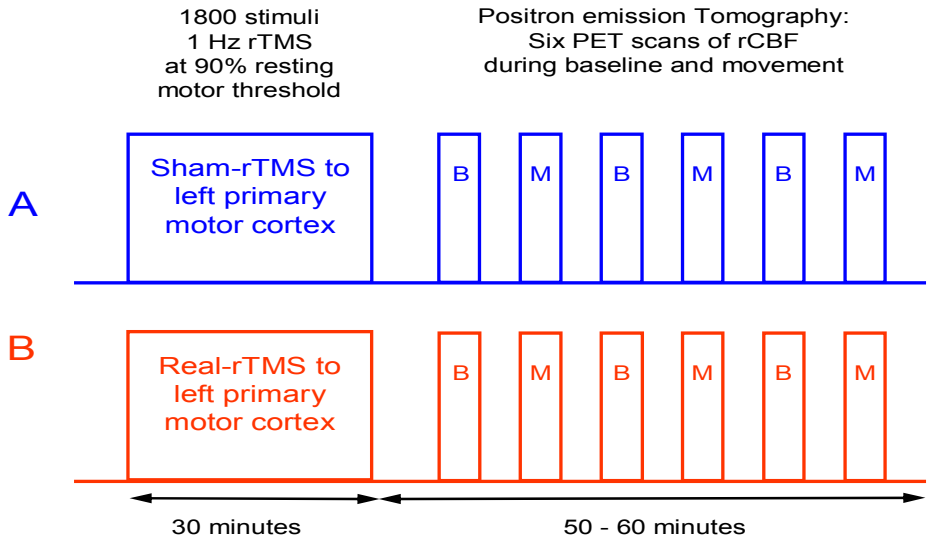

Figure 3.1: Experimental design.
Subjects received 1Hz real or sham rTMS on separate days. Changes in regional cerebral blood flow were mapped using positron emission tomography (PET). Six sequential H215O-PET scans were acquired at baseline (B) or during the freely selected movement task (M) in an alternating order during an hour after the end of rTMS. The order of intervention (real v sham rTMS) and experimental conditions were counterbalanced across subjects.

3.2.3 Repetitive transcranial magnetic stimulation (rTMS)

In each rTMS session, 1800 biphasic stimuli were given over left primary motor hand area using a MagStim-rapid stimulator connected to four booster modules (MagStim Company, Whitland, Wales, UK; www.magstim.com). All subjects received two 15-minutes trains of 1Hz rTMS separated by an inter-train interval of one minute. Stimulation intensity was set to 90% of resting motor threshold (RMT) of the right first dorsal interosseus (FDI) muscle. A standard figure-of-eight shaped coil (Double 70mm - Coil Type P/N 9925, MagStim Company, Whitland, Wales, UK) was used for real rTMS. For sham rTMS a specially designed sham coil that induced no magnetic field but provided a comparable acoustic stimulus was used (MagStim Company, Whitland, Wales, UK). The coil was positioned with the handle at 45^{o} to the sagittal plane. The current flow of the initial rising phase of the biphasic

pulse in the TMS coil induced a current flowing from posterior-to-anterior in the underlying motor cortex.

The site of rTMS stimulation was located at the "motor hot spot", defined functionally as the point of maximum evoked motor response in the relaxed right FDI muscle. The resting motor threshold was defined as the lowest stimulus intensity that elicited at least five twitches in ten consecutive stimuli given over the “motor hot spot”. The FDI muscle was used to define the motor threshold because TMS-evoked twitches are clearly visible and it has a threshold similar to other intrinsic hand muscles. This ensured that the intensity used for rTMS was below motor threshold for all the hand muscles. The use of sub-threshold intensity (i) avoided muscle twitches during rTMS that could modulate central processing via sensory afferents and (ii) reduced the spread of the stimulation away from the targeted site. An intensity of 90% RMT was used because this is above the threshold for activating corticospinal output projections. The latter is usually assessed by measuring active motor threshold (the intensity needed to produce EMG activation in pre-contracting muscles), and is equivalent to approximately 80% RMT. Thus it is certain that the rTMS pulses would produce synaptic activation in at least some of the anatomical targets of M1.

3.2.4 Motor Task

Subjects underwent six sequential $H_2{}^{15}O$-PET scans on each of the two separate days. All scans were acquired during the first hour after 30 minutes of 1Hz rTMS to the motor cortex. Normalized rCBF-dependent uptake (referred to hereafter as rCBF) was used as an index of regional synaptic activity during two experimental conditions: baseline (referred to as condition "B") and random selection of finger movements (referred to as condition "M"). Three PET scans were acquired for each of the experimental conditions in an alternating order (B-M-B-M-B-M or M-B-M-B-M-B). Subjects were required to fixate a cross on the centre of a screen located 0.7m in front of their face. A pacing tone sounded every 2 seconds during both conditions. During the movement task, subjects were required to freely select and execute brisk flexion movements with the index, middle, ring or little finger of their right hand. They were asked to make a fresh choice on each trial, regardless of

previous moves, so as to produce a random sequence. The instructions emphasised that each choice should be independent of previous choices. Subjects were told to actively prepare the forthcoming movement and execute the movement as soon as they heard the pacing tone. To ensure a stable level of task performance, the random selection task started about 20 seconds prior to the onset of the PET scan and lasted for the entire 90-second period of data acquisition. During the baseline condition, subjects were instructed to watch the fixation point and listen to the tones.

Subjects' responses were made on four buttons, set under their fingertips on a moulded wrist splint. All responses were recorded by computer (Apple Macintosh 7300) using COGENT Cognitive Interface Software (Wellcome Dept. of Imaging Neuroscience, London, UK). The data were subsequently analysed using Matlab 6.0 (Mathworks, Sherborn, MA) and SPSS 8.0 (SPSS Inc., Chicago, Illinois, USA).

3.2.5 Behavioural assessment

In addition to the random selection task during scanning, subjects performed two finger-tapping tasks with their right hand after the first, third, and fifth PET scan. In the 'simple tapping task' subjects tapped their right index finger as many times as possible during a ten second interval. In the 'sequential tapping task' subjects were asked to repeat an ascending sequence (index, middle, ring, little finger) as quickly as possible for ten seconds. To familiarise subjects with the task and to reduce learning effects during sequential PET scans, subjects performed each of the three tasks twice in the PET scanner prior to rTMS on both scanning sessions

From each task, the mean interval between responses and the mean duration of button presses were calculated, as indices of motor performance. These values were entered into a paired-samples t-test to look for differences after real rTMS compared to sham rTMS. The free selection movement task during scanning was paced, therefore only the mean duration of button presses was considered as a kinematic variable of interest. Simpson's equitability index (Simpson, 1949) was calculated for sequential response pairs and taken as a measure of the randomness of the sequence. This index varies between 0 and 1. A value of 1 indicates that, over a series of responses, any given response was equally likely to be followed by

any other response. Data from the three repetitions of this task, during each scan, were analysed to provide two values of randomness for each subject: one after sham rTMS and one after real rTMS. These values were entered into a paired-samples t-test to look for rTMS related differences. Significance was set at $P < 0.05$.

3.2.6 PET data acquisition

PET was performed using a CTI ECAT HR+ scanner (CTI, Knoxville, TN) in three-dimensional mode with inter-detector collimating septa removed. The axial field of view was 155 mm providing whole brain coverage including cerebellum. The subjects lay supine in the scanner. A padded helmet with a chinstrap, fixed to the headrest, reduced head movement. A TV monitor was adjusted to give subjects an unrestricted view of the instructions and fixation point.

Regional cerebral blood flow was assessed using $H_2{}^{15}O$. Six to ten mCi (mean 8.9 mCi) were delivered intravenously over 20s to the left arm. Image acquisition began 5s before the rising phase of the count curve, approximately 25-35s after injection, and continued for 90s. Correction for tissue and helmet attenuation was made using a transmission scan from $^{68}Ga/^{68}Ge$ sources at the start of each scanning session. The interscan interval was approximately 8 minutes. Corrected data were reconstructed by three dimensional filtered back-projection (Hanning filter, cut off frequency 0.5 cycles/pixel) and scatter correction. Sixty-three transverse planes were obtained with 128 x 128 pixel image matrix, with a pixel size of 2.4 x 2.1 x 2.1 mm, and a resolution of about 6 mm at full width half maximum.

Anatomic structural images were acquired prior to rTMS stimulation, with the position of the centre of the eight-shaped TMS coil marked on the skull with a capsule containing cod liver oil. Structural scans were acquired using a VISION MR scanner at 2 Tesla (Siemens, Erlangen, Germany) with a T1 MPRAGE sequence (TE=4ms, TR=9.5s, TI=600ms, resolution 1x1x1.5 mm, 108 axial slices. This structural image also excluded asymptomatic structural brain abnormalities. In all subjects the cod liver oil capsule marking the motor hot spot was clearly visible, located over the central sulcus. Examples of the TMS coil placement scans for one subject can be seen in Figure 3.2.

Figure 3.2

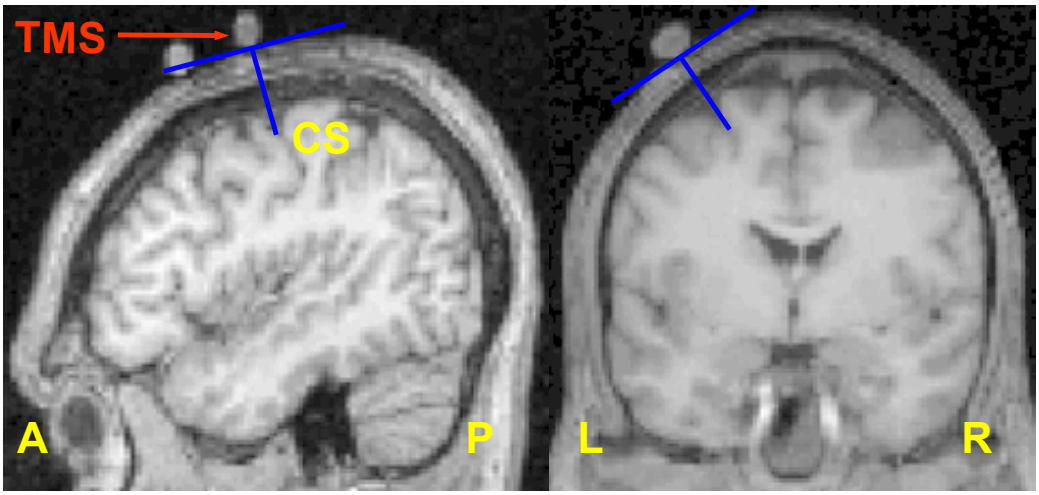

Figure 3.2: Position and orientation of TMS coil relative to the central sulcus (CS) shown in one subject.
N.B. Capsules marking the position of the premotor cortex, visible in the sagittal scans anterior to A, are part of a different experiment.

3.2.7 Image Analysis

Image preprocessing was as described in Chapter 2.

The primary analysis employed a general linear model that included twelve covariates modelling the task (movement selection versus baseline) separately for each consecutive scan pair, first to third, under each condition of treatment (real versus sham rTMS). The effect of global differences in cerebral blood flow among scans was removed by treating global activity as a confound and scaling to a nominal grand mean global activity of 50 ml/100g/min (Friston et al., 1995b). This statistical model enabled characterisation of the main effects of rTMS (real versus sham) and task (movement versus baseline) and for movement-by-rTMS interactions, as well as modelling the effects of time and time by condition by task interactions. For the main effect of movement, the reporting criterion was set at $P < 0.05$, corrected for multiple non-independent comparisons over the whole brain. Results for the main effects of rTMS and rTMS by movement interactions are reported at $P < 0.05$, using a small volume correction (16mm radius sphere centred on the maxima of the main effect of movement, Table 3.2).

Changes in effective connectivity within the motor network were assessed using the 'Psychophysiological Interaction' (PPI) method described in Chapter 2. The first PPI was used to investigate the effect of rTMS on the connectivity between the site of stimulation and other cortical areas i.e. to identify areas whose activity was differently coupled with the rTMS site after stimulation. The index area used as the physiological variable consisted of the first eigenvariate of the rCBF signal from a sphere (radius 8mm) centred on the voxel in primary motor cortex with maximally increased activity after real-rTMS (Table 3.3). The eigenvector was adjusted to remove subject-specific effects. This ensures that the analysis is sensitive to within-subject variation in activity, and the results do not reflect between-subject differences. A covariate of interest (a regressor representing the interaction between physiological activity and experimental condition) was obtained by multiplying the physiological variable by the TMS specific effect. Having included the effects of the physiological component (activity in the index region) and the psychological component (real-rTMS versus sham-rTMS) in the same model, SPM was used to test for the PPI (an example of a design matrix is displayed in Figure 3.6). The resulting SPM [t] reflects the significance of the PPI, where a significant value indicates a difference in the regression slopes linking the activity in the index area to activity in other brain areas, depending on the type of rTMS (real or sham). In order to quantify the effects of rTMS on the motor network identified by the primary analysis, regression slopes were plotted for areas where $P < 0.05$ (corrected for a 16mm radius sphere centred on the maxima of the main effect of movement). In this PPI, a significant increase in the regression slope between two areas represents a reduction in the magnitude of the response of the index area (the site of rTMS) to putative input from another brain area. This is because the slope represents the ratio of changes in the significant area to changes at the rTMS site. Therefore, positive interactions identify regions whose activity during movement is associated with a smaller response at the site of rTMS after stimulation.

The second analysis of effective connectivity was designed to look for changes in the degree of coupling between components of the motor network involved in the movement task after rTMS. Three areas ipsilateral to the site of stimulation where chosen, based on the known anatomical connections with the site of stimulation and

the areas involved in action preparation and execution: left primary sensorimotor hand area, left dorsal premotor cortex and left SMA. Three separate PPI analyses were performed, one for each area. In each case the physiological variable was the first eigenvariate of the rCBF signal from a region of interest (sphere 8-mm radius) identified previously by the main effect of movement. The covariate of interest was constructed and tested using SPM as described above. In these three PPI analyses, a significant increase in the regression slope between two areas (a positive interaction) can be interpreted as an increase in movement-related coupling between the index area and significant sites after real rTMS.

3.3 Results

Subjects did not report any adverse side effects during the course of the study, nor were any motor responses evoked during the 30 minutes of rTMS. Mean resting motor threshold was 62%, ranging from 46% to 72% of maximum output of the MagStim-rapid stimulator.

3.3.1 Behavioural Data

No significant effect of 1Hz rTMS was seen on the rate and duration of finger presses during simple and sequential finger tapping. All eight subjects performed the random movement selection task during scanning without difficulty. Likewise for the simple index tapping performed between scans, there were no difficulties. However, during the sequential tapping task between scans one subject failed to make any presses with their ring or little fingers, and was therefore excluded from the analysis of these data. Table 3.1 shows the averaged group values (mean $\pm$ SD) of the variables used to asses behaviour following 30 minutes of 1Hz rTMS, either in terms of motor performance or free selection of movement. Statistical analysis of these behavioural data excluded any behavioural confound in the neurophysiological analyses in the sense there were no effects of rTMS on any performance index.

For the simple tapping task there was no effect of rTMS on the duration of button presses or on the interval between button presses. For the sequential tapping task there was no effect of rTMS on duration of button presses or on the interval between presses. For freely selected movements, rTMS had no effect on the randomness of responses measured by Simpson's equitability index or on the duration of button presses.

Table 3.1: Behavioural Data

	Post-Sham	Post-TMS	t	P
Index Tapping (n=8)				
Duration(ms)	111.73 (+/-21.296)	119.79 (+/-22.36)	-1.49 df = 7	0.18
Interval (ms)	198.16 (+/-16.19)	199.48 (+/-18.39)	-0.38 df = 7	0.71
Sequential Tapping (n=7)				
Duration (ms)	242.22 (+/-180.98)	244.61 (+/-154.68)	-0.12 df = 6	0.91
Interval (ms)	310.68 (+/-80.53)	324.26 (+/-67.6)	-0.73 df = 6	0.5
Random Selection Task (n=8)				
Duration (ms)	234.89 (+/-50.89)	224.5 (+/-57.87)	0.83 df = 7	0.43
Simpson's Equitability Index	0.77 (+/-0.13)	0.76 (+/-0.13)	0.59 df = 7	0.57

Table 3.1: Mean group data (+/-SD) of kinematic measures (duration of press and interval between presses for the index tapping and sequential tapping tasks, plus duration of press for the free selection task. For the random selection task Simpson's Equitability Index, mean (+/- SD) is a measure of randomness. The equitability index ranges from 0 (non-random) to 1 (fully random)

3.3.2 Imaging Data

A conventional analysis was used to investigate the distributed changes in synaptic activity associated with prolonged sub-motor threshold 1Hz rTMS. Analyses of effective connectivity addressed two distinct issues. First, identification of cortical areas whose influence on the stimulation site was attenuated by rTMS and second, assessment of changes in movement-related coupling within the motor network, after rTMS has been used to alter the excitability of primary motor cortex.

Figure 3.3

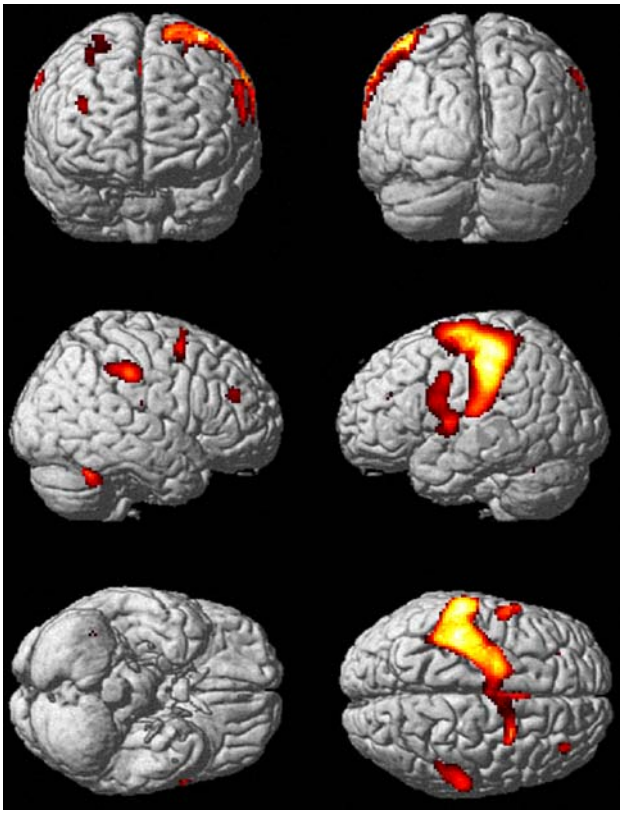

Figure 3.3: Regional Activations during freely selected finger movements (Main effect of movement).
Results are displayed as statistical parametric maps on rendered projections of a single subject structural MR in stereotactic space. The coloured areas indicate all significant voxels showing a movement-related activation at P< 0.05 (corrected for multiple comparisons).

3.3.2.1 Movement-Related Activations (Main effect of task)

The movement task activated a number of motor areas compatible with freely selected right hand movements (Table 3.2, Figure 3.3, reported at P < 0.05 corrected for multiple comparisons). These included the left primary sensorimotor cortex, extending to the left dorsal premotor cortex and left supplementary motor area (SMA). Additional activations were also seen in the right dorsal premotor cortex, right SMA, right rostral motor cingulate cortex and left ventral premotor cortex. There were also bilateral activations in the lateral prefrontal cortex and the cerebellum.

Table 3.2: Main Effect of Movement

Brain Region		MNI Co-ordinates of peak activation			Z-value of peak activation	P value whole volume corrected
		x	y	z		
Sensorimotor	Left	-42	-26	56	> 8	P < 0.001
Primary Sensory	Left	-58	-26	42	7.81	P < 0.001
Premotor (PMd)	Left	-20	-4	64	6.85	P < 0.001
	Left	-26	-14	68	7.12	P < 0.001
	Right	30	4	52	5.25	P = 0.004
Premotor (PMv)	Left	-58	8	24	5.96	P < 0.001
	Left	-56	2	34	6.47	P < 0.001
	Left	-52	-4	6	5.64	P < 0.001
SMA	Left	-10	-2	52	6.09	P < 0.001
	Left	-12	-4	56	5.98	P < 0.001
	Right	8	0	54	5.17	P = 0.005
Cingulate motor (rostral)	Right	10	18	30	4.87	P = 0.002
	Right	2	8	48	6.11	P < 0.001
Cerebellum	Left	-26	-56	-26	5.91	P < 0.001
	Right	24	-52	-26	7.69	P < 0.001
Insula	Left	-44	-2	0	5.55	P = 0.001
	Left	-34	-4	-2	5.64	P < 0.001
SII (Post central sulcus)	Left	-58	-20	16	6.44	P < 0.001
Anterior Inferior Parietal/	Right	60	-24	40	5.71	P < 0.001
Intraparietal Sulcus	Right	50	-30	40	5.19	P = 0.005
	Right	52	-38	40	5.05	P = 0.009
Prefrontal	Left	-28	36	24	4.83	P = 0.024
	Right	36	40	26	5.43	P = 0.001
	Right	26	8	68	5.07	P = 0.008
	Right	22	6	58	5.05	P = 0.009

Table 3.2: Maxima of regional increases in rCBF during movement compared to baseline.

3.3.2.2 Changes in rCBF induced by rTMS (Main effect of rTMS)

Compared to sham, real rTMS caused widespread increases and decreases in rCBF throughout the brain (Table 3.3). There were no significant main effects of time, or time-by-condition interactions, indicating that rTMS induced sustained changes in rCBF for at least one hour.

The left primary motor hand area that was directly targeted by rTMS showed a sustained increase in rCBF after real-rTMS (averaged over move and baseline

conditions) (Figure 3.4). Real rTMS also induced bilateral increases in rCBF in the dorsal premotor cortices (Figure 3.4) and cerebellum. Other motor areas showing lasting increases included left caudal SMA, left basal ganglia and bilateral foci in the inferior parietal lobule. There was also greater activity in the right prefrontal area and bilateral parietal regions.

There were no decreases in rCBF at or near the site of stimulation (Table 3.3b). However, significant decreases in rCBF were seen in the right cingulate motor cortex and the left ventral premotor area. Additional rCBF decreases were located in frontal operculum, superior temporal gyrus, right cerebellum and lateral prefrontal cortices.

3.3.2.3 rTMS-induced changes in task-related activation (Movement-by-rTMS interaction)

Increases in task specific activation (movement versus baseline) after real rTMS (versus sham rTMS) were found in two areas. These were left primary sensorimotor cortex (x = -30, y = –24, z = 48, Z score = 3.6, P = 0.028) and right dorsal premotor cortex (x = 30, y = 4, z = 54, Z score = 3.55, P = 0.033). Figure 3.5 shows the anatomical location of these activations. Real-rTMS caused no task-specific decreases in activation.

Figure 3.4

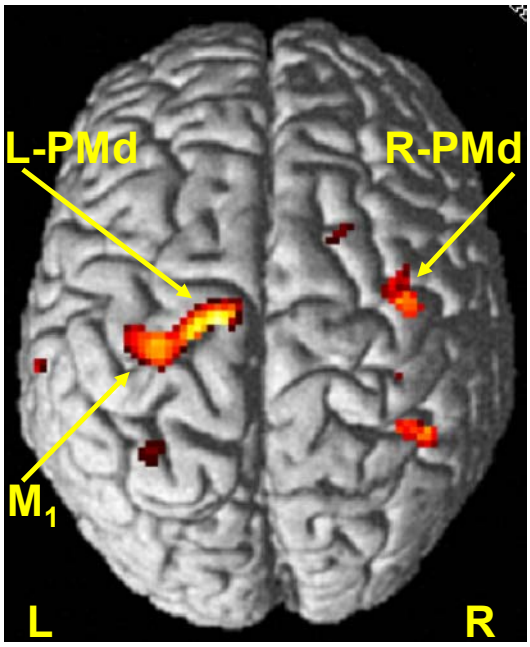

Figure 3.4: Regional increases in rCBF after rTMS to the Left Motor Cortex (Main effect of rTMS)
Left primary motor and bilateral increases in rCBF displayed on a rendered projection of a single subject anatomical MRI scan. Results are displayed at P < 0.001 uncorrected, masked by main effect of movement, P < 0.001 uncorrected (because these effects are orthogonal this corresponds to P < 0.00001). Parameter estimates showing mean (± SE) activation during the four experimental conditions are also displayed.

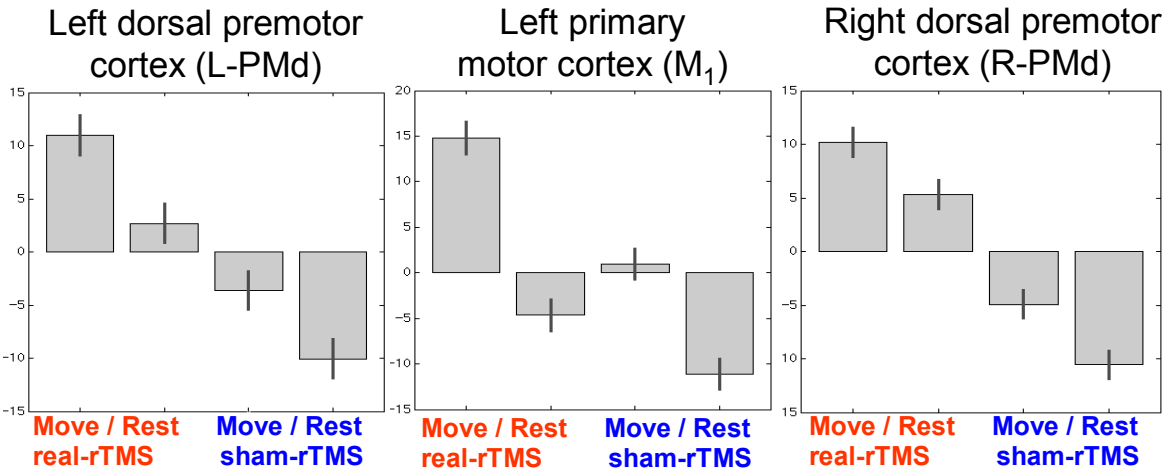

Table 3.3: Main Effect of rTMS

Brain Region		MNI Co-ordinates of peak activation			Z-value of peak activation	P value SVC
		x	y	z		
a)Increased rCBF						
Sensorimotor	Left	-30	-26	62	4.02	P = 0.007
PreMotor (PMd)	Left	-14	-16	68	4.93	P < 0.001
	Left	-18	-18	66	4.96	P < 0.001
	Right	40	-10	64	7.06	P < 0.001
	Right	38	-4	62	4.81	P < 0.001
SMA	Left	-12	-18	58	3.99	P = 0.001
Cerebellum	Left	-20	-56	-36	4.51	P = 0.001
	Left	-26	-60	-24	5.31	P < 0.001
	Right	22	-54	-18	6.67	P < 0.001
Putamen	Left	-24	-12	2	3.44	P = 0.045
Anterior Inferior Parietal	Left	-66	-30	38	3.56	P = 0.032
	Right	38	-32	40	3.64	P = 0.025
	Right	54	-34	30	3.81	P = 0.014
	Right	40	-50	48	6.02	P < 0.001
Insula	Left	-32	-12	-8	4.82	P = 0.001
Prefrontal	Right	20	10	70	3.38	P = 0.054
b) Decreased rCBF						
Premotor (PMv)	Left	-50	6	24	3.6	P = 0.028
Cingulate motor (Caudal)	Right	2	0	38	3.75	P = 0.017
Cingulate motor (Rostral)	Right	6	20	48	5.15	P < 0.001
	Right	6	14	52	3.89	P = 0.011
	Right	10	14	52	3.49	P = 0.039
Cerebellum	Right	40	-56	-22	4.73	P < 0.001
S II (post central sulcus)	Left	-44	-24	36	3.56	P = 0.031
Operculum (44/45)	Left	-46	12	2	5.21	P < 0.001
	Left	-44	10	-6	5.06	P < 0.001
Prefrontal	Left	-22	42	28	4.23	P = 0.003
	Right	38	8	52	4.3	P = 0.003
	Right	34	12	50	3.77	P = 0.017
	Right	36	10	52	3.96	P = 0.009
Superior Temporal Gyrus	Left	-58	-8	-2	6.17	P < 0.001
	Left	-52	-8	2	6.22	P < 0.001

Table 3.3a: Main effect of rTMS (increases): Maxima of regional increases in normalized rCBF after real-rTMS. *3.3b*: Main effect of rTMS (decreases): Maxima of regional rCBF decreases after rTMS. P < 0.05 (small volume correction, using values in Table 3.2).

Figure 3.5

a) Left primary motor cortex: x = -30, y = -24, z = 48

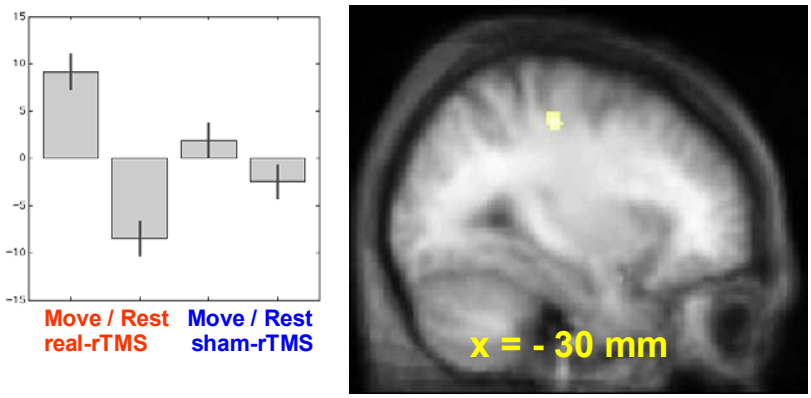

b) Right dorsal premotor cortex: x = 30, y = 4, z = 54

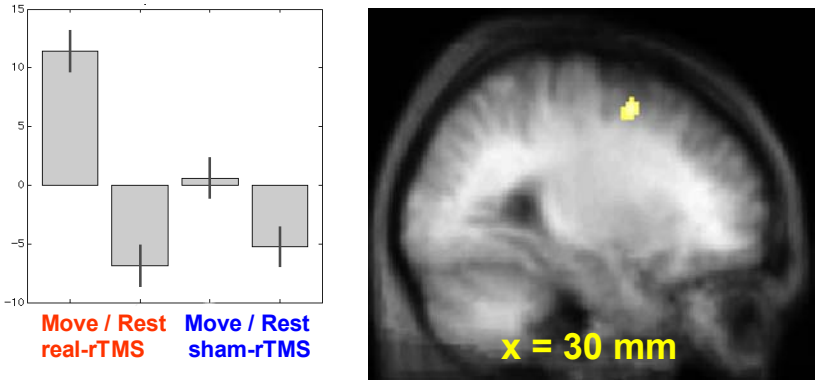

Figure 3.5: Areas of the brain showing different responses during movement after real-rTMS compared to sham-rTMS (Interaction between movement and rTMS).
Results are displayed on coronal sections of averaged anatomical MRI scans at P < 0.001 uncorrected, masked by main effect of movement as for Figure 3.4. Localisation of activation and parameter estimates for **(3.5a)** left sensorimotor site and **(3.5b)** right premotor site.

3.3.2.4 Changes in effective connectivity between the stimulated area and non-primary motor areas. (Psychophysiological interactions)

Figure 3.6 and Table 3.4a show the results of the first psychophysiological interaction analysis, using the synaptic activity (as indexed by rCBF) from the site of maximal rTMS-induced increase in the stimulated cortex (x = -30, y = -26, z = 62) as the physiological variable. Table 3.4a lists the co-ordinates of the maxima of sites shown in Figure 3.6a, with corrected P-values. After real-rTMS, changes in activity in the left premotor (x = -14, y = -6, z = 66) and motor cingulate (x = -4, y = 14, z = 34) cortices were associated with a reduction in the magnitude of the response of the index area (the site of rTMS). A trend towards this effect was also found in a region of left sensorimotor cortex (x = -38, y = -20, z = 46). As explained in the methods section, one interpretation of this finding is that the sensitivity of the site of stimulation to input from these distal areas has been reduced by rTMS.

3.3.2.5 Changes in effective connectivity between primary and non-primary motor areas

Figure 3.7 and Table 3.4b-d summarise the results of three psychophysiological interaction analyses looking for changes in coupling between components of the motor system activated during the movement task. When activity in left sensorimotor hand area (x = -42, y = -26, z = 56) was used as the physiological component, there was an increase in coupling between the index area and an additional ipsilateral left sensorimotor area (x = -38, y = -20, z = 46) after rTMS (Figure 3.7a & b, Table 3.4b). The PPI analysis based on activity in the left dorsal premotor area (x = -26, y = -14, z = 68) demonstrated that after rTMS, there was increased coupling with areas in the left and right primary sensorimotor cortex (Fig. 3.7c & d, Table 3.4c). A third analysis used the activity in left SMA (x = -12, y = -4, z = 56) as the physiological variable. It can be seen from Table 3.4d and Figures 3.7e & f that rTMS increases the coupling between the left SMA and the left sensorimotor cortex (x = -30, y = -26, z = 54).

Table 3.4: Psychophysiological Interactions

Brain Region		**MNI Co-ordinates of peak activation**			**Z-value of peak activation**	**P value SVC**
		x	**y**	**z**		
a) Main effect of rTMS increase (-30 -26 62) as index region for PPI						
Sensorimotor	Left	-38	-20	46	3.28	0.07
Premotor (PMd)	Left	-14	-6	66	3.59	0.029
Cingulate motor (rostral)	Left	-4	14	34	3.62	0.026
b) Sensorimotor (-42 -26 56) as index region for PPI						
Sensorimotor	Left	-38	-20	46	3.61	0.028
c) PMd (-26 -14 68) as index region for PPI						
Sensorimotor	Left	-36	-22	44	3.32	0.061
	Right	44	-22	42	4.03	0.007
d) SMA (-12 -4 56) as index region for PPI						
Sensorimotor	Left	-34	-22	48	3.69	0.021
	Left	-30	-26	54	4.04	0.006

Table 3.4: Psychophysiological Interactions. $P < 0.05$ (small volume correction, using values in table 3.2). *3.4a:* TMS site as index area: Co-ordinates of brain regions to which the TMS site is less sensitive after rTMS. *3.4 b-d):* Three movement-related activations as index areas. Co-ordinates of brain regions showing increased coupling with (3.4a) left sensorimotor region, (3.4b) left dorsal premotor region and (3.4c) left SMA after real-rTMS, compared to sham-rTMS.

Figure 3.6

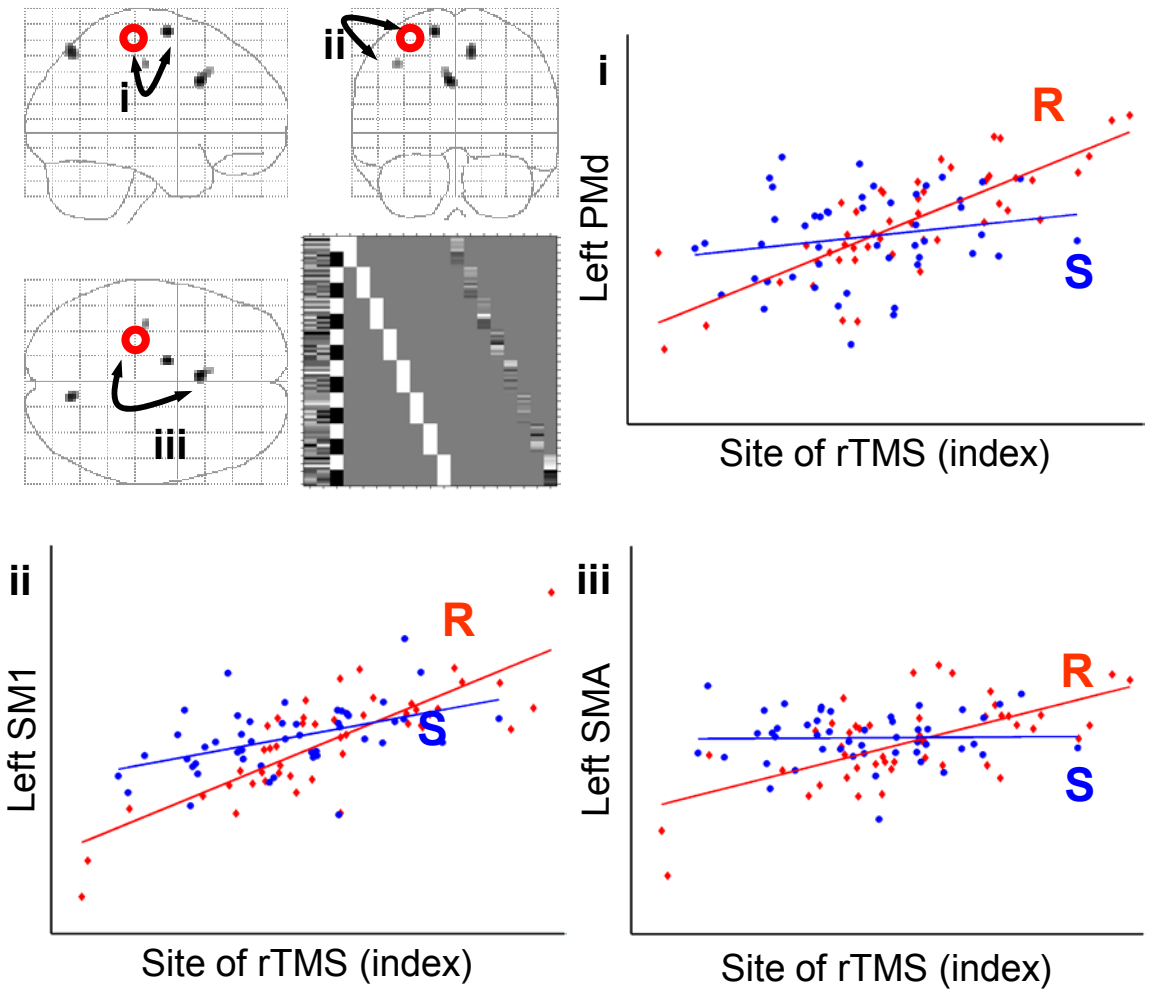

Figure 3.6: Changes in Effective Connectivity (Psychophysiological interaction) with the site of rTMS stimulation.
3.6) Areas showing positive PPI with the site of rCBF increase in left sensorimotor cortex after rTMS. Results are displayed as statistical parametric maps in sagittal, coronal and transverse projections in stereotactic space. The greyscale areas show all significant voxels at P<0.001, uncorrected. The black circle shows the location of the region of interest used as the physiological variate in the interaction. The design matrix is displayed alongside the statistical parametric maps.
Graphical representations illustrating the psychophysiological interactions between the site of rTMS region of interest (x = -30, y = -26, z = 62) (abscissa) and significant areas. Regression lines between the activity in the two regions have been fitted: sham-rTMS = 'S' (circles) and real-rTMS = 'R' (crosses).
3.6i) Proximate left sensorimotor region (x = -38, y = –20, z = 46), marked **'i'**. **3.6ii)** Left dorsal premotor area (x = -14, y = –6, z = 66), marked **'ii'**. **3.6iii)** Left mesial motor area (x = -4, y = 14, z = 34), marked **'iii'**.

Figure 3.7

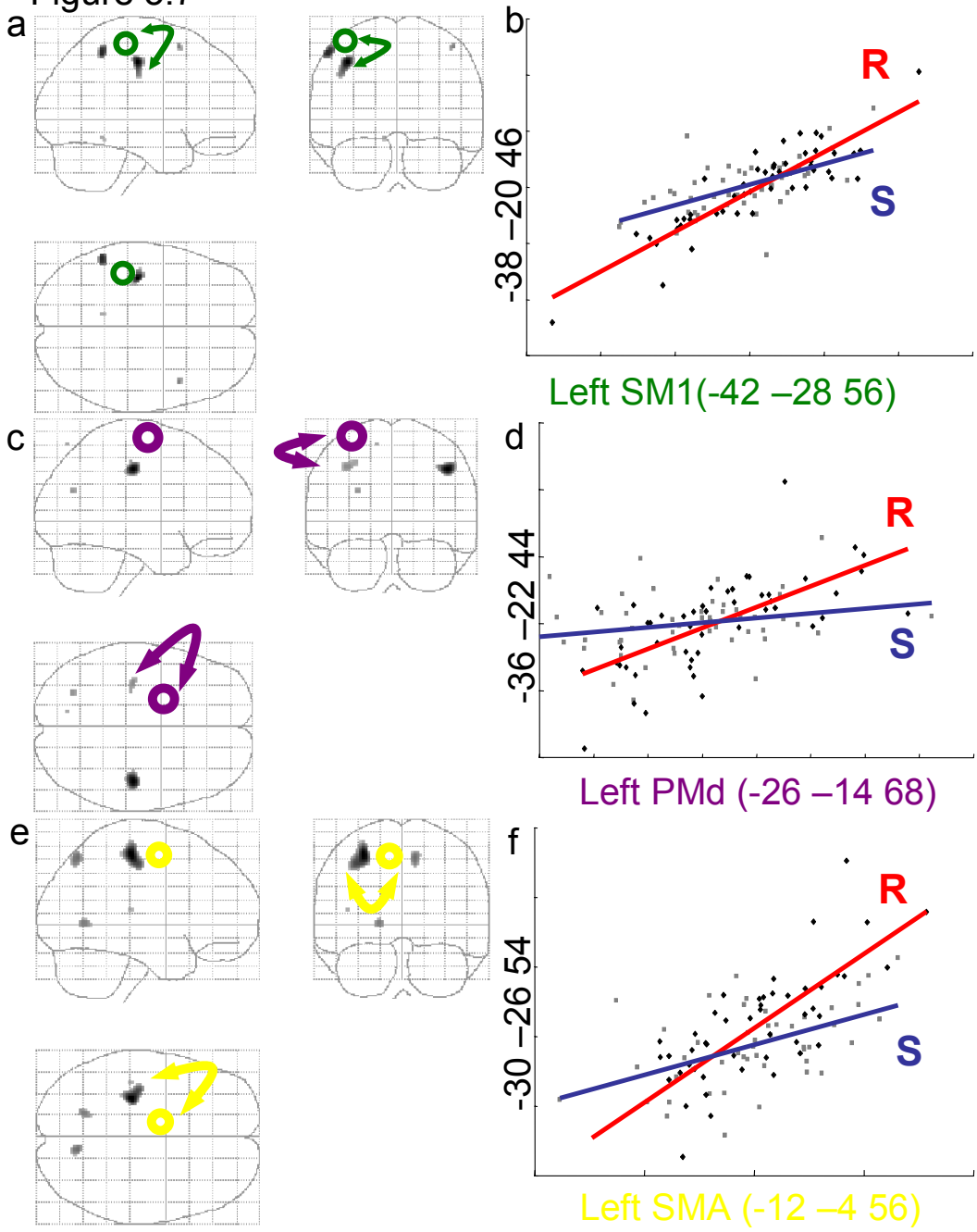

Figure 3.7: Changes in Effective Connectivity (Psychophysiological interaction) with the movement-related activations. **3.7a**: Positive PPI with left sensorimotor region of interest (x = -42, y = -26, z = 56). **3.7b**: PPI between left sensorimotor region of interest (abscissa) and a proximate left sensorimotor region (x = -38, y = –20, z = 46). **3.7c**: Positive PPI with left premotor region of interest (x = -26, y = -14, z = 68). **3.7d**: PPI between left premotor region of interest (abscissa) and left sensorimotor region (x = -36, y = –22, z = 44). **3.7e**: Positive PPI with the left SMA region of interest (x = -12, y = -4, z = 56). **3.7f**: PPI between left SMA region of interest (abscissa) and left sensorimotor region (x = -30, y = -26, z = 54).

Figure 3.8

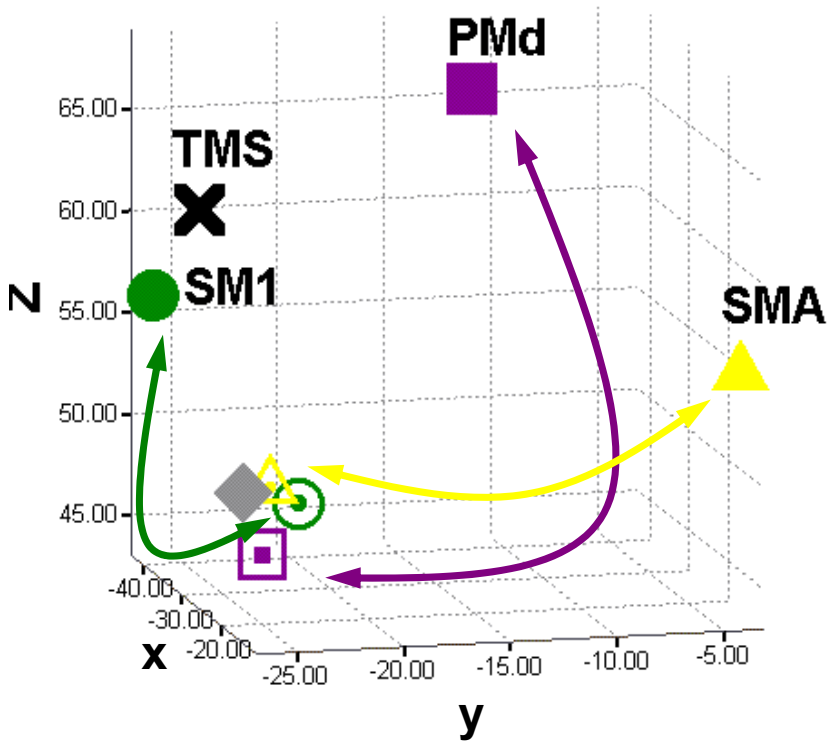

Figure 3.8:Three-dimensional representation of the relative positions of the primary motor cortex sites identified in the three PPI analyses shown in figures 3.7a-f.
The solid circle, square and triangle symbols represent the regions of interest (the maxima in the main effect of movement) whose activity was used to create the covariate of interest (see methods). The hollow circle, square and triangle symbols indicate the relative position of the sites in primary motor cortex that are more strongly coupled with activity in SM1, PMd and SMA respectively, after rTMS.
The solid diamond indicates the position of the SM1 site seen in the Movement-by-rTMS interaction (see figure 3.5). 'X' marks the site of stimulation with 1Hz rTMS.

3.4 Discussion

The findings of this experiment are discussed in two sections. First, the neural correlates of reduced cortical excitability following 1Hz rTMS. Second, mechanisms by which the brain maintains functional integrity in the context of altered cortical excitability.

3.4.1 Neural correlates of reduced cortical excitability

Widespread changes in rCBF were seen within the motor system following a period of subthreshold rTMS, including increased rCBF at the site of stimulation, that were stable for up to one hour following the end of stimulation. These data extend previous $H_2{}^{15}O$-PET studies which had described increases in neuronal activity in motor areas during rTMS of the motor cortex (Fox et al., 1997;Siebner et al., 2001). In addition to local effects, there are statistically significant alterations in synaptic activity in areas not stimulated directly with rTMS. Changes in rCBF at non-stimulated sites have been previously reported in studies using supra-threshold stimulation at 1Hz (Fox et al., 1997). Remote effects may be mediated by cortico-subcortical relays (Strafella et al., 2001) or via cortico-cortical connections (Wassermann et al., 1998;Siebner et al., 2000). They may represent a conditioning effect of rTMS caused by a spread of excitation via these connections. Alternatively, remote effects may reflect compensatory responses to maintain normal function of the motor system (see below).

There are two mechanisms by which rTMS can decrease cortical and cortico-spinal excitability (see Chapter 2) while increasing rCBF (synaptic activity). If 1Hz rTMS increases the activity of inhibitory interneurones, which is metabolically demanding (Ackermann et al., 1984;Nudo and Masterton, 1986), this will increase rCBF while reducing the responsiveness of the stimulated cortical area to further stimulation. Alternatively, rTMS may reduce synaptic efficacy in the motor cortex, such that, for a given excitatory input, there is less postsynaptic activity i.e. long-term depression. Reduced efficacy of synapses terminating on pyramidal cells would account for the observed decrease in excitability as TMS effects are generated transsynaptically (see Chapter 2). Compensatory excitatory presynaptic input to pyramidal cells

would result in increased synaptic activity (increased rCBF), without increased output (i.e. decreased corticospinal excitability). These compensatory changes may arise from intrinsic connections mediating cortical gain control (Abbott et al., 1997) or reflect compensatory extrinsic inputs. This explanation is in good accordance with the reduced sensitivity of primary motor cortex to somatosensory cortical activity, as shown by Tsuji and Rothwell (2002). In this study, an analysis of effective connectivity further corroborates this notion. The site of rTMS became less responsive to activity in motor areas involved in the execution of freely selected movements; specifically premotor cortex, mesial motor areas and an inferolateral part of the primary motor cortex (see Figure 3.6 and Table 3.4a).

In this study, the site of increased rCBF at the site of stimulation with rTMS was 13mm superior and medial to the maximal activation of the left sensorimotor cortex during freely selected movement. This may be because the site of stimulation with rTMS was located by generating twitches in the FDI muscle, whereas the movement task used the full range of finger flexors and extensors. Also, the activation during movement may represent a conflation of sensory and motor effects, as compared to the purely motor site stimulated with rTMS.

3.4.2 Maintenance of functional integrity during modulation of cortical excitability

The right dorsal premotor cortex (contralateral to the site of stimulation) showed increased activation during freely selected finger movements of the right hand (Figure 3.5). This reinforcement of movement-related activation in the contralateral premotor cortex has interesting parallels with a TMS study published recently by (Johansen-Berg et al., 2002b). In this study, stimulation of the contralesional PMd with single-pulse TMS increased reaction times for stoke patients more than for healthy controls and the degree of slowing correlated with impairment. The authors concluded that, following stroke, increased activity in contralesional premotor cortex (Weiller et al., 1992;Seitz et al., 1998;Johansen-Berg et al., 2002b) during movement of the affected limb is of functional significance for motor recovery. The fact that contralesional premotor activation appears to be functionally important after stroke raises the possibility that similar mechanisms may occur after rTMS in healthy subjects, enabling unchanged motor performance.

The second set of PPI analyses demonstrate that after rTMS activity in caudal SMA, dorsal premotor and primary motor cortices became more tightly coupled with a distinct sensorimotor cluster in the primary hand area. This cluster was close to the area in left primary sensorimotor cortex seen in the movement-by-rTMS interaction (Figure 3.8). It is worth noting that these sites were located inferiorly to the sensorimotor site that showed maximal activation during movement. This does not imply that 1Hz rTMS remodels motor representations per se, but having rendered a superficial part of primary motor cortex less sensitive to inputs from premotor and mesial motor areas (see Figure 3.6), other regions within the primary sensorimotor cortex become responsive during movement. The intensity chosen for rTMS modulates more superficial portions of the primary sensorimotor cortex because the strength of stimulation attenuates with increasing vertical distance from the plane of the coil. Regions of primary sensorimotor cortex deep in the central sulcus would be less affected by rTMS and therefore capable of responding to input from premotor cortex and SMA during movement. Such operational remapping of motor representations may contribute to compensatory mechanisms for rTMS-induced reductions in cortical excitability. This is discussed further in Chapter 7.

3.5 Conclusion

This experiment adds to the body of evidence that low-intensity rTMS to the primary motor hand area induces long-lasting changes in neural activity in local and remote brain regions. However, the motor system may compensate for this by increasing activity in the contralateral premotor cortex, similar to that seen in stroke (Johansen-Berg et al., 2002b). In addition, sites in primary sensorimotor cortex that are unlikely to have been affected by rTMS increase their movement-related activity and strengthen their connectivity with other components of the motor network, suggesting an acute remodelling of motor representations within the primary sensorimotor cortex. Mapping these patterns of reorganisation in the motor system may provide a useful method to study acute compensatory plasticity of the human brain and may help to understand how the brain reacts in response to more permanent lesions. In order to confirm that reorganisation of motor representations occur during movement after rTMS, and to provide further anatomical detail regarding the location of the sites of activation with regard to detailed motor maps, it may be necessary to use the superior spatial resolution of fMRI.

Chapter 4

The role of premotor activity in task performance after 1Hz rTMS

4.1 Introduction

Aims of Experiment 2:

1. Investigate the functional relevance of the contralateral PMd activation seen in experiment1

Prolonged periods of 1Hz repetitive Transcranial Magnetic Stimulation (rTMS) impair the function of the targeted cortical area for several minutes (Kosslyn et al., 1999;Hilgetag et al., 2001;Knecht et al., 2002). The experiment presented in Chapter 3 used functional neuroimaging to identify two brain areas with relatively increased synaptic activity during a simple motor task following 1Hz rTMS (Figure 3.5). These were the right dorsal premotor cortex (contralateral to the site of stimulation and ipsilateral to the movement) and the left primary motor cortex deep in the central sulcus (ipsilateral to the site of stimulation and contralateral to the movement). It was suggested that the increased activity in these areas may represent induced plasticity in the motor system, enabling preserved motor performance in simple motor tasks.

This pattern of changes has interesting parallels with imaging studies of movement related activity after stroke, where increased activity has been reported in contralesional motor areas (Chollet et al., 1991;Weiller et al., 1992;Cramer et al., 1997;Cao et al., 1998;Seitz et al., 1998;Cuadrado et al., 1999;Marshall et al., 2000;Carey et al., 2002;Johansen-Berg et al., 2002a) during movement of the affected limb. The functional relevance of these activations was examined in a TMS study published recently by (Johansen-Berg et al., 2002b). In this study stimulation of the contralesional PMd with single-pulse TMS during a reaction time task lead to increased reaction times for stoke patients but not for healthy controls. In addition, the degree of slowing induced by TMS correlated with motor impairment. The authors concluded that contralesional premotor activation appears to be functionally important after stroke. This raises the possibility that similar mechanisms may occur

after rTMS in healthy subjects, enabling unchanged motor performance as seen in the previous experiment.

The use of single pulses or short bursts (less than 500ms) of repetitive TMS to disrupt behaviour during a task has been described as a ‘virtual lesion’ or perturbation technique (Walsh and Rushworth, 1999). When a cortical area is active during a behavioural task, electrical currents induced by TMS will add ‘noise’ to organized neural activity in a temporally discrete fashion, leading to a deficit in neuronal computation and ensuing task performance. Schluter et al (Schluter et al., 1998) demonstrated that, in healthy subjects, there is an asymmetry in the premotor contribution to performance during simple and choice reaction tasks. TMS to left premotor cortex at short cue-stimulus intervals increased reaction times for right and left handed responses in a choice reaction time task; whereas TMS to right premotor cortex only increased reaction times for left handed responses. During simple reaction time tasks, TMS to left and right premotor cortices did not increase reaction times with either hand.

This experiment was designed to test the hypothesis that a lasting disruption of function in left M1 by 1Hz rTMS renders the motor system susceptible to an acute perturbation of the activity in right PMd with short trains of 20Hz rTMS. The task used in Chapter 3 is not suitable for an experiment using single pulses or short trains of rTMS to cause a deficit in task performance. This is because the measure of task performance is the selection of a ‘random’ sequence of finger movements. With only four movements to choose from, it is unlikely that an acute intervention would significantly affect the randomness of the sequence. The movements are paced; therefore reaction times cannot be used as a measure of performance. A suitable task for this experiment needed to include a readily measured metric of task performance and an element of movement selection that would engage premotor areas. For these reasons, a choice reaction task was selected, based on the experiments described by (Schluter et al., 1998).

4.2 MATERIALS AND METHODS

4.2.1 Subjects

Six healthy, right-handed volunteers (one male) aged between 22 and 38 (mean age: 28), with no history of neurological disorder or head injury, were recruited from the Institute of Neurology, University College London, UK. Written informed consent was obtained from all participants. The study was approved by the joint ethics committee for the National Hospital for Neurology and Neurosurgery and the Institute of Neurology.

4.2.2 Study design

The study had a 2x3 factorial design. The factors were 1Hz rTMS (two levels: pre and post); and 20Hz rapid rTMS (three levels: none, early or late). The study design is illustrated in Figure 4.1a.

4.2.3 Motor Task

Subjects were seated 60 cm from a computer screen, with their right arm placed on the table and their index and middle fingers resting on response keys. Coloured symbols were displayed for 100ms on the screen and subjects had to respond as quickly as possible by pressing either their index or middle finger. If the red circle or blue triangle appeared subjects responded with their middle finger, if the red triangle or blue circle appeared they responded with their index finger. Neither the shape nor colour alone determined the response; this made the task reasonably difficult and ensured that reaction times were relatively long. The motor task is shown in Figure 4.1b.

Each block contained 60 trials, 12 with no TMS, 24 with ‘early’ 20Hz rTMS and 24 with ‘late’ 20Hz rTMS. The inter-trial interval was 2s. The onset of 20Hz rTMS pulses was measured from the onset of cues on the screen. 4 pulses at 20 Hz (200ms) were delivered starting at 0 to 50 ms after stimulus onset (early 20Hz rTMS) or 100 to 150ms after stimulus onset (late 20Hz rTMS). The timing of ‘early’ and ‘late’ 20Hz rTMS is shown in Figure 4.1b.

All subjects performed 4-6 blocks of practice trials with no TMS, during which time they were encouraged to respond as quickly and accurately as possible, and they were given feedback on their performance.

During the experiment, all subjects performed four blocks of 60 trials before receiving 1Hz rTMS, and four blocks of 60 trials after 1Hz rTMS. During these blocks subjects were magnetically stimulated over their right hemisphere (ipsilateral to the hand being used for the task) (see Figure 4.1a).

Figure 4.1

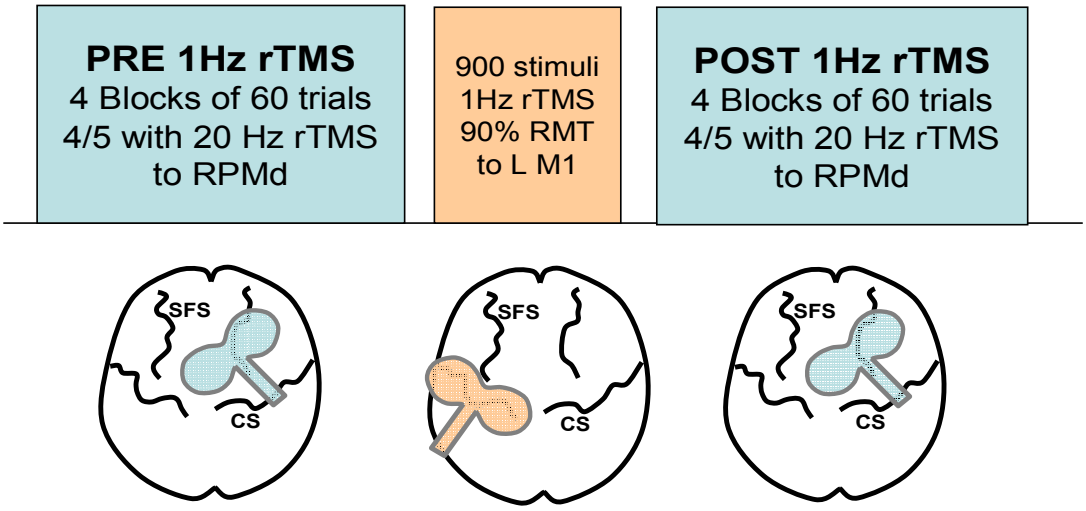

Figure 4.1a: Study Design and site of rTMS stimulation
All subjects performed 4 blocks 60 trials of the choice reaction time task (PRE), during which they received 20 Hz rTMS to right premotor cortex (blue) on 4/5 trials. They then received 1Hz rTMS to left primary motor cortex (orange) before completing a further 4 blocks of 60 trials (POST).
SFS: superior frontal sulcus CS: central sulcus

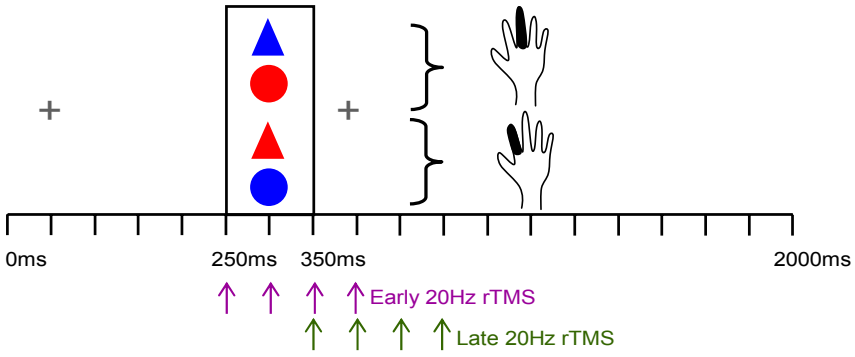

Figure 4.1b: Choice Reaction Task.
Subjects were instructed to respond as quickly and accurately as possible by pressing their right index or middle finger when the relevant stimuli were presented for 100ms. 20 Hz perturbing rTMS at 90% resting motor threshold was applied on 4/5 trials to subjects' right dorsal premotor cortex during ('early') or after ('late') stimulus presentation. Grey and black arrows show the timing of early and late 20 Hz pulses respectively. Subjects performed four blocks of 60 trials before and immediately after receiving 900 stimuli of 1Hz rTMS at 90% RMT to left M1.

4.2.4 20 Hz Repetitive transcranial magnetic stimulation

20Hz rTMS comprised 4 biphasic stimuli given over the right premotor cortex using a MagStim-rapid stimulator connected to four booster modules (MagStim Company, Whitland, Wales, UK; www.magstim.com). Stimulation intensity was set to 90% of resting motor threshold (RMT) of the left first dorsal interosseus (FDI) muscle. A standard figure-of-eight shaped coil (Double 70mm - Coil Type P/N 9925, MagStim Company, Whitland, Wales, UK) was used. The coil was positioned with the handle at 45^{o} to the sagital plane. The current flow of the initial rising phase of the biphasic pulse in the TMS coil induced a current flowing from posterior-to-anterior in the underlying premotor cortex.

The site of 20Hz rTMS stimulation was the dorsal premotor cortex: 2cm anterior and 1cm medial to the "motor hot spot", defined functionally as the point of maximum evoked motor response in the relaxed left FDI muscle. Previous studies (Schluter et al., 1998;Johansen-Berg et al., 2002b) have indicated that TMS at this site has dissociable effects on similar tasks in healthy controls and stroke patients. The resting motor threshold was defined as the lowest stimulus intensity that elicited at least five twitches in ten consecutive stimuli given over the “motor hot spot”. Previous work (Gerschlager et al., 2001) has shown that premotor cortex is more sensitive to TMS that M1. By using a stimulus intensity of 90% RMT it is likely that the 20Hz rTMS pulses will disrupt cortical activity in PMd, without eliciting responses in M1.

4.2.5 1Hz Repetitive transcranial magnetic stimulation (rTMS)

900 stimuli of 1 Hz rTMS were given over left M1 as described in Chapter 3.

4.2.6 Behavioural assessment

All response times were recorded and subsequently analyzed using SPSS 11.0 (SPSS Inc., Chicago, Illinois, USA). For each subject the mean reaction times for each block were normalized by taking the percentage change in reaction time (RT) with early or late 20Hz rTMS stimulation, relative to none. These changes in RT were entered into an ANOVA comparing the effects of early and late stimulation before and at four time points after 1Hz conditioning rTMS. Significance was set at $P < 0.05$ following Greenhouse-Geiser correction for non-sphericity.

4.3 Results

Subjects did not report any adverse side effects during the course of the study, nor were any motor responses observed during the 15 minutes of rTMS. Mean resting motor threshold for right FDI was 49%, ranging from 41% to 58% of maximum output of the MagStim-rapid stimulator. Mean RMT for Left FDI was 53%, ranging from 43% to 61% of maximum output of the same MagStim-rapid stimulator.

4.3.1 Behavioural Data

The numbers of errors were small (>90% accuracy), and were not significantly different after 1Hz rTMS ($t = 1.38$, $P = 0.227$). Incorrect responses were excluded from the analysis of reaction times.

To assess relative differences in the acute effects of 20Hz rTMS, on reaction times before and after conditioning 1Hz rTMS, changes in reaction time (RT) were analyzed using a repeated measures general linear model. There was a significant main effect of 1Hz rTMS ($F = 4.71$, $P = 0.02$) and of 20Hz rTMS ($F = 51.17$, $P < 0.001$).

The significant main effect of conditioning rTMS is the key result here and suggests that increases in RT, induced by premotor perturbations, are seen with, and only with, conditioning rTMS to the primary motor cortex.

There was no significant interaction between 1 and 20 Hz rTMS ($F = 0.5$, $P = 0.64$), suggesting that 1Hz rTMS conditioning did not have a differential effect on the impact of early and late 20Hz rTMS. Post-hoc t-tests were used to further characterize the main effect of 1Hz rTMS. These t-tests compared percentage change in RT provoked by early and late 20Hz rTMS before 1Hz rTMS to the percentage change in RT at the four different time point after 1Hz rTMS. There was a significant increase in RT with 20Hz rTMS in the second post rTMS block ($P = 0.03$ for early 20Hz rTMS and $P = 0.001$ for late 20Hz rTMS). These data are shown in Figure 4.2.

Figure 4.2

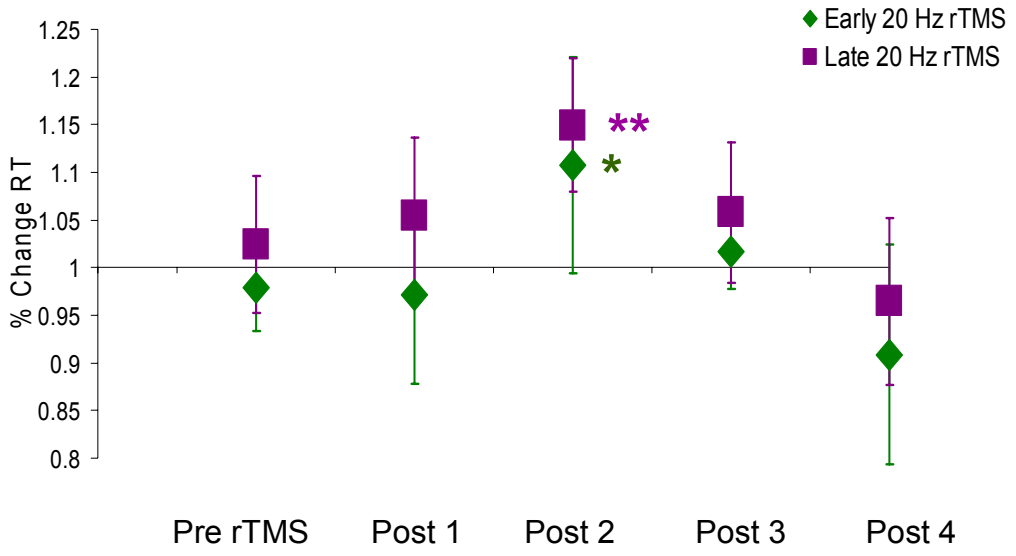

Figure 3: Results
Percentage change in reaction times induced by early (green) and late (purple) 20Hz perturbing rTMS to right PMd compared to trials with no 20Hz perturbing rTMS before and after 1Hz conditioning rTMS to left M1. *: P = 0.03, **: P = 0.001. These p-values pertain to significant differences between pre and post 1Hz rTMS.

4.4 Discussion

The aim of this experiment was to use short (200 ms) bursts of rapid repetitive TMS as a 'virtual lesion' to investigate the functional relevance of premotor activation seen during the movement task in Chapter 3.

In that experiment prolonged trains of sub-threshold 1Hz repetitive TMS were used as a method of modulating or conditioning cortical excitability. Following this intervention, task-dependent changes in rCBF (a marker of synaptic activity) were observed with no change in motor performance. Specifically, increases in rCBF were seen during movement after real rTMS (compared to sham) in Area 4p in the stimulated hemisphere and in the dorsal premotor cortex in the unstimulated hemisphere. There was no change in motor performance, measured with finger tapping speed and duration of presses. In this follow-up experiment, it has been shown that disrupting the right dorsal premotor cortex during a choice reaction time task (right handed responses) affects task performance after 1Hz rTMS to left M1.

4.4.1 Degeneracy in the Motor System revealed by rTMS

This result establishes an important paradigm for characterising functional anatomy, namely the identification of degeneracy in cortical systems (Price and Friston, 2002). The concept of "degeneracy" as a ubiquitous biological property was introduced by Edelman and colleagues (Tononi et al., 1999;Edelman and Gally, 2001) and refers to the ability of biological systems that are structurally different to perform the same function. In cognitive neuroanatomy, degeneracy has emerged as an important feature of functional brain architectures and provides an important substrate for functional recovery after focal lesions (Price and Friston, 2002). Degeneracy is a many-to-one structure-function mapping and, in this context, implies that more than one set of cortical structures can support the same function (maintenance of performance on a choice reaction time task). Using functional neuroimaging (Chapter 3) it was demonstrated that the right pre-motor region was more active during freely selected finger movements made with the right hand after conditioning left M1 with 1Hz rTMS. This suggests that either, or both, the motor

and pre-motor regions may be sufficient for task performance and the possibility of a degenerate mapping from structure (motor and premotor regions) to function (as measured by reaction times). The order of degeneracy is defined as the minimal number of lesions required to impair function. There is an important connection between the order of degeneracy and the order of 'contribution' (Price and Friston, 2002). In contribution analyses one examines the sensitivity of some function or performance P to lesioning a system's components (e.g. cortical areas). This sensitivity can be summarised mathematically as:

$$C_i = \frac{\partial P}{\partial L_i}$$

Where L_i quantifies the lesion to area i. In this example, rTMS to either the motor or premotor components did not increase reaction times and, consequently, there was no evidence for first-order contributions from either area. This means neither is necessary but both may be sufficient. This can be tested with the second order contribution,

$$C_{ij} = \frac{\partial^2 P}{\partial L_i \partial L_j}$$

which means the effects of lesioning area i, depends on lesioning j. This requires two lesions and is precisely what is observed: decreased performance, induced by perturbing (20Hz) rTMS in the ipsilateral premotor area, depends on compromising the contralateral motor cortex with conditioning (1Hz) rTMS. In this example, the long-lasting disruptive effects of conditioning 1HZ rTMS and the transient disruption of 20Hz rTMS were used to simultaneously 'lesion' two areas. By showing these interventions interact, to impair performance, a second-order contribution is established and it is possible to infer second-order degeneracy. Establishing the order of degeneracy using TMS and contribution analyses of this sort may play a key role in rehabilitation and a mechanistic understanding of compensatory mechanisms in patients. Degeneracy should not be confused with redundancy. Redundancy refers to the joint recruitment of two or more regions when only one is necessary. The co-activation of degenerate regions may or may not be redundant.

4.4.2 Combining prolonged 1Hz rTMS with the 'virtual lesion' approach

Previous work using a very similar experimental protocol (Schluter et al., 1998;Johansen-Berg et al., 2002b) has suggested that disrupting the right dorsal premotor cortex with TMS during right-handed choice reaction time tasks does not affect performance in healthy controls. The results presented in this chapter concur with these previous findings. There were no significant effects of early or late 20Hz perturbing rTMS on reaction times during the blocks of trials performed before 1Hz conditioning rTMS (Figure 4.2). Following stimulation to left M1 with 1Hz rTMS, 20 Hz rTMS to right PMd slowed reaction times made with the right hand when applied at cue onset (early) or offset (late). Following conditioning of left M1 with 1Hz rTMS, 20 Hz perturbing rTMS to right PMd slowed reaction times made with the right hand when applied at cue onset (early) or offset (late). This suggests that the increase in movement related activity in right premotor cortex after 1Hz conditioning rTMS reported in Chapter 3 may be functionally relevant for maintaining task performance.

It should be noted however that the movement task performed during PET scanning is not the same as the task used in the current experiment. This is because for this second experiment it was necessary to use a motor task with a measure of performance that could be acutely disrupted by TMS. It would be of interest to repeat the imaging experiment using a choice reaction time task, looking for right PMd activation during the task after 1Hz rTMS to left M1.

Another possibility is that the interaction between the effects of 20Hz rTMS on task performance and 1Hz rTMS is due to a non-specific effect of 20Hz rTMS on performance that is somehow altered after 1Hz rTMS. It is difficult to imagine a mechanism by which this might occur. A suitable control for this eventuality would have been to use an additional site for 20Hz rTMS, such as the vertex, or a control task which should not have been affected by premotor stimulation e.g. a simple reaction time task with no element of movement selection (Schluter et al., 1998).

In contrast to previous work examining the effects of single pulses of TMS on reaction times during simple and choice reaction time tasks in healthy controls and stroke patients (Schluter et al., 1998;Johansen-Berg et al., 2002b;Werhahn et al., 2003), this study used a subthreshold intensity to disrupt PMd during task

performance. This was done deliberately in order to avoid causing twitches in the left hand and to reduce the likelihood of stimulating the right primary motor cortex during 20 Hz rTMS. Previous studies have examined the effects of single TMS pulses delivered at a range of time intervals after stimulus presentation. This is the first study combining the lasting disruptive effects of 1Hz conditioning rTMS with the acute disruptive effects of high-frequency rTMS. A short train of rTMS pulses was used to induce a 'virtual lesion' because no prior information was available regarding the temporal window during which TMS might disrupt task performance under these experimental conditions. By electing to use a 200ms duration train of pulses, information pertaining to the temporal specificity of premotor cortical involvement was compromised. However, this information could be recovered by using single pulses of TMS delivered at various time intervals after stimulus presentation (Schluter et al., 1998;Johansen-Berg et al., 2002b;Werhahn et al., 2003).

This experiment focussed on the effects of disrupting right PMd. This was not the only motor area to show increased movement related activity after 1Hz conditioning rTMS to left M1 (Figure 3.5). In common with several imaging studies of motor activation in stroke patients, an increase in movement-related activity was seen in the left primary motor cortex (or the affected hemisphere in stroke patients), contralateral to the moving hand. By using the virtual lesion TMS technique in stroke patients Werhahn et al. (Werhahn et al., 2003) have shown that supra-threshold stimulation to the lesioned M1 slowed reaction times in a simple motor task. TMS caused a greater degree of slowing in patients with good recovery, suggesting that activity in the affected hemisphere in chronic stroke patents is important for motor function. In order to examine the functional relevance of increased M1 activity in the stimulated cortex after 1Hz conditioning rTMS it would be necessary to demonstrate a differential effect of supra-threshold perturbing TMS to M1 on reaction times before and after 1Hz conditioning rTMS. However, the use of suprathreshold stimuli would, by definition, cause movements in the contralateral hand during the generation of motor responses, and this has been shown to affect reaction times in a variety of motor tasks (Gerloff et al., 1997;Ziemann et al., 1997;Chen et al., 1997c;Gerloff et al., 1998b).

4.5 Conclusion

This experiment demonstrates the functional relevance of compensatory plasticity in the human motor system following modulation of cortical excitability with 1Hz rTMS. These data have interesting parallels with previously published work in stroke patients (Johansen-Berg et al., 2002b;Werhahn et al., 2003;Fridman et al., 2004) and provide a framework for future research into the effects of rTMS on the motor system.

Chapter 5

Effects of 1Hz rTMS on synaptic activity: contralateral and ipsilateral changes in functional anatomy

5.1 Introduction

Aims of Experiment 3:

1. Replicate the main effect of rTMS seen in Experiment 1
2. Explore the functional correlates of contralateral rCBF changes
3. Generalise the effects on rTMS to a different motor task

In Chapter 3, rCBF increases were observed in motor areas in both the stimulated and non-stimulated hemispheres following 1Hz rTMS at 90% resting MT to left M1. The literature reviewed in Chapter 2 suggests that 1Hz rTMS may have opposite effects on the excitability of the stimulated and non-stimulated primary motor cortex. Kobayashi et al. showed a difference in the effects of 1Hz rTMS on motor performance, specifically, an improvement in performance of a sequential key-pressing task with the hand ipsilateral to the stimulated hemisphere following 1Hz rTMS at 90% RMT, and no change in performance with the hand contralateral to the site of stimulation (Kobayashi et al., 2004). Based on these findings, one might predict opposite effects on movement–related activity with the right and left hands after unilateral rTMS, even if task performance remained unchanged.

This chapter presents a second functional imaging experiment using the techniques described in Chapter 3 to investigate the neural correlates of rTMS effects on activity during movement of the left and right hand (ipsilateral and contralateral to the site of stimulation respectively). Changes in neural activity at the site of stimulation and at remote cortical and subcortical sites associated with thirty minutes subthreshold stimulation were examined to replicate of the effects of rTMS reported in Chapter 3. Movement by rTMS interactions for left and right handed movements were used to characterise differences in the local and transcallosal effects of rTMS on movement-related responses. These results were explored further using PPIs. The PPI analyses described in Chapter 3 were repeated in this second study, looking for similarities and differences in the context a different motor task.

5.2 MATERIALS AND METHODS

5.2.1 Subjects

Ten healthy, right-handed volunteers (two female) aged between 23 and 63 (mean age: 35), with no history of neurological disorder or head injury, were recruited from the database of volunteers at the Functional Imaging Laboratory, Institute of Neurology, University College London, UK. Written informed consent was obtained from all participants. The study was approved by the joint ethics committee for the National Hospital for Neurology and Neurosurgery and the Institute of Neurology. The administration of radioactivity was covered under the Motor Studies Licence from the Administration of Radioactive Substances Advisory Committee held at the Functional Imaging Laboratory (RPC528-890 (14364)).

5.2.2 Study design

The study conformed to a 2x3 factorial design, with two levels per factor: "intervention" (real-rTMS versus sham-rTMS) and three levels of the factor "task" (movement right, movement left and baseline). Figure 5.1 illustrates the study design. Real and sham rTMS were given on two separate days, at least one week apart. The order of intervention was counterbalanced across subjects. The effects of rTMS were assessed by consecutive PET measurements of regional cerebral blood flow (rCBF) during the first hour after rTMS. Within each scanning session the baseline and movement tasks were alternated. The order of tasks was kept constant within a subject between sessions, but counterbalanced across subjects.

5.2.3 Repetitive transcranial magnetic stimulation (rTMS)

rTMS was performed in an identical manner to that described in Chapter 3.

Figure 5.1

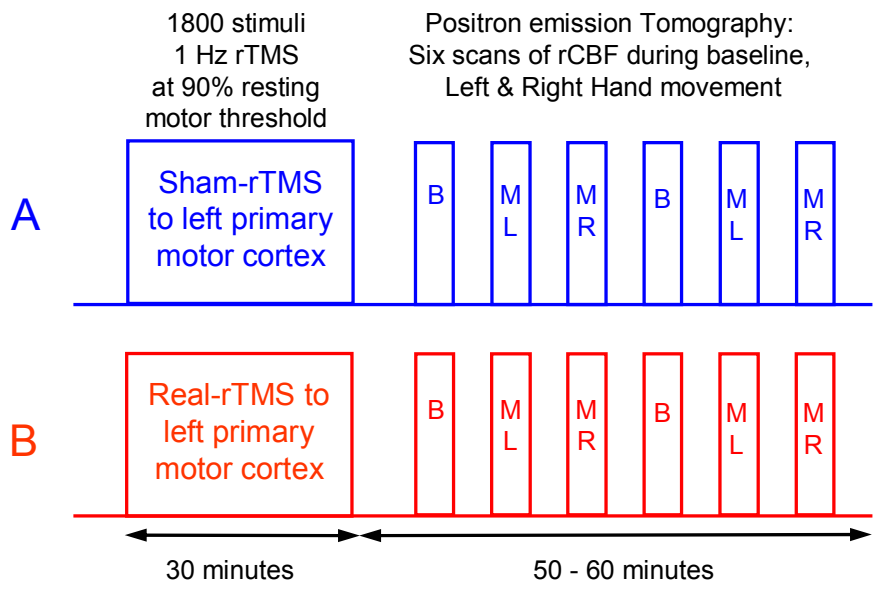

Figure 5.1: Experimental Design.
Subjects received real or sham 1Hz rTMS on separate days. Changes in regional cerebral blood flow were mapped using positron emission tomography (PET). Six sequential H215O-PET scans were acquired at baseline (B) or during the movement task: finger tapping with left (ML) or right (MR) hand, in an alternating order during an hour after the end of rTMS. The order of intervention (real-rTMS (red) v sham-rTMS (blue)) and experimental conditions were counterbalanced across subjects.

5.2.4 Motor Task

Subjects underwent six sequential $H_2{}^{15}O$-PET scans on each of the two separate days. All scans were acquired during the first hour after 30 minutes of 1Hz rTMS to the left motor cortex. Normalized rCBF was used as an index of regional synaptic activity during three experimental conditions: baseline (referred to as condition "B") and paced finger tapping with the right or left hand (referred to as conditions "LM" and “RM”). Two PET scans were acquired for each of the experimental conditions in an alternating order. Subjects were required to watch a display indicating which finger to tap, on a screen located 0.7m in front of their face. A pacing tone was presented every 0.5 seconds during all conditions. During the movement task, subjects were required to execute tapping movements of the finger indicated on the screen (index, middle, ring or little) in time with the pacing tones. They were instructed which hand to use prior to the block. During the baseline condition they

were instructed to watch the display, but not move. To ensure a stable level of task performance, the paced tapping task started about 20 seconds prior to the onset of the PET scan and lasted for the entire 90-second period of data acquisition.

Subjects' responses were made on four buttons, set under their fingertips on a moulded wrist splint. All responses were recorded by computer (Apple Macintosh 7300) using COGENT Cognitive Interface Software (Wellcome Dept. of Imaging Neuroscience, London, UK). The data were analysed using Matlab 6.0 (Mathworks, Sherborn, MA) and SPSS 11.0 (SPSS Inc., Chicago, Illinois, USA).

5.2.5 Behavioural assessment

As in Chapter 3, subjects performed two additional finger-tapping tasks with their right and left hands after each PET scan. In the 'index tapping task' subjects tapped their right or left index finger as many times as possible during a ten second interval. In the 'sequential tapping task' subjects were asked to repeat an ascending sequence (index, middle, ring, little finger) as quickly as possible for ten seconds. To familiarise subjects with the tasks and to reduce learning effects during sequential PET scans, subjects performed each of the tasks twice in the PET scanner prior to rTMS on both scanning sessions.

From each task, the interval between consecutive taps was calculated. For each condition the mean inter-tap intervals (ITI) and coefficients of variation (CV) were computed as indices of motor performance. The CV is a measure of variability, correcting for differences between the means (SD *100/mean). The ITIs and CVs for each task (index and sequential tapping) were subjected to two way ANOVAs with repeated measures, with the following factors: TMS (real and sham) and Hand (right and left).

5.2.6 PET data acquisition

The method of PET data acquisition was identical to that described in Chapter 3.

5.2.7 Image Analysis

Initial image processing was as described in Chapter 2.

The primary analysis employed a general linear model that included six covariates modelling the task (left move, right move and baseline) under each condition of treatment (real versus sham rTMS). The effect of global differences in cerebral blood flow among scans was removed by treating global activity as a confound and scaling to a nominal grand mean global activity of 50 ml/100g/min (Friston *et al*., 1995b). This statistical model enabled characterisation of the main effects of rTMS (real versus sham rTMS) and task (left move versus baseline or right move versus baseline) and movement-by-rTMS interactions.

Changes in effective connectivity were assessed using the 'Psychophysiological Interaction' (PPI) method Friston *et al*. (1997) described in Chapter 2. Three sets of PPIs were performed where the index areas, used as the physiological variable, comprised the first eigenvariate of the rCBF signal from a sphere (radius 8mm) centred on voxels outlined below:

1) The site of stimulation with rTMS was used as the index area to identify those brain regions where rTMS significantly altered the degree of coupling to the site of stimulation. The index area was centred on the maxima of the main effect of rTMS closest to the average location of the fiducials marking the site of stimulation with rTMS.

2) In addition, a site contralateral to the site of stimulation was used as an index area: the maxima of the main effect of rTMS in the motor cortex of the right hemisphere.

3) The maxima of the main effects of movement (left and right hands) were used as index regions to look for brain regions showing a difference in movement-related coupling after rTMS. These sites comprised left and right M1 and SMA.

The results of the movement-by-rTMS interactions were explored further by looking for changes in effective connectivity between the areas showing significant interactions and other parts of the motor network. The index regions were centred on the voxels in the right and left cerebellar cortices where a significant movement-by-rTMS interaction was seen during right (increased movement related activity) and left (decreased movement related activity) hand movements respectively.

Put simply, the interactions observed were further explored using PPIs to see how these interactions might have been mediated by other areas.

5.3 Results

Subjects did not report any adverse side effects during the course of the study, nor were any motor responses evoked during the 30 minutes of rTMS. Mean resting motor threshold was 58.4%, ranging from 44% to 75% of maximum output of the MagStim-rapid stimulator. However, in two subjects with high motor thresholds (74% and 75% stimulator output) there were problems with the TMS equipment, due to coil overheating, and it was not possible to deliver 1800 stimuli within 30 minutes. Data from these two subjects were therefore excluded from further analysis.

5.3.1 Behavioural Data

During scanning, subjects performed a paced finger tapping task. They were monitored to ensure that they were performing the finger tapping task satisfactorily. This included making an equal number of taps with each finger during any given movement scan.

In the index tapping tasks, subjects showed a clear right handed advantage in the mean inter-trial intervals (Table 5.1) ($F = 8.49$, $df = 7$, $P = 0.02$). There were no such differences for right and left hands in the sequential tapping task. There was no main effect of rTMS on tapping speed or variability for either task or hand.

Table 5.1: Behavioural Data

		Task	Index Finger Tapping			Sequential Finger Tapping	
		rTMS	Sham	Real		Sham	Real
Hand	**Measure**						
Right	ITI (ms)	mean	201.5	207.6	*	252.9	272.8
		sd	(+/-12.1)	(+/-16.0)		(+/-36.3)	(+/-48.0)
	CV (%)	mean	20.4	21.9		55.6	84.5
		sd	(+/-5.0)	(+/-6.4)		(+/-14.1)	(+/-34.2)
Left	ITI (ms)	mean	224.8	224.9	*	267	267.6
		sd	(+/-17.4)	(+/-15.9)		(+/-40.3)	(+/-57.5)
	CV (%)	mean	22.5	22.3		81.9	121.1
		sd	(+/-8.3)	(+/-3.7)		(+/-30.1)	(+/-74.2)

Table 5.1: Mean group data (+/-SD) of kinematic measures (interval between presses and coefficient of variation for index tapping and sequential tapping tasks, for left and right hands. *P<0.05 for the comparison of right and left hand index tapping rates.

5.3.2 Imaging Data

The distributed changes in rCBF associated with prolonged subthreshold 1Hz rTMS, movement and movement-by rTMS interactions were examined. Analyses of effective connectivity were used to examine the effects of rTMS at the site of stimulation, in the contralateral motor cortex, and in regions showing significant move-by rTMS interactions. These rTMS-induced effects were modelled, using PPIs as changes in movement-related coupling within the motor network, after rTMS.

5.3.2.1 Movement-Related Activations (Main effect of task)

The contrasts for the main effect of hand movement demonstrated a wide range of areas involved in right and left finger tapping. The results can be seen in Table 5.2a & b and Figure 5.2a & b. The key areas involved in right hand movement included left primary motor cortex, right cerebellum, left basal ganglia (including mediodorsal thalamus and putamen) and left supplementary motor area (SMA). Left hand movements were associated with increased activity in right primary motor cortex, right SMA, bilateral cerebellum and basal ganglia (including mediodorsal thalamus and putamen). Results are reported at P<0.001 (uncorrected).

Figure 5.2

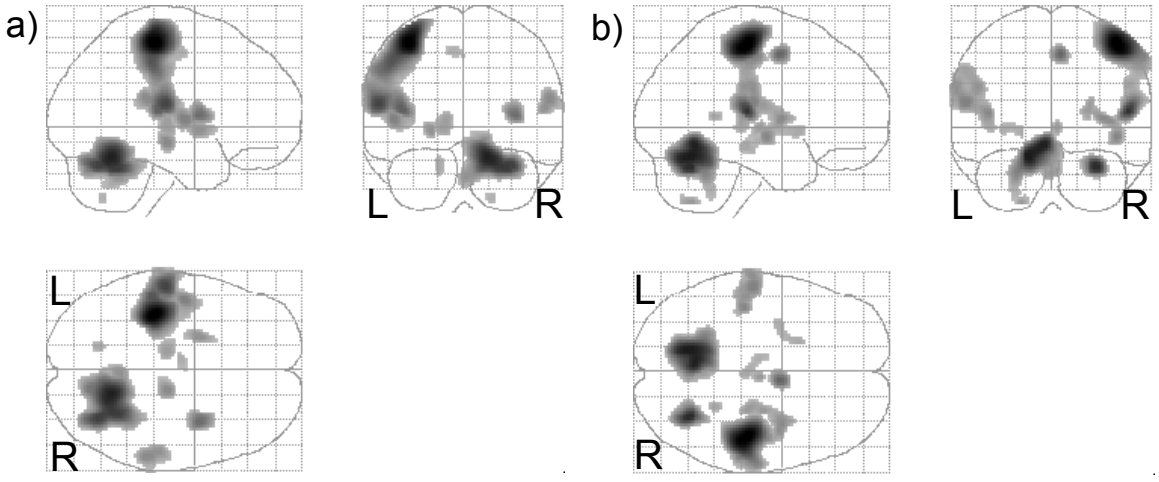

Figure 5.2: Regional Activations during finger tapping (Simple main effect of movement)
Results are displayed as statistical parametric maps on sagittal, coronal and transverse projections in stereotactic space. The greyscale areas indicate all significant voxels showing a movement-related activation at P< 0.001 (uncorrected). **5.2a)** Right hand **5.2b)** Left Hand

Table 5.2: Main Effects of Movement

Anatomy		MNI co-ordinates x	y	z	Z score	P (FWE-cor)	P (uncorrected)
5.2a) Right Hand							
Primary Motor (4a)	*L*	-36	-28	58	6.91	<0.001	
SMA / CMA	*L*	-6	-10	52	3.42	0.999	<0.001
Rostral CMA	*R*	4	-4	48	3.11	1	0.001
Cerebellar Lobule VI	*L*	-16	-66	-26	3.52	0.994	<0.001
	R	30	-54	-28	5.8	<0.001	<0.001
	R	32	-64	-26	5.71	0.001	<0.001
Cerebellar Lobule V	*R*	16	-56	-20	6.27	<0.001	<0.001
Cerebellum Lobule VIIIB	*R*	18	-62	-48	3.3	1	<0.001
Putamen	*L*	-22	2	-2	4.09	0.55	<0.001
Ventral posterolateral thalamus	*L*	-12	-20	2	3.8	0.884	<0.001
Substantia Nigra	*R*	14	-20	-10	4.26	0.347	<0.001
S II	*L*	-58	-20	16	5.61	0.001	<0.001
Insula	*L*	-42	-26	12	5.1	0.012	<0.001
	R	36	4	8	4.83	0.04	<0.001
Superior Temporal	*R*	56	-24	14	4.05	0.599	<0.001
	R	58	-32	20	4.25	0.35	<0.001
5.2b) Left Hand							
Primary Motor (4a)	*R*	44	-24	58	6.27	<0.001	<0.001
SMA / CMA	*R*	6	-2	50	4.61	0.1	<0.001
Cerebellar Lobule V	*L*	-6	-60	-12	5.74	<0.001	<0.001
Cerebellar Lobule V	*L*	-14	-60	-18	5.8	<0.001	<0.001
Cerebellar Lobule VI	*R*	30	-62	-26	5.56	0.001	<0.001
Cerebellum Lobule VIIIB	*L*	-20	-62	-50	3.73	0.933	<0.001
Putamen	*L*	-32	-2	0	3.37	1	<0.001
	L	-24	2	-2	3.3	1	<0.001
	L	-20	12	-2	3.44	0.999	<0.001
Substantia Nigra	*R*	2	-24	-12	3.47	0.998	<0.001
Ventral posterolateral thalamus	*L*	-8	-16	-8	3.32	1	<0.001
Mediodorsal thalamus	*R*	4	-16	0	3.73	0.933	<0.001
S II	*L*	-64	-20	26	3.91	0.78	<0.001
	L	-58	-20	18	4.18	0.431	<0.001
	R	52	-26	30	3.57	0.989	<0.001
Insula	*R*	36	0	6	3.99	0.673	<0.001
	R	44	-10	-6	4.07	0.568	<0.001
Superior Temporal	*L*	-42	-26	10	4.06	0.584	<0.001
	R	52	-24	12	5.38	0.003	<0.001
Precuneus	*R*	24	-46	8	3.53	0.994	<0.001

Table 5.2: Maxima of regional increases in rCBF during movement compared to baseline.

5.3.2.2 Changes in rCBF induced by rTMS (Main effect of rTMS)

The main effects of rTMS on rCBF in the motor system are shown in Table 5.3a & b and Figure 5.3. Results for the main effects of rTMS are reported at $P < 0.05$, using a small volume correction (16mm radius sphere centred on the maxima of the main effect of movement, Table 5.2a&b). In agreement with the data presented in Chapter 3, there is an increase in rCBF in the left primary motor cortex (the site of stimulation with 1Hz rTMS) and bilateral increases in rCBF in the pre-motor cortices. There are additional increases in rCBF in the left putamen, globus pallidus and in motor and non-motor areas of the right cerebellum. There are extensive decreases in rCBF bilaterally in motor and non-motor basal ganglia and cerebellum.

Figure 5.3

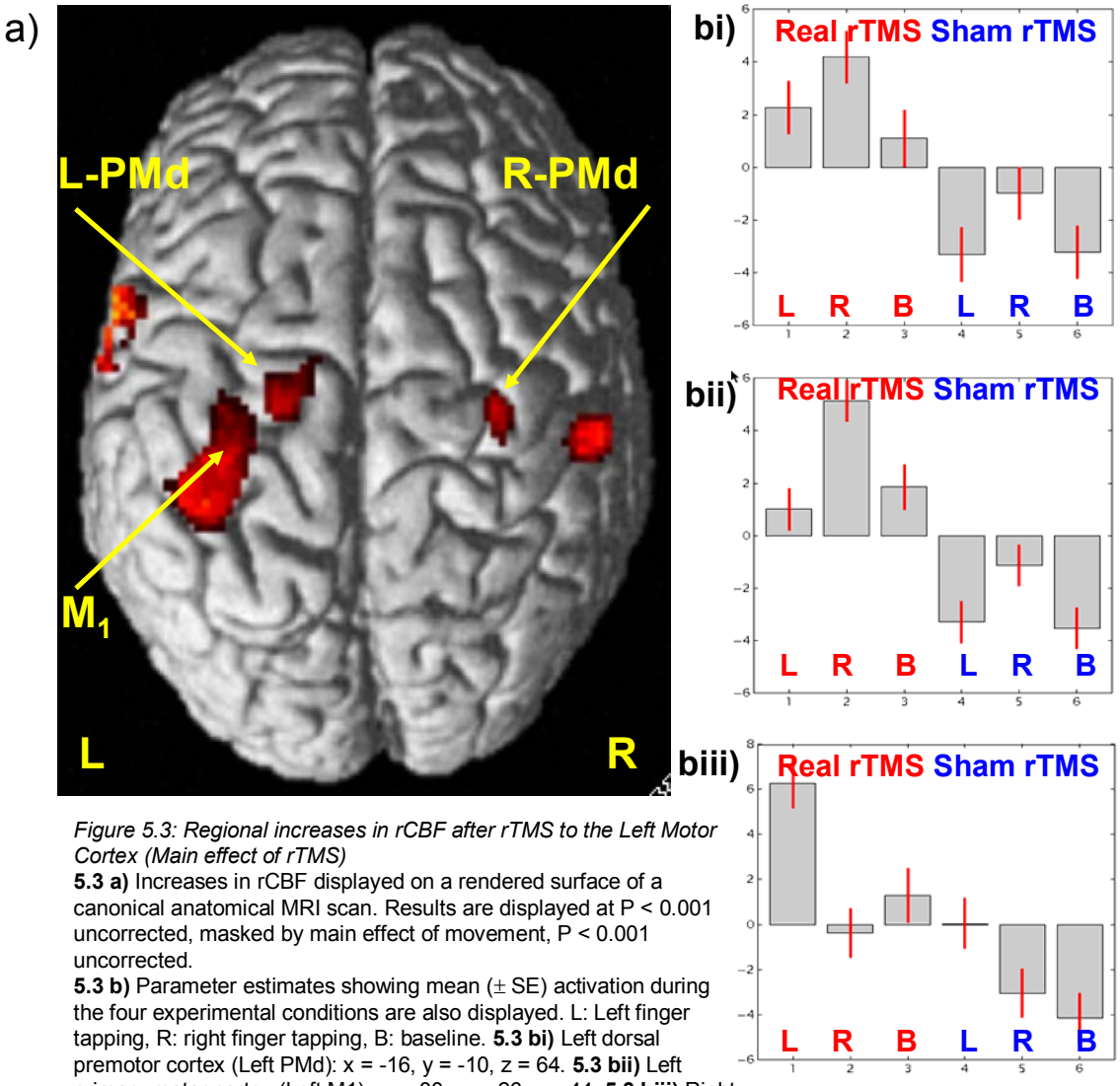

Figure 5.3: Regional increases in rCBF after rTMS to the Left Motor Cortex (Main effect of rTMS)
5.3 a) Increases in rCBF displayed on a rendered surface of a canonical anatomical MRI scan. Results are displayed at $P < 0.001$ uncorrected, masked by main effect of movement, $P < 0.001$ uncorrected.
5.3 b) Parameter estimates showing mean (± SE) activation during the four experimental conditions are also displayed. L: Left finger tapping, R: right finger tapping, B: baseline. **5.3 bi)** Left dorsal premotor cortex (Left PMd): x = -16, y = -10, z = 64. **5.3 bii)** Left primary motor cortex (Left M1): x = -30, y = -26, z = 44. **5.3 biii)** Right dorsal premotor cortex (Right PMd): x = 30, y = -18, z = 62.

Anatomy		MNI co-ordinates			Z score	P (SVC-cor)	P (uncorrected)
		x	y	z			
5.3a) Increased rCBF							
Motor Areas							
Primary Motor (4p)	*L*	-30	-26	44	5.6	<0.001	<0.001
PMd	*L*	-16	-10	64	3.93	0.009	<0.001
	R	30	-18	62	3.76	0.016	<0.001
CMA	*R*	8	-14	40	4.2	0.004	<0.001
Cerebellar Lobule VI	*R*	34	-58	-22	4.02	0.007	<0.001
Putamen	*L*	-28	2	12	4.04	0.005	<0.001
	L	-20	2	-8	5.64	<0.001	<0.001
	L	-32	-10	-2	5.17	<0.001	<0.001
Globus Pallidus	*L*	-25	-14	-2	3.75	0.017	<0.001
	L	-20	-8	-4	4.46	0.001	<0.001
Non-Motor Areas							
Cerebellar Lobule VIIA	*R*	24	-66	-44	4.41	0.002	<0.001
Intraparietal Sulcus	*L*	-32	-40	50	4.1	0.005	<0.001
Supramarginal Gyrus	*L*	-42	-38	50	4.08	0.005	<0.001
	R	54	-24	34	4.99	<0.001	<0.001
Post Central Gyrus	*L*	-55	-8	22	3.47	0.04	<0.001
	L	-64	-6	18	4.5	0.001	<0.001
Insula	*L*	-34	-5	4	4.57	0.001	<0.001
	R	42	-26	6	3.84	0.012	<0.001
5.3b) Decreased rCBF							
Motor Areas							
Cerebellar Lobule VI	*R*	22	-66	-14	4.52	0.001	<0.001
Cerebellar Lobule V	*L*	-12	-54	-18	3.53	0.033	<0.001
	L	-10	-46	-24	5.27	<0.001	<0.001
Cerebellar Lobule IV	*L*	-8	-46	-18	4.98	<0.001	<0.001
Middle Cerebellar Peduncle	*R*	4	-30	-26	Inf	<0.001	<0.001
Superior Cerebellar Peduncle	*L*	-2	-28	-16	5.04	<0.001	<0.001
	R	2	-26	-18	5.57	<0.001	<0.001
Ventral posterolateral thalamus	*L*	-10	-20	-8	3.88	0.011	<0.001
Non-Motor Areas							
Cerebellar Vermis VI	*R*	4	-72	-14	3.53	0.033	<0.001
Mediodorsal thalamus	*L*	-6	-22	4	4.91	<0.001	<0.001
	R	2	-10	2	4.59	<0.001	<0.001
Anterior Thalamic nucleus	*R*	6	-6	2	6.15	<0.001	<0.001
Supramarginal Gyrus	*L*	-62	-30	38	4.32	0.002	<0.001
Parietal Operculum	*R*	52	-26	14	3.57	0.03	<0.001
Posterior Temporal	*L*	-34	-30	18	3.41	0.047	<0.001
Superior Temporal Gyrus	*R*	64	-32	6	3.4	0.049	<0.001
Internal Capsule	*R*	32	2	16	4.55	0.001	<0.001
Insula	*R*	36	10	6	6.04	<0.001	<0.001
Precuneus	*R*	26	-52	10	4.92	<0.001	<0.001

Table 5.3a: Main effect of rTMS (increases): Maxima of regional increases in normalized rCBF after real-rTMS. 5.3b: Main effect of rTMS (decreases): Maxima of regional rCBF decreases after rTMS. P < 0.05 (small volume correction, using values in Table 5.2) and P < 0.001, uncorrected.

Table 5.4: Move-by-rTMS Interactions

Anatomy		MNI co-ordinates x	y	z	Z score	P (SVC-cor)	P (uncorrected)
5.4a) rTMS > Sham Right Move							
Non-Motor Areas							
Cerebellar lobule VIIB	*R*	26	-80	-48	3.19		0.001
Precuneus	*R*	2	-54	30	3.12		0.001
Frontal pole	*L*	-4	68	18	3.09		0.001
5.4b) rTMS < Sham Left Move							
Non-Motor Areas							
Cerebellar Crus I	*L*	-50	-72	-34	3.4		<0.001
Intraparietal Sulcus	*R*	42	-52	58	3.75		<0.001

Table 5.4: Maxima of regional increases (5.4a) and decreases (5.4b) in rCBF after rTMS. P < 0.05 (small volume correction using values in Table 5.2 and P < 0.001, uncorrected.

5.3.2.3 rTMS-induced changes in task-related activation (Movement-by-rTMS interaction)

The movement by rTMS interactions were different for right and left handed finger movements. During the paced finger tapping task performed with the right hand, there were increases in movement related activity in the lateral right cerebellum (non-motor area) after real rTMS (Figure 5.4a & Table 5.4a). During paced finger tapping performed with the left hand, there were decreases in movement related activity in the left lateral cerebellum (Crus 1, a non-motor area) (Figure5.4b & Table 5.4b) and right intraparietal sulcus after real rTMS.

Figure 5.4

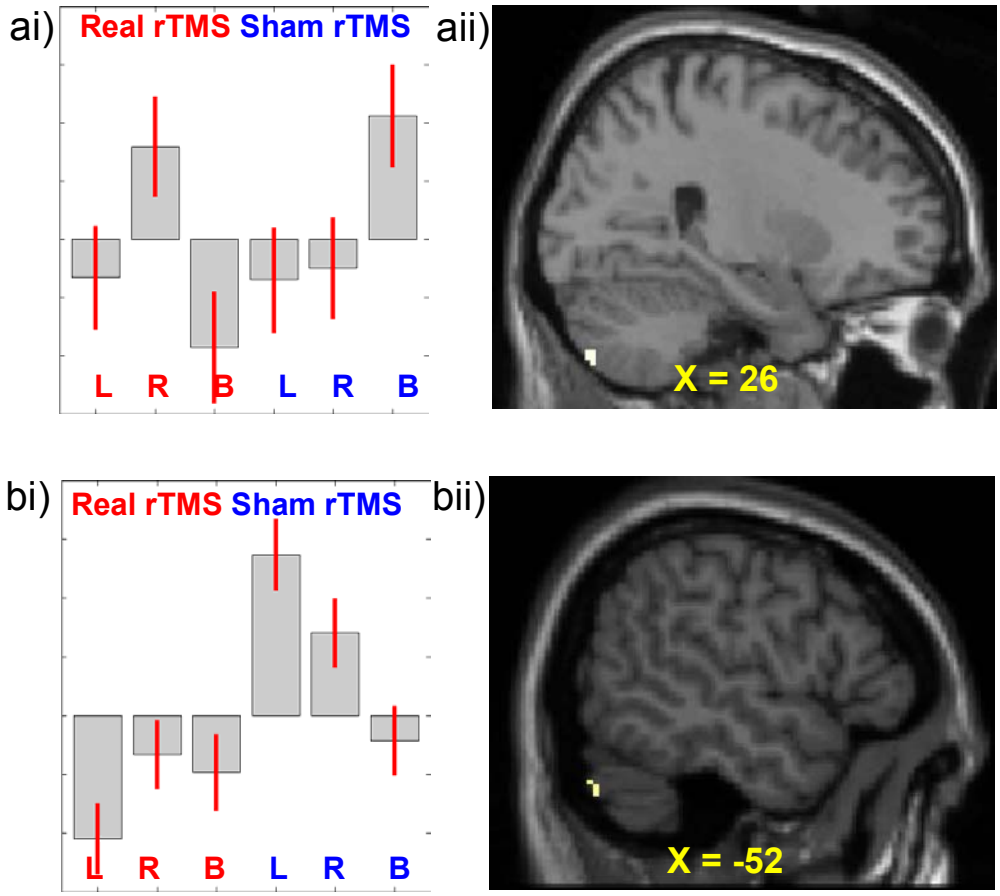

Figure 5.4: Areas of the brain showing different responses during movement after real-rTMS compared to sham-rTMS (Interaction between movement and rTMS).
5.4 ai) Parameter estimates and **5.4 aii)** localisation of activation for Right cerebellar site (x = 26, y = -80, z = -48) showing increased movement-related activity after rTMS.
5.4 bi) Parameter estimates and **5.4 bii)** localisation of activation for Left cerebellar site (x = 26, y = -80, z = -48) showing decreased movement-related activity after rTMS. Results are displayed on sagital sections of canonical anatomical MRI scans at P < 0.001 uncorrected.

5.3.2.4 Changes in effective connectivity between the site of stimulation, transcallosal M1 and motor areas (Psychophysiological interactions).

There were specific a priori hypotheses regarding the two PPIs performed using index areas based on the maxima of the main effect of rTMS. In line with the hypothesis described in Chapter 3, a significant positive PPI based on the maxima from the stimulated hemisphere, was interpreted as a reduction in the sensitivity of this area to inputs. In contrast, the transcallosal effects of 1Hz rTMS are thought to cause increased excitability. Therefore, a significant negative PPI was interpreted

as representing areas to whose inputs contralateral (right) M1 becomes more sensitive.

Figure 5.5a and Table 5.5a show the results of PPI analysis, using the synaptic activity (as indexed by rCBF) from the site of maximal rTMS-induced increase in the stimulated cortex as the physiological variable. Table 5.5a lists the co-ordinates of the maxima of sites shown in Figure 5.5a. After real rTMS, changes in activity in the right posterior non-motor cerebellum were associated with a reduction in the magnitude of the response of the index area (the site of rTMS).

Figure 5.5b and Table 5.5b show the results of the PPI analysis using the synaptic activity from the site of maximal rTMS-induced increase in the non-stimulated cortex as the physiological variable. Table 5.5b lists the co-ordinates of the maxima of sites shown in Figure 5.5b. As predicted, after real-rTMS, changes in activity in the right SMA, primary sensorimotor cortex and intraparietal sulcus were associated with an increase in the magnitude of the response of the index area (contralateral to the site of rTMS).

Table 5.5: Psychophysiological Interactions: maxima of rTMS effects

Anatomy		**MNI co-ordinates** x	y	z	**Z score**	**P** (SVC)	**P** (uncorrected)
5.5a) Positive PPI: -26 -18 68							
Non-Motor Areas							
Cerebellar Crus I	*R*	36	-90	-30	3.25	1	0.001
Inferior Frontal Gyrus	*L*	-58	12	26	3.11	1	0.001
Anterior Temporal Pole	*L*	-52	0	-42	3.11	1	0.001
5.5b) Negative PPI: 30 -18 62							
Motor Areas							
SMA	*R*	2	-14	76	3.43	0.999	<0.001
Non-Motor Areas							
Intraparietal Sulcus	*R*	50	-52	58	4.32	0.296	<0.001
Post central gyrus	*R*	46	-16	32	3.79	0.908	<0.001
Superior Temporal Cortex	*L*	-36	-22	0	4.01	0.67	<0.001

Table 5.5a: Maxima of main effect of rTMS in Left M1 as index area: Co-ordinates of brain regions to which the TMS site is less sensitive after rTMS. *5.5b*: Maxima of main effect of rTMS in Right M1 as index area: Co-ordinates of brain regions to which the TMS site is more sensitive after rTMS. $P < 0.05$ (small volume correction, using values in table 5.2) and $P < 0.001$, uncorrected.

Figure 5.5

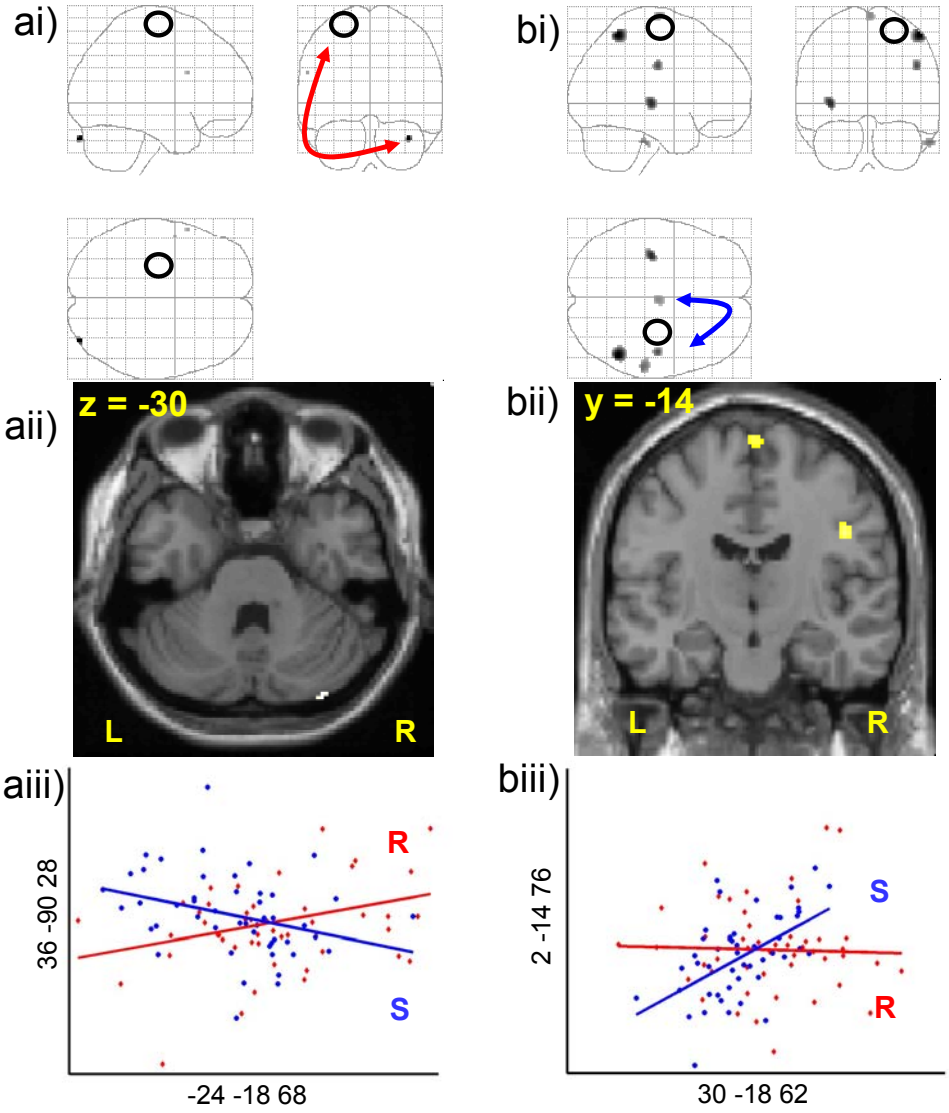

Figure 5.5: Changes in Effective Connectivity (Psychophysiological interaction) with the site of rTMS stimulation.
5.5 ai) Areas showing positive PPI with the site of rCBF increase in left sensorimotor cortex after rTMS (x = -24, y = -18, z = 68), displayed as statistical parametric maps in sagittal, coronal and transverse projections in stereotactic space. The greyscale areas show all significant voxels at P<0.001, uncorrected. The black circle shows the location of the region of interest used as the physiological variate in the interaction. **5.5 aii)** Localisation of right cerebellar site (x = 36, y = -90, z = -30) displayed on axial section of canonical anatomical MRI scan. **5.5 aiii)** Graphical representation illustrating the psychophysiological interactions between the site of rTMS region of interest (abscissa) and right cerebellum. Regression lines between the activity in the two regions have been fitted: sham-rTMS = 'S' (blue) and real-rTMS = 'R' (red).
5.5 bi) Areas showing negative PPI with the site of rCBF increase in right sensorimotor cortex after rTMS (x = 30, y = -18, z = 62) displayed as described in 5.5 ai. **5.5 bii)** Localisation of right SMA site (x = 2, y = -14, z = 76) displayed on coronal section of canonical anatomical MRI scan. **5.5 biii)** Graphical representation illustrating the psychophysiological interactions between the site of rTMS region of interest (abscissa) and right SMA.

5.3.2.5 Changes in effective connectivity between primary and non-primary motor areas

Figures 5.6a-d and Table 5.6a-h summarise the results of four PPIs looking for changes in effective connectivity between cortical motor areas activated during the left and right finger tapping task. There is a significant negative PPI between all the index regions (left M1, left SMA, right M1 and right SMA) and the right superior parietal cortex (Figures and Tables 5.6 & 5.7 a & bii).

In addition, the analysis based on activity in right sensorimotor hand area showed a significant negative PPI with the right premotor area (Figure and Table 5.7b). The analysis based on activity in the right supplementary motor area (Figures and Tables 5.7c-d) showed a significant positive PPI with left SMA and right ventrolateral thalamus. The implications of this profile of PPIs are discussed below.

Table 5.6: Psychophysiological Interactions: Maxima of Main Effects of Right Finger Tapping

Anatomy		**MNI co-ordinates** x	y	z	**Z score**	**P** (SVC-cor)	**P** (uncorrected)
Left M1 (-36 -28 58)							
5.6ai) Positive PPI							
Non-Motor Areas							
Superior Frontal Gyrus	*L*	-2	60	12	3.64		< 0.001
Superior Frontal Gyrus	*R*	6	48	28	3.13		0.001
Posterior Orbital Gyrus	*R*	24	12	-20	3.24		0.001
Precuneus	*R*	4	-52	28	3.64		< 0.001
5.6aii) Negative PPI							
Non-Motor Areas							
Intra Parietal Sulcus	*R*	32	-72	42	3.25		0.001
Inferior Temporal Sulcus	*R*	54	-46	-12	3.25		0.001
Superior Temporal Gyrus	*L*	-68	-12	-10	3.1		0.001
Left SMA (-6 -10 52)							
5.6bi) Positive PPI							
Non-Motor Areas							
Posterior Orbital Gyrus	*R*	24	10	-16	3.32		<0.001
Precuneus	*R*	6	-54	30	3.28		0.001
5.6bii) Negative PPI							
Non-Motor Areas							
Cerebellar Crus I	*L*	-56	-66	-22	3.21		0.001
Supramarginal Gyrus	*R*	50	-34	30	3.36	0.054	<0.001
Angular Gyrus	*R*	30	-78	54	3.48		<0.001

Table 5.6a: Co-ordinates of brain regions showing positive (ai) and negative (aii) PPIs with Left M1. *5.6b* Co-ordinates of brain regions showing positive (ai) and negative (aii) PPIs with Left SMA. P < 0.05 (small volume correction, using values in table 5.2) and P < 0.001, uncorrected.

Table 5.7: Psychophysiological Interactions: Maxima of Main Effects of Left Finger Tapping

Anatomy		MNI co-ordinates			Z score	P (SVC-cor)	P (uncorrected)
		x	y	z			
Right M1 (44 -24 58)							
5.7ai) Positive PPI							
NIL							
5.7aii) Negative PPI							
Motor Areas							
PMd	*R*	20	-2	52	3.3	0.062	<0.001
Cerebellar Lobule IV	*L*	-10	-42	-28	3.18		0.001
Non-Motor Areas							
Superior Parietal Lobule	*R*	42	-48	58	3.95		<0.001
Planum Temporale	*L*	-38	-24	4	4.23	0.003	<0.001
superior temporal gyrus	*L*	-32	8	-28	3.77		<0.001
superior temporal sulcus	*R*	56	-40	10	3.13		0.001
Hippocampus	*L*	-34	-32	-8	3.16		0.001
precuneus	*L*	-8	-52	34	3.16		0.001
Posterior Orbital Gyrus	*R*	26	42	-18	3.85		<0.001
Right SMA (6 -2 50)							
5.7bi) Positive PPI							
Motor Areas							
SMA	*L*	-2	-12	54	3.46	0.041	<0.001
Ventrolateral thalamus	*R*	16	-2	10	3.11	0.106	0.001
5.7bii) Negative PPI							
Motor							
CMA (caudal)	*R*	4	0	44	3.61	0.026	<0.001
Non-Motor Areas							
Superior Parietal Lobule	*R*	34	-52	56	3.74		<0.001
Supra Marginal Gyrus	*R*	50	-38	28	3.37	0.053	<0.001
superior temporal gyrus	*R*	60	10	-12	3.42		<0.001
Transverse Temporal Gyrus	*L*	-40	-26	8	3.35	0.056	<0.001
Cingulate Sulcus	*L*	-14	-26	46	3.24		0.001

Table 5.7a: Co-ordinates of brain regions showing positive (ai) and negative (aii) PPIs with Right M1. *5.7b* Co-ordinates of brain regions showing positive (ai) and negative (aii) PPIs with Right SMA. P < 0.05 (small volume correction, using values in table 5.2) and P < 0.001, uncorrected.

Figure 5.6

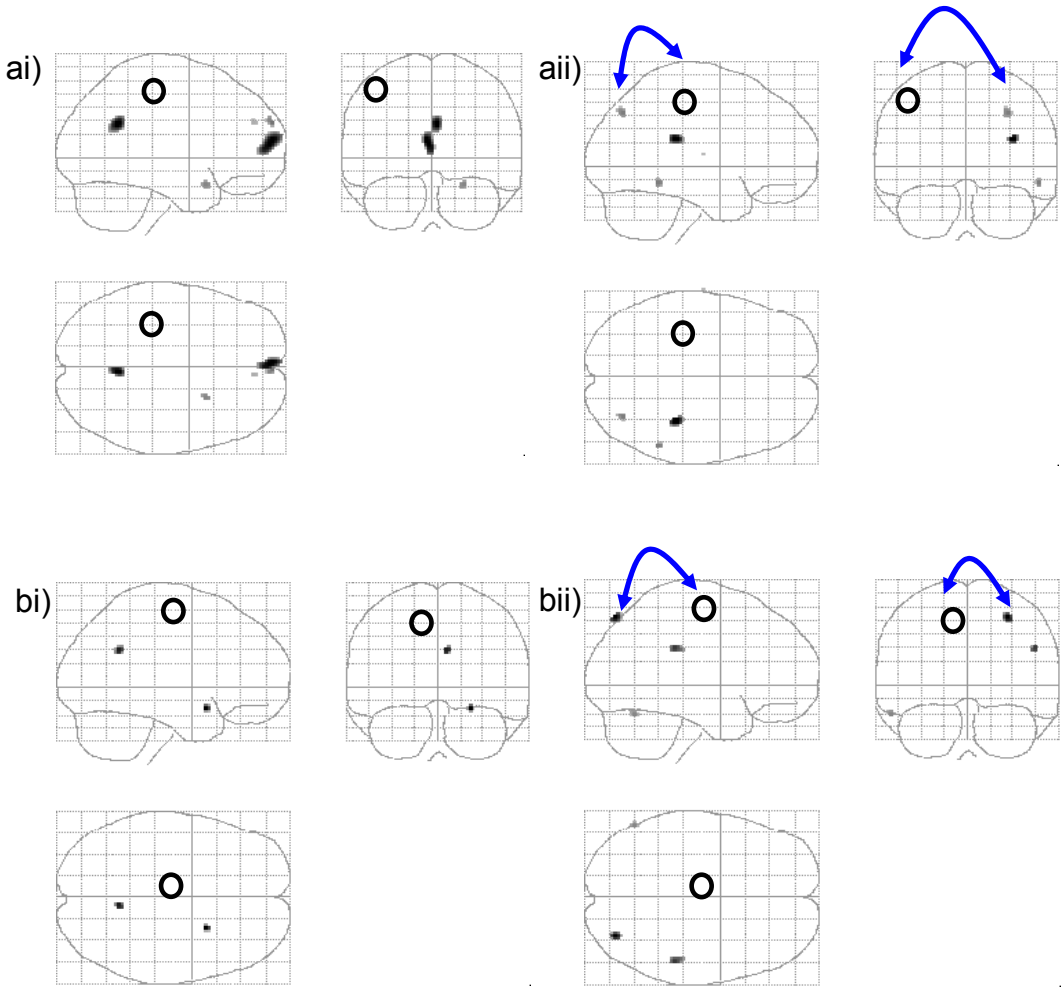

Figure 5.6: Changes in Effective Connectivity (Psychophysiological interaction) with Right finger tapping activations.
Areas showing **5.6 ai)** positive and **5.6 aii)** negative PPI with left sensorimotor region of interest (x = -36, y = -28, z = 58) during movement-related activity after real-rTMS compared to sham-rTMS, displayed as described for Figure 5.5 ai.
Areas showing **5.6 bi)** positive and **5.6 bii)** negative PPI with left SMA region of interest (x = -6, y = -10, z = 52) during movement-related activity after real-rTMS compared to sham-rTMS, displayed as described for Figure 5.5 ai.

Figure 5.7

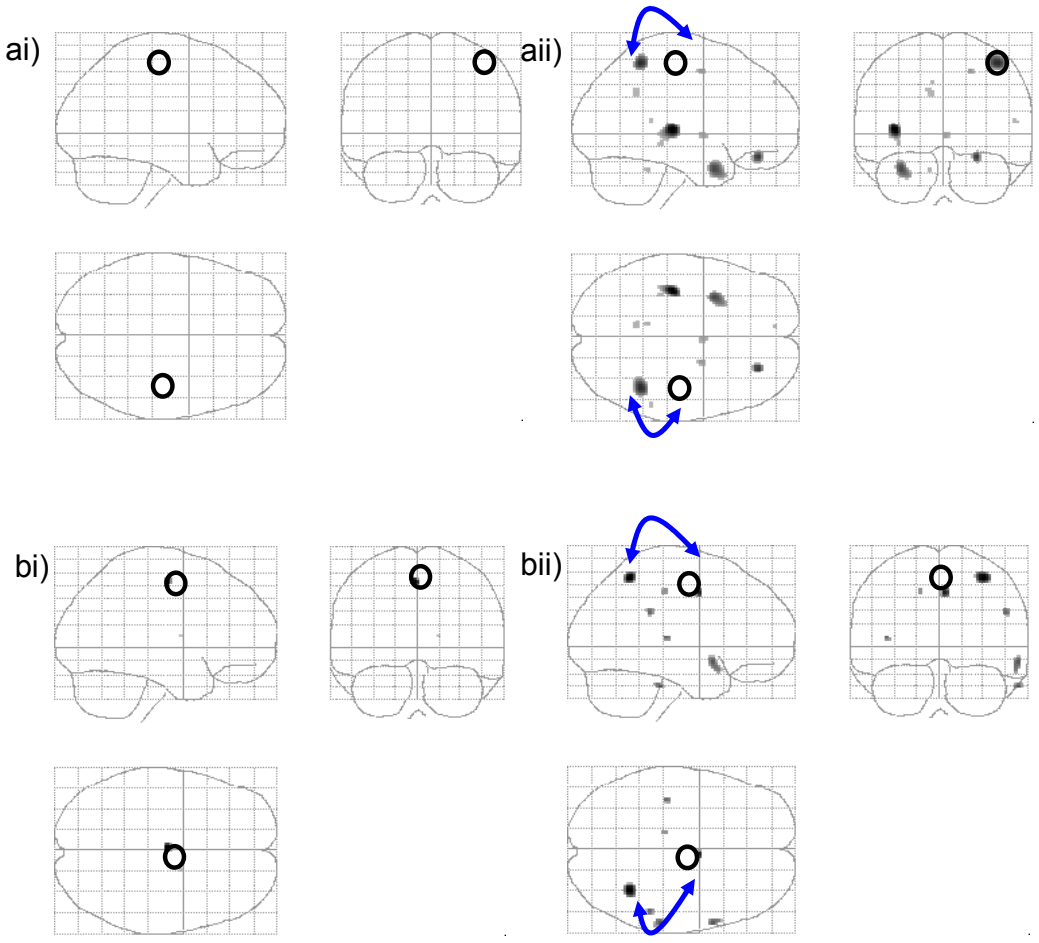

Figure 5.7: Changes in Effective Connectivity (Psychophysiological interaction) with Left finger tapping activations.
Areas showing **5.7 ai)** positive and **5.7 aii)** negative PPI with right sensorimotor region of interest (x = 44, y = -24, z = 58) during movement-related activity after real-rTMS compared to sham-rTMS, displayed as described for Figure 5.5 ai.
Areas showing **5.7 bi)** positive and **5.7 bii)** negative PPI with right SMA region of interest (x = 6, y = -2, z = 50) during movement-related activity after real-rTMS compared to sham-rTMS, displayed as described for Figure 5.5 ai.

5.3.2.6 Changes in effective connectivity with areas showing significant movement-by-rTMS interactions

Two psychophysiological interactions were performed using the areas in right and left cerebellum where a significant movement by rTMS interaction was seen (positive and negative interaction during right and left hand movement respectively) as index regions. When activity in the right cerebellum was used as the physiological component, there was a significant PPI with the right superior motor cerebellum and the left putamen and posterior ventrolateral thalamus (Figure 5.8a,

Table 5.8a); and a significant negative PPI with the left SMA (Figure 5.8b, Table 5.8b). When activity in the left cerebellum was used as the physiological component, there was a significant positive PPI with the right prefrontal cortex (x = 22, y = 12, z = -34) (Figure 5.8c, Table 5.8c).

Figure 5.8

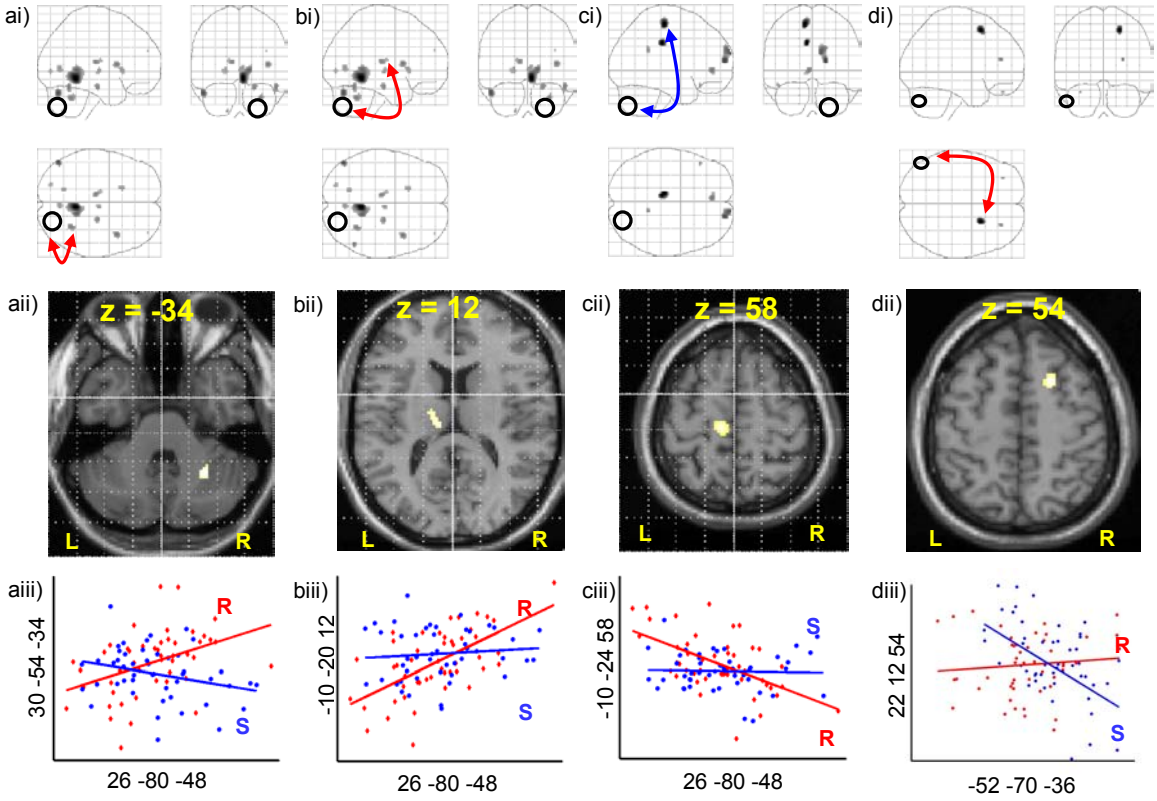

Figure 5.8: Changes in Effective Connectivity (Psychophysiological interaction) with movement by rTMS interaction sites.

5.8 a&bi) Positive PPI with right cerebellum (x = 26, y = -80, z = -48), **5.8 ci)** Negative PPI with right cerebellum (x = 26, y = -80, z = -48) and **5.8 di)** Positive PPI with left cerebellum (x = -52, y= =-70, z = -36). Results displayed as described for Figure 5.5 ai.

5.8 a–d ii) Anatomical localisation of sites with significant PPIs displayed on axial sections of a canonical structural MRI.

5.8 a-d iii) Graphical representations illustrating the psychophysiological interactions between index regions (abscissa) and **5.8 aiii)** right cerebellar nucleus (x = 30, y = -54, z = -34), **5.8 biii)** left thalamus (x = -10, y = -20, z = 12), **5.8 ciii)** left SMA (x = -10, y = -24, z = 58) and **5.8 diii)** right PMd (x = 22, y = 12, z = 54). Regression lines between the activity in the two regions have been fitted: sham-rTMS = 'S' (blue) and real-rTMS = 'R' (red).

Table 5.8: Psychophysiological Interactions: Maxima of Move-by-rTMS Interactions

Anatomy		MNI co-ordinates			Z score	P (SVC-cor)	P (uncorrected)
		x	y	z			
Right Cerebellum (26 -80 -48)							
5.8ai) Positive PPI							
Motor Areas							
Cerebellar lobule IV	*R*	6	-46	-8	4.6	0.005	<0.001
Cerebellar lobule V	*R*	30	-54	-34	3.56	0.03	<0.001
Cerebellar lobule VIIIA	*L*	-16	-64	-50	3.3		<0.001
Putamen	*L*	-18	18	2	3.38	0.059	<0.001
Posterior Ventrolateral thalamus	*L*	-10	-20	12	3.54	0.033	<0.001
Non-Motor Areas							
Cerebellar Crus I	*L*	-50	-72	-26	3.96		<0.001
Mediodorsal Thalamus	*R*	4	-14	0	3.41	0.047	<0.001
Precuneus	*R*	4	-70	4	3.37		<0.001
Precuneus	*R*	14	-46	2	3.77		<0.001
Insula	*R*	40	10	10	3.61	0.026	<0.001
Inferior occipital gyrus	*R*	52	-56	-18	3.57		<0.001
5.8aii) Negative PPI							
Motor Areas							
SMA	*L*	-10	-24	58	3.98	0.008	<0.001
Non-Motor Areas							
Inferior Frontal Sulcus	*R*	18	60	14	3.62		<0.001
Anterior Cingulate Sulcus	*L*	-4	44	0	3.41		<0.001
Precuneus	*R*	12	-46	26	3.26		0.001
Left Cerebellum (-50 -72 -34)							
5.8bi) Positive PPI							
Non-Motor Areas							
Superior Frontal Sulcus	*R*	22	12	54	3.8	0.86	<0.001
5.8bii) Negative PPI							
Motor Areas							
Cerebellar lobule V	*L*	-18	-52	-12	3.12	1	0.001
Non-Motor Areas							
Parietal Operculum	*L*	-52	-30	20	3.8	0.865	<0.001
Parietal Operculum	*L*	-42	-24	14	3.7	0.938	<0.001
Insula	*L*	-36	-6	10	3.28	1	0.001
Anterior Temporal	*R*	52	-24	14	3.22	1	0.001
Superior Temporal Sulcus	*L*	-60	-36	8	3.16	1	0.001
Anterior Temporal	*R*	48	-10	-6	3.83	0.838	<0.001

Table 5.8a: Co-ordinates of brain regions showing positive (ai) and negative (aii) PPIs with Right cerebellum. *5.8b* Co-ordinates of brain regions showing positive (ai) and negative (aii) PPIs with Left cerebellum. $P < 0.05$ (small volume correction, using values in table 5.2) and $P < 0.001$, uncorrected.

Figure 5.9

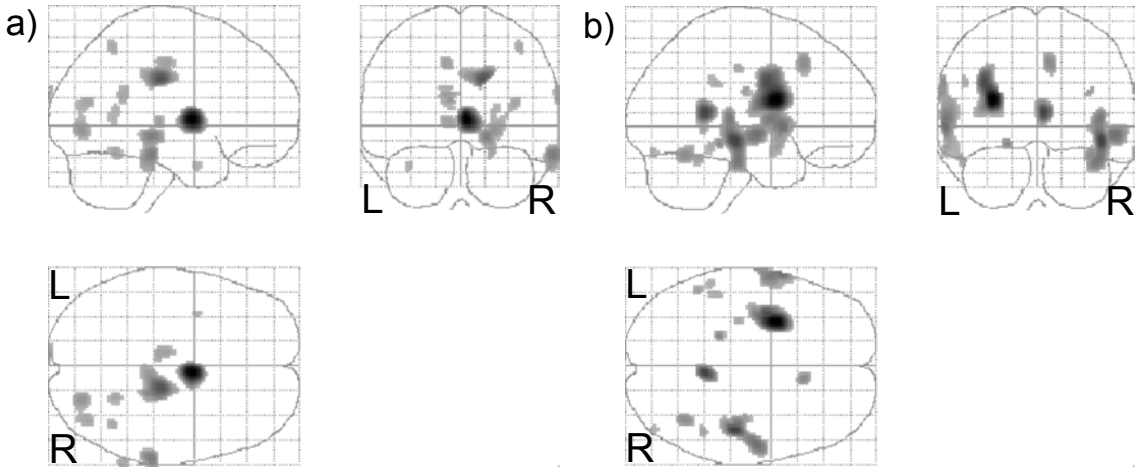

Figure 5.2: Differences in the Main Effect of rTMS between experiments
Results are displayed as statistical parametric maps on sagittal, coronal and transverse projections in stereotactic space. The grey scale areas indicate all significant voxels showing increased rCBF after 1Hz rTMS at P< 0.05 (whole volume corrected). **5.9a)** Expt 1> Expt 2 **5.9b)** Expt 1< Expt 2

5.4 Discussion

The discussion of this experiment will focus on three aspects of the results. First: the effects of 1Hz rTMS on rCBF with those seen in Chapter 3. Second: differences in the effects of rTMS on movement-related activity in the stimulated and non-stimulated hemisphere. Third: differences in movement-related changes in rCBF and connectivity of the motor network that may be task-dependent.

5.4.1 Main effect of rTMS

The first aim of this experiment was to replicate the findings presented in Chapter 3 pertaining to the main effect of 1Hz rTMS to left M1 at 90% resting motor threshold (RMT) on rCBF. Inspection of the data in Figures 3.4 and 5.3 and the maxima reported in Tables 3.3 and 5.3 suggest this has been achieved. It can be seen that there are increases in rCBF in the primary motor cortex in the stimulated left hemisphere following 1Hz rTMS, and bilateral increases in rCBF in the dorsal premotor cortices. There are also increases in rCBF in mesial motor areas, the putamen, cerebellum and parietal cortices in both experiments, and decreases in prefrontal and superior temporal regions. The decreases in rCBF seen in the cingulate motor area in Chapter 3 were not seen in this experiment. A formal statistical comparison between the main effects of rTMS in the two experiments is shown in Figure 5.9. There are significant differences between the two experiments (that could be related to the task), but these are not seen in the primary motor areas or lateral and medial premotor cortices.

As discussed in Chapter 3, remote effects of rTMS may represent a conditioning effect of rTMS caused by a spread of excitation via cortico-cortical connections, or they may reflect compensatory responses to maintain normal function of the motor system. In light of the similarities in the main effects of rTMS, between these two experiments, using very different motor paradigms, the majority of the remote effects are more simply explained by the first mechanism.

In Chapter 3, two mechanisms were outlined by which rTMS could decrease cortical and cortico-spinal excitability while increasing rCBF (synaptic activity). Increased rCBF is caused by increased synaptic activity therefore the increase in rCBF contralateral to the site of stimulation reflects increased synaptic activity following

1Hz rTMS. The literature reviewed in Chapter 2 suggests that a loss of transcallosal inhibition is a likely cause of increased cortical excitability in the non-stimulated primary motor cortex. During the period of reduced interhemispheric inhibition, any inputs to the non-stimulated M1 will evoke disinhibition in M1. This may be associated with increased rCBF even under resting conditions, explaining the increased rCBF in the unstimulated hemisphere.

5.4.2 Differences in task-related movement after rTMS

The second aim of this experiment was to examine the functional correlates of the contralateral rCBF changes described in Chapter 3. To enable this, right and left hand movements were included in this second experiment. During right finger tapping there was increased activity in right cerebellum after 1Hz rTMS, whereas during left finger tapping there was decreased activity in left cerebellum. This suggests that the functional correlates of changes in synaptic activity (rCBF), induced by 1Hz rTMS are different at the site of stimulation, and in the contralateral hemisphere. This is in keeping with the differences in cortical excitability seen in the stimulated and unstimulated hemispheres (see Chapter 2).

Kobayashi et al report an improvement in a sequential key-pressing task when performed with the hand ipsilateral to the site of stimulation (Kobayashi et al., 2004). They postulate that this may be due to a 'release' from transcallosal inhibition. In the current experiment, a very simple task was performed; with no real capacity for improvement (the rate at which subjects tap was paced). It is therefore possible that instead of seeing an improvement in performance with the hand ipsilateral to the site of stimulation (left hand), a decrease in movement-related activity is observed in the cerebellum because the same level of performance can be achieved more efficiently. Conversely, when performing paced finger tapping with the right hand more activity is seen in the right cerebellum, compensating for decreased excitability of the left M1. Task performance was not impaired, suggesting that this may contribute to compensatory mechanisms.

5.4.3 Changes in coupling within the motor system following rTMS may be task dependent

The task used in this experiment is different to that described in Chapter 3. The auditory paced (2 Hz), visually cued finger tapping task used here led to activations in the primary motor cortex, cerebellum and SMA. The visual cues guiding finger movements followed an obvious and invariant sequence, and were easily 'over-learned'. Studies by Jenkins et al. show increased responses during new sequences, compared to pre-learnt sequences in lateral motor areas (Jenkins et al., 1994). In Chapter 3 the task required selection of which finger to move as subjects were required to generate a 'random' sequence. The slower rate of tapping (0.5 Hz) meant that there was more time for motor preparation. Passingham has suggested that more anterior cortical motor regions are engaged during these processes (Passingham, 1997). This is reflected in the activations reported as the main effect of movement in Chapter 3, which included dorsal pre-motor and dorsolateral prefrontal areas (see Figure 3.3 and Table 3.2). It is therefore not surprising that the two different experimental tasks result in different patterns of motor activation.

In addition to the differences in the main effect of movement seen in the two experiments, there are marked differences in the movement by rTMS interactions. In Chapter 3, increases in movement-related activation in left primary motor cortex and right premotor cortex (ipsilateral to the moving hand) are seen following rTMS. The data presented in Chapter 4 suggested that the increased movement-related activity in right PMd is implicated in maintaining task performance. The analysis of effective connectivity presented in Chapter 3 suggests that during a period of abnormal excitability, induced in superficial M1 (Area 4a), there is increased coupling between premotor areas (PMd and SMA) and an inferomedial area of M1 (Area 4p). This is the same part of M1 that showed increased motor-related activity after rTMS. The data presented in this chapter do not show this pattern. Following rTMS, there are no increases in movement-related activity in M1 or other cortical motor areas for right or left finger tapping. There is an increased movement-related response in the right cerebellum during right finger tapping and decreased movement-related response in the left cerebellum and right intraparietal sulcus during left finger tapping. The changes in effective connectivity seen with the motor

areas (M1 and SMA), derived from the maxima of the main effect of right and left hand movement reflect this difference. With both right and left finger tapping, a negative PPI is seen between the index area and the right intraparietal sulcus. This may reflect increased responsiveness of the right M1 and SMA to parietal inputs, for example during the period of increased cortical excitability in the non-stimulated hemisphere, or decreased input from parietal cortex to left M1 and SMA following rTMS. Given the increase in movement-related activity in right cerebellum, increased movement-related coupling between cerebellar areas and thalamus, and decreased coupling between cerebellum and secondary motor areas during right finger movements, motor performance may be maintained by compensatory activity in cerebello-thalamic systems when left M1 excitability is reduced.

5.5 Conclusion

This experiment replicates the results presented in Chapter 3 pertaining to the effects of low-intensity 1Hz rTMS to the primary motor hand area on neural activity in local and remote brain regions. This experiment also reinforces the position that increases in rCBF (as observed in the stimulated and non-stimulated motor cortices) can reflect increased and decreased cortical excitability, and therefore changes in rCBF do not map directly to changes in regional excitability. The differences in movement by rTMS interaction with left and right hand movements also suggests that increases and decreases in cortical excitability have measurable effects on the network of areas engaged during a motor task and that these are widespread with an asymmetric organisation.

This experiment provides additional evidence that the adult human motor system is able to maintain task performance during focal changes in excitability, by increasing movement-related activity in distal components of the motor network. The differences in movement by rTMS interactions and rTMS effects on movement-related coupling reported in this chapter and Chapter 3 suggest that compensatory activity in the motor system after 1Hz rTMS may depend on the specific task that is being performed. This finding may generalise to other lesions, such as stroke.

Chapter 6

The effects of 1Hz rTMS on motor activity: characterised with fMRI and dynamic causal modelling.

6.1 Introduction

Aims of Experiment 4:

1. Explore the anatomical details of M1 plasticity using fMRI.
2. Explore the functional sequelae of rTMS effects on inter-regional coupling using dynamic causal modelling.

In Chapter 3, changes were seen in movement-related responses in the primary motor cortex, inferior and medial to the site of stimulation. These were attributed to a possible remodelling of the somatotopic representations of finger movement in primary motor cortex. Previous experiments have shown that altering cortical excitability with TMS (in combination with manipulations to reduce GABA-ergic inhibition) can leading to remodelling of motor cortex as measured with TMS techniques (Ziemann et al., 2002). To examine this potential remodelling further, this final experiment uses the improved spatial resolution of functional magnetic resonance imaging (fMRI) to assess changes in motor representations in single subjects. Recent work with has confirmed early PET findings (Colebatch et al., 1991;Grafton et al., 1991) that multiple, overlapping sensorimotor representations of distinct hand and finger movements exist in human primary motor cortex (Sanes et al., 1995;Rao et al., 1995), and that it is possible to resolve individual finger movements with fMRI (Indovina and Sanes, 2001).

In this experiment a simple visually cued and paced (1Hz) task was used, with the order of cued finger tapping following a random sequence. This experimental design controls the number of movements with each finger, which is important for somatotopic mapping, while cueing movements in an unpredictable sequence, which engages premotor cortex (Jenkins et al., 1994).

In addition to providing improved spatial resolution, fMRI data can be acquired with a much finer temporal resolution than PET data. Therefore dynamic causal modelling (Friston et al., 2003) can be used to detect changes in connectivity or

coupling among motor areas as a result of rTMS. In this chapter DCM will be used to investigate the effect of rTMS on the efficacy of connections between the premotor cortices and the primary motor cortex during a motor task. The analyses of effective connectivity presented in Chapter 3 suggest that, after 1Hz rTMS, there is an increase in movement-related coupling or effective connectivity between the dorsal premotor cortex, the SMA and the primary motor cortex. However, it is not clear if this represents an increase in the strength of inputs from the premotor areas or an increase in the excitability or responsiveness of the primary motor cortex to the inputs. Dynamic causal modelling was used to resolve this ambiguity by examining which of the connections between these areas are significantly modulated by rTMS.

The data presented in Chapters 3 and 4 suggest a role for the non-stimulated premotor cortex (ipsilateral to the moving hand) in maintaining task performance after rTMS, but it is not clear how this is achieved. In this final experiment, DCM will be used to examine the changes in the connectivity of the right premotor cortex, left premotor and primary motor cortex following rTMS. This may provide some mechanistic insights into how the right premotor cortex contributes to motor performance during altered cortical excitability.

6.2 Materials and Methods

6.2.1 Subjects

Six healthy, right-handed volunteers (two female) aged between 26 and 48 (mean age: 33), with no history of neurological disorder or head injury, were recruited from the database of volunteers at the Functional Imaging Laboratory, Institute of Neurology, University College London, UK. Written informed consent was obtained from all participants. The study was approved by the joint ethics committee for the National Hospital for Neurology and Neurosurgery and the Institute of Neurology.

6.2.2 Study design

The study conformed to a 2x2x2 factorial design, with two levels per factor: "intervention" (real-rTMS versus sham-rTMS), "movement" (movement versus rest) and “vibration” (vibrotactile stimulation versus none). Figure 6.1 illustrates the study design. Real and sham-rTMS were given on two separate days, at least one week apart. The order of intervention was counterbalanced across subjects. The effects of rTMS on movement and vibration-induced changes in synaptic activity were assessed by fMRI measurements of Blood Oxygenation Dependent signal (BOLD). Within each scanning session the order of the four conditions alternated. The order of conditions was kept constant within a subject between sessions, but counterbalanced across subjects. The effects of the ‘vibration’ factor are not presented in this thesis.

6.2.3 1Hz Repetitive transcranial magnetic stimulation (rTMS)

rTMS was performed in an identical manner to that described in Chapter 3 for real rTMS. Sham rTMS was performed using the same MagStim TMS coil as for real rTMS, but at an intensity of 20% RMT. This was administered to provide scalp stimulation to control for somatosensory input during rTMS.

Figure 6.1

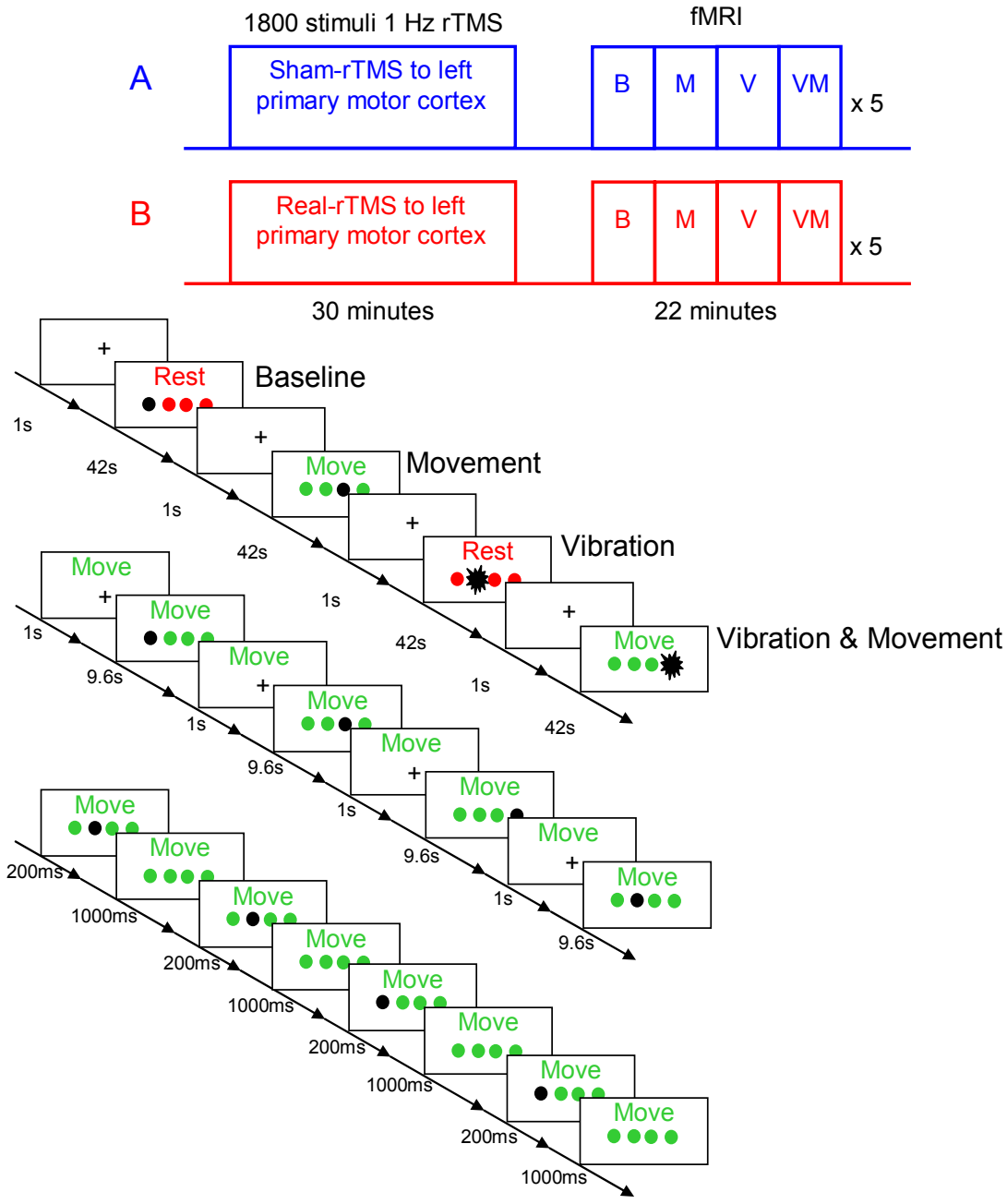

Figure 6.1: Experimental design.
Subjects received 1Hz real or sham rTMS on separate days. Changes in synaptic activity were mapped using BOLD fMRI. 340 scans were acquired over 22 minutes after the end of rTMS. The order of intervention (real v sham rTMS) and experimental conditions were counterbalanced across subjects.

6.2.4 Motor Task

Subjects underwent one 15 minute session of fMRI on each of the two separate days. All fMRI sessions were completed within 22 minutes after 30 minutes of 1Hz rTMS to the motor cortex. There were four conditions, each lasting 42.4s: baseline ("B"), vibration alone ("V"), paced finger movement alone ("M") and vibration with finger tapping ("VM"). Subjects were required to watch a display indicating whether they should tap their finger (green visual cues) or remain still (red visual cues). Movement was cued at 1Hz by flashes of cues corresponding to each finger. During the movement and vibration with movement conditions, subjects were required to execute a single button press with the indicated finger in synchrony with the visual cues. During the baseline and vibration conditions they were instructed to watch the display, but not move. During all conditions there were eight consecutive visual cues / vibrations / presses of one finger, before switching to another. The order of finger movements was random. To ensure a stable level of task performance, all subjects practiced the task for ten minutes prior to rTMS on each session.

Subjects' responses were made on four buttons, set under their fingertips on a response pad. Each response pad had a hollow centre, in which was located a plastic point arranged to be in light contact with the finger pad. Each plastic point was mounted on a piezoelectric component (T220-H3BS-304, Piezo Systems, Cambridge, USA) to deliver discrete vibrotactile stimulation to each fingertip. All responses were recorded on a personal computer (Dell PC) using COGENT 1.25v Cognitive Interface Software (Wellcome Dept. of Imaging Neuroscience, London, UK). The data were analysed using Matlab 6.5 (Mathworks, Sherborn, MA).

6.2.5 fMRI Data Acquisition

Subjects lay supine, with head fixation provided by foam pads. Visual instructions were projected onto a screen at the end of the scanner bore, and viewed via a mirror mounted on the head-coil. Headphones and earplugs were provided. Functional imaging data were acquired using an Allegra MR scanner at 3 Tesla (Siemens, Erlangen, Germany) with a T2*-weighted echo-planar image (EPI) sequence (echo time = 30 ms, repeat time = 2860 ms, resolution = 3 x 3 x 2mm, with 1mm gap between slices, 44 axial slices, flip angle = 90 degrees).

6.2.6 Structural MRI Acquisition

In all subjects, the position of the centre of the eight-shaped TMS coil was marked on the skull with a capsule containing cod liver oil. High-resolution anatomic structural images were acquired after rTMS stimulation, with the TMS surface markers in place, using an Allegra MR scanner at 3 Tesla (Siemens, Erlangen, Germany) with a T1 MDEFT sequence (echo time = 2.48 ms, repeat time = 7.92 ms, inversion time = 910 ms, 1 mm isotropic resolution, sagittal slices). This structural image also excluded asymptomatic structural brain abnormalities. In all subjects the cod liver oil capsule marking the motor hot spot was clearly visible, located over the central sulcus. TMS coil placement scans for all subjects are shown seen in Figure 6.2.

Figure 6.2

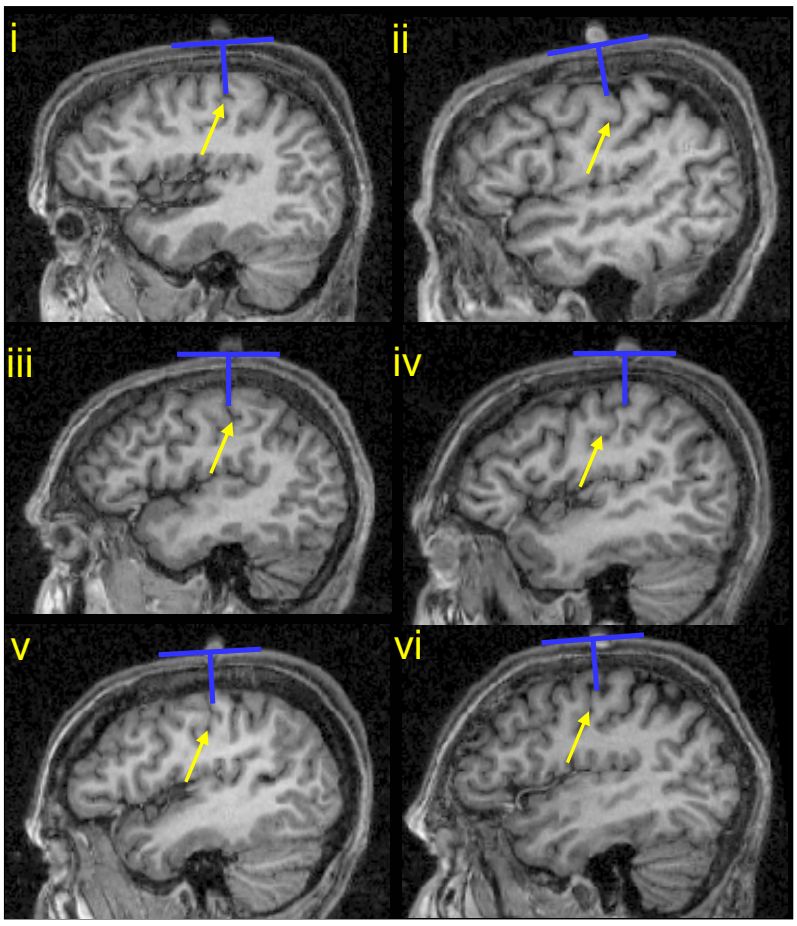

Figure 6.2: Position and orientation of TMS coil (blue) relative to the central sulcus (yellow arrow) in all subjects.

6.2.7 Image Analysis

All image analysis was performed using Statistical Parametric Mapping software, SPM2 (Wellcome Department of Imaging Neuroscience, UCL, UK. http://www.fil.ion.ucl.ac.uk/spm). For each subject, the first five volumes were discarded to allow steady-state magnetisation. The remaining 335 functional images from both sessions (670 volumes in total) were realigned to the first image of the sham-rTMS session by rigid body transformation to correct for head movements and phase-shift during volume acquisition (Friston et al., 1995a), and unwarped as described in Chapter 2. All images were then normalised to a standardised anatomic space (Talairach and Tournoux, 1988), by matching to a standardised EPI template using linear and non-linear spatial transformations (Friston et al., 1995a). Each image was smoothed with an isotropic Gaussian kernel of 6 mm full-width at half-maximum, to accommodate inter-subject differences in anatomy and enable the application of Gaussian Field corrections during inference (Friston et al., 1995a).

Two separate analyses were performed. The aim of the first analysis was to examine differences in the location of the maxima for individual finger movements after real and sham rTMS. A general linear model was specified that included 32 regressors modelling the task (baseline, vibration, movement, vibration with movement) separately for each finger under each condition of treatment (real-rTMS versus sham-rTMS). Incorrect presses or misses were modelled separately. This statistical model enabled localisation of activations associated with movement of each finger individually before and after rTMS. Data from each subject were analysed separately. For all subjects the main effect of movement was used to constrain the search for finger movement and rTMS interactions. For each subject the maxima of the simple main effect of movement for index, middle, ring and little fingers after sham rTMS were displayed on individual subjects' MRI scans. The maxima of the main effect of movement of the index and little fingers were examined for rTMS effects.

The aim of the second analysis was to determine the effects of rTMS on the coupling between cortical motor areas involved in task performance. A second,

simpler linear model was used to identify regions of interest which would be used in a series of dynamic causal models (DCMs). This model included five regressors per session (real and sham rTMS): rest, vibrotactile stimulation, movement, movement and vibrotactile stimulation and a new condition that specified the onset of changes between tapping movements with different fingers ('switch' condition). Misses or incorrect presses were modelled separately. The maxima of the ensuing SPM analysis defined the regions or nodes of the DCM. Note that this model does not include the effects of individual fingers, and provides a simpler characterisation of the functional anatomy.

The first set of DCMs examined the effect of rTMS on the efficacy of connections between primary and premotor cortices. Maxima were identified in left premotor cortex from the main effect of movement and in primary motor cortex from the interaction between 'switch' and rTMS. Two DCMs were examined allowing for rTMS induced plasticity in afferents to M1 and self connections intrinsic to M1. The aim of using these models was to disambiguate between changes in the strength of intrinsic and extrinsic connectivity as explanations for changes in motor excitability. Using Bayesian model comparison it was possible to test whether one or other of the models was a better explanation if the observed responses. The two models are shown in Figure 6.9.

The second DCMs examined the effect of rTMS on the efficacy of connections between primary motor cortex and mesial motor areas (SMA/CMA). Maxima were identified in left SMA/CMA from the main effect of movement, and in the primary motor cortex from the interaction between movement and rTMS. The two models are shown in Figure 6.10.

The third DCMs explored the contribution of the right premotor cortex. The interactions between three regions were examined. The regions of interest were the maxima of the main effect of movement in Left PMd and the maxima of the interaction between rTMS and 'switch' in M1 and Right PMd. The two models are shown in Figure 6.11. The question here was; does R PMd mediate its effects on L M1 directly or vicariously through L PMd. This question was addressed by seeing if an increase in right to left PMd connections had more evidence than left to right.

The inputs for the dynamic causal models comprised rTMS (1 or 0 depending on the session), switch and movement. Each model was estimated separately for each subject. For each model fMRI responses (sphere of radius 6mm) were selected as described above (see Table 6.1 for the maxima of the regions of interest). Principle eigenvariates were extracted from all regions and entered into the DCM analysis to estimate intrinsic connections and how these were influenced by the factor rTMS. Bayesian inferences were based on the probability that changes in the coupling parameters exceeded 0. In each case, alternative models were compared using Bayes Factors as described Penny et al. to see if either model provided a better description of the data (Penny et al., 2004).

6.3 Results

Subjects did not report any adverse side effects during the course of the study, nor were any motor responses evoked during the 30 minutes of rTMS. Mean resting motor threshold was 53%, ranging from 45% to 62% of maximum output of the MagStim-rapid stimulator.

6.3.1 Behavioural Data

Subjects made between zero and twelve mistakes (incorrect presses, missed presses) per session during fMRI scanning. The average numbers of mistakes per session were 3 and 5 for sham and real sessions respectively. A two-tailed t-test showed no significant difference in the numbers of mistakes per session.

6.3.2 Imaging Data

6.3.2.1 Somatotopic mapping in the primary motor hand area.

All subjects showed a stereotypical pattern of activation in the anterior bank of the central sulcus (primary motor area) during movement. This contrast was used to constrain test of individual finger movements (Figures 6.3-8a & b). For each subject the maxima of the effect of movement for index, middle, ring and little fingers after sham rTMS were displayed on the individuals' structural MR scan (Figures 6.3-8 c). In the majority of subjects it is possible to detect distinct but overlapping areas of activation for individual finger movements. The maxima for individual finger movements in primary motor cortex are reported in Table 6.2. The maxima of index and little finger movement following real (red) and sham (blue) rTMS are shown in Figures 6.3-8 d & e. Inspection of the data from all six subjects reveals no consistent pattern in the change of locations of these maxima following rTMS (see also table 6.1). Subjects 1 and 4 show shift towards a more inferior activation during index finger movement after real rTMS as hypothesised, however this was not consistently observed in other subjects.

Table 6.1 Motor Mapping

			MNI Co-ordinates of peak activation			Z-score	P value	
		rTMS	x	y	z		FWE	UC
Subject 1	ME		-36	-20	56	Inf	P<0.001	
	Index	Sham	-36	-20	58	4.92		P<0.001
		Real	-36	-20	56	2		P<0.001
	Middle	Sham	-36	-20	58	5.94		P<0.001
		Real	-34	-20	56	4.32		P<0.001
	Ring	Sham	-34	-22	56	5.9		P<0.001
		Real	-34	-18	56	4.49		P<0.001
	Little	Sham	-36	-18	56	5.3		P<0.001
		Real	-34	-20	56	9.07	P<0.001	
Subject 2	ME		-40	-20	56	6.06	P<0.001	
	Index	Sham	-40	-22	56	1.87		P<0.05
		Real	-32	-18	58	2.1		P<0.05
	Middle	Sham	-40	-24	50	2.35		P<0.001
		Real	-42	-18	56	2.17		P<0.05
	Ring	Sham	0	0	0	0		
		Real	-34	-22	54	1.83		P<0.05
	Little	Sham	-40	-22	58	5.32		P<0.001
		Real	-44	-20	64	1.82		P<0.05
Subject 3	ME		-32	-28	58	Inf	P<0.001	
	Index	Sham	-34	-28	54	6.15	P<0.001	
		Real	-32	-28	58	6.78	P<0.001	
	Middle	Sham	-32	-28	58	7.37	P<0.001	
		Real	-34	-28	56	7.42	P<0.001	
	Ring	Sham	-32	-28	56	Inf	P<0.001	
		Real	-34	-28	56	Inf	P<0.001	
	Little	Sham	-30	-28	60	7.74	P<0.001	
		Real	-34	-28	56	Inf	P<0.001	
Subject 4	ME		-38	-30	56	Inf	P<0.001	
	Index	Sham	-36	-30	70	4.53		P<0.001
		Real	-36	-28	56	4.37		P<0.001
	Middle	Sham	-38	-30	56	3.51		P<0.001
		Real	-38	-30	54	5.47	P<0.001	
	Ring	Sham	-36	32	56	3.98		P<0.001
		Real	-38	-30	56	Inf	P<0.001	
	Little	Sham	-42	-30	60	6.08	P<0.001	
		Real	-36	-30	56	8.79	P<0.001	
Subject 5	ME		-40	-18	62	Inf	P<0.001	
	Index	Sham	-38	-18	58	6.11	P<0.001	
		Real	-38	-18	56	7.28	P<0.001	
	Middle	Sham	-40	-20	62	6.75	P<0.001	
		Real	-38	-18	60	6.99	P<0.001	
	Ring	Sham	-40	-22	58	6.01	P<0.001	
		Real	-40	-18	62	6.52	P<0.001	
	Little	Sham	-40	-18	60	6.67	P<0.001	
		Real	-38	-20	62	7.56	P<0.001	
Subject 6	ME		-36	-24	58	Inf	P<0.001	
	Index	Sham	-36	-26	60	5.11	P<0.05	
		Real	-42	-22	56	3.86		P<0.001
	Middle	Sham	-36	-24	58	5.33	P<0.05	
		Real	-38	-24	58	3.69		P<0.001
	Ring	Sham	-36	-24	58	4.7		P<0.001
		Real	-36	-22	56	3.07		P<0.001
	Little	Sham	-34	-24	60	6.78	P<0.05	
		Real	-36	-24	60	4.5		P<0.001

Table 6.2: Maxima of simple main effect of individual finger movement.

Figure 6.3: Motor Mapping Subject 1

6.3 a

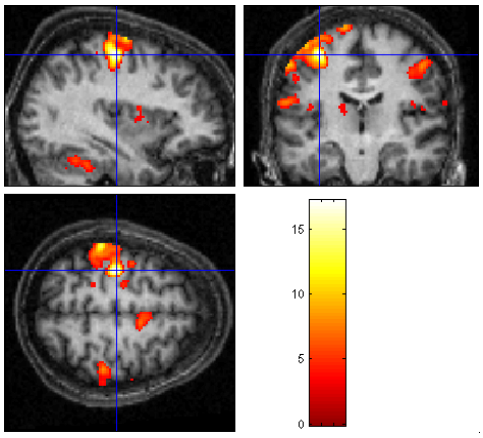

6.3 b

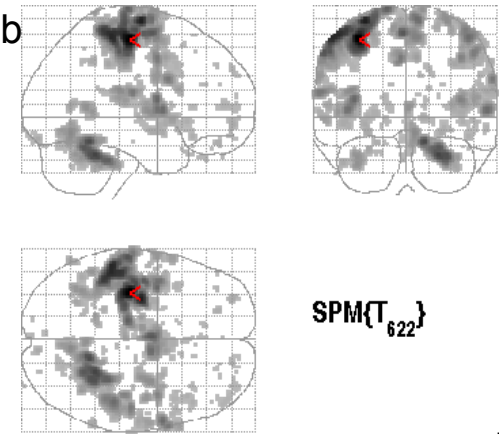

Main effect of move P<0.0001 uncorrected.
a) Maxima of effect in primary motor cortex (-36 -24 58) displayed on subject's structural
b) Maximum intensity projection

6.3 c

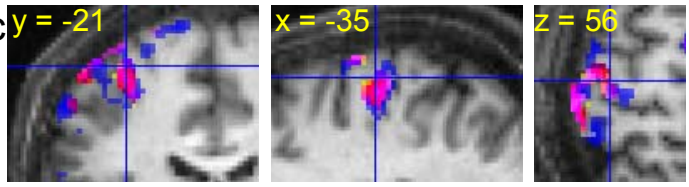

c) Mapping of individual finger movements P<0.05 uncorrected, masked by main effect movement Displayed on axial, sagittal and coronal sections. Red: index, yellow: middle, blue: ring and magenta: little finger

6.3 d

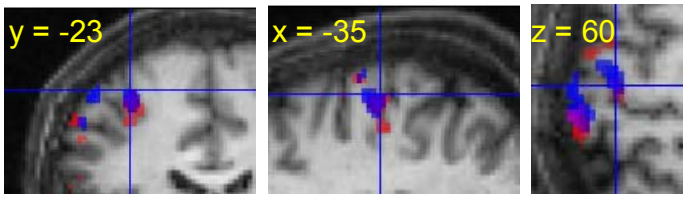

d) Mapping of Index finger movements P<0.05 uncorrected, masked by main effect movement
Displayed on axial, sagittal and coronal sections. Red - post real rTMS, Blue – post sham rTMS

6.3 e

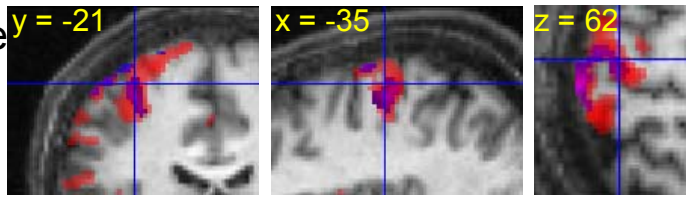

e) Mapping of Little finger movements P<0.05 uncorrected, masked by main effect movement
Displayed on axial, sagittal and coronal sections. Red - post real rTMS, Blue – post sham rTMS

Figure 6.4: Motor Mapping Subject 2

6.4 a

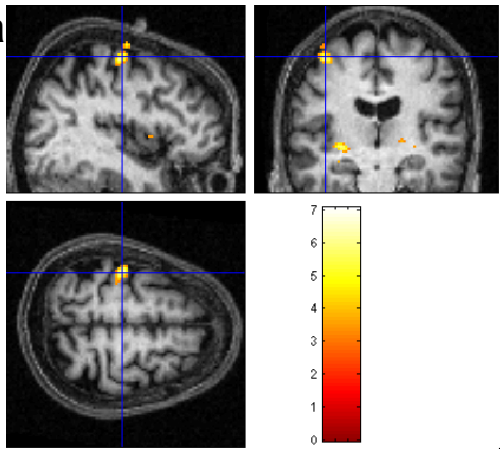

6.4 b

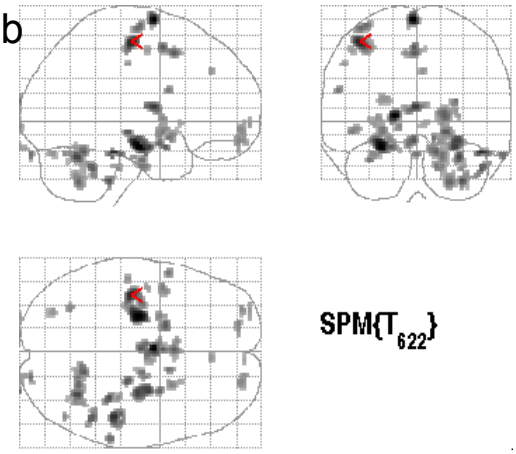

Main effect of move P<0.001 uncorrected.
a) Maxima of effect in primary motor cortex (-36 -24 58) displayed on subject's structural
b) Maximum intensity projection

6.4 c

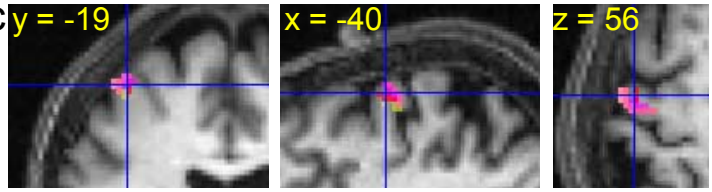

c) Mapping of individual finger movements P<0.05 uncorrected, masked by main effect movement Displayed on axial, sagittal and coronal sections. Red: index, yellow: middle, blue: ring and magenta: little finger

6.4 d

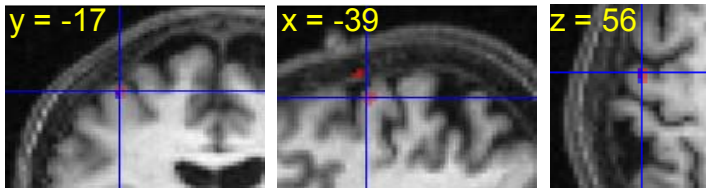

d) Mapping of Index finger movements P<0.05 uncorrected, masked by main effect movement
Displayed on axial, sagittal and coronal sections. Red - post real rTMS, Blue – post sham rTMS

6.4 e

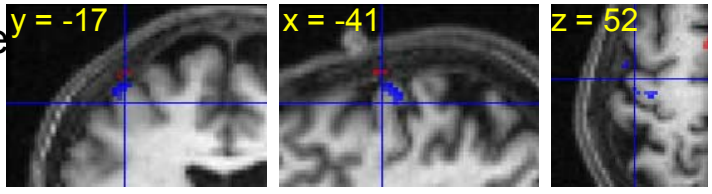

e) Mapping of Little finger movements P<0.05 uncorrected, masked by main effect movement
Displayed on axial, sagittal and coronal sections. Red - post real rTMS, Blue – post sham rTMS

Figure 6.5: Motor Mapping Subject 3

6.5 a

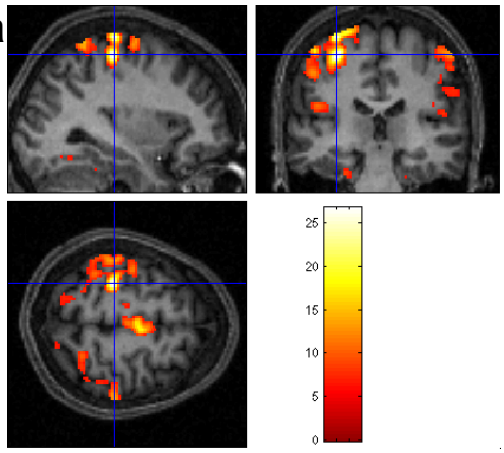

6.5 b

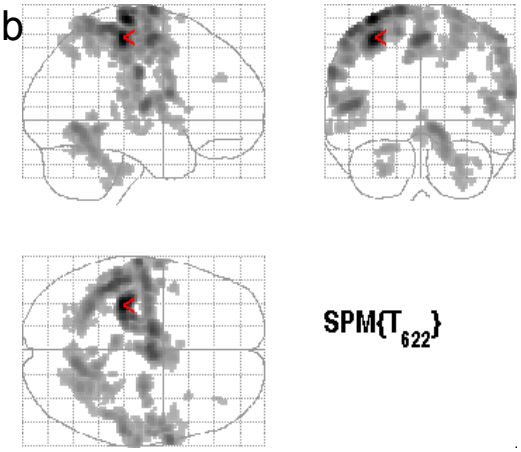

Main effect of move P<0.000000001 uncorrected.

a) Maxima of effect in primary motor cortex (-36 -24 58) displayed on subject's structural

b) Maximum intensity projection

6.5 c

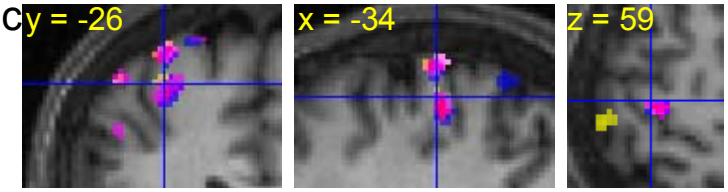

c) Mapping of individual finger movements P<0.05 uncorrected, masked by main effect movement Displayed on axial, sagittal and coronal sections. Red: index, yellow: middle, blue: ring and magenta: little finger

6.5 d

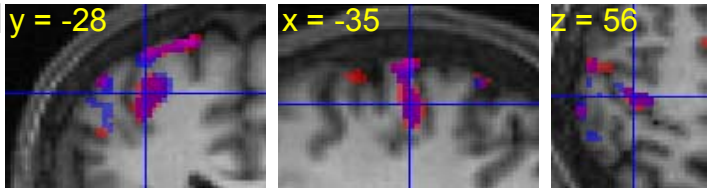

d) Mapping of Index finger movements P<0.05 uncorrected, masked by main effect movement
Displayed on axial, sagittal and coronal sections. Red - post real rTMS, Blue – post sham rTMS

6.5 e

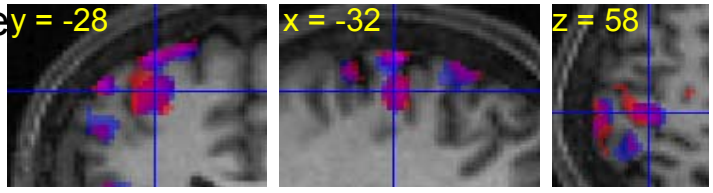

e) Mapping of Little finger movements P<0.05 uncorrected, masked by main effect movement
Displayed on axial, sagittal and coronal sections. Red - post real rTMS, Blue – post sham rTMS

Figure 6.6: Motor Mapping Subject 4

6.6 a

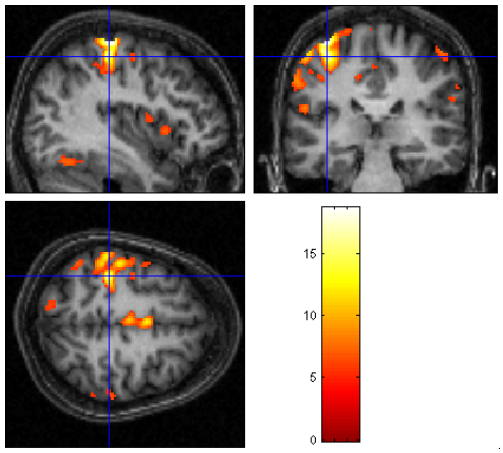

6.6 b

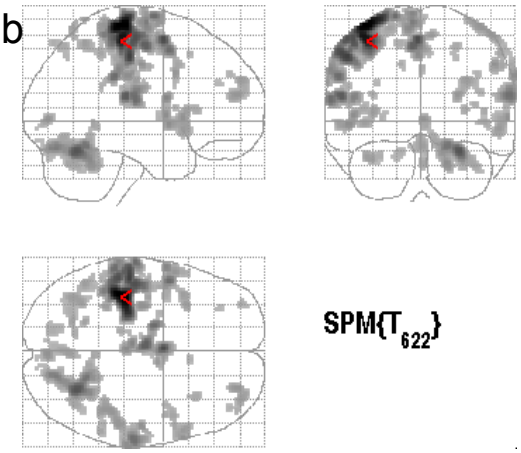

Main effect of move P<0.0000001 uncorrected.
a) Maxima of effect in primary motor cortex (-36 -24 58) displayed on subject's structural
b) Maximum intensity projection

6.6 c

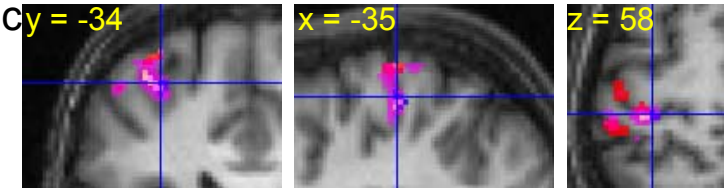

c) Mapping of individual finger movements P<0.05 uncorrected, masked by main effect movement
Displayed on axial, sagittal and coronal sections. Red: index, yellow: middle, blue: ring and magenta: little finger

6.6 d

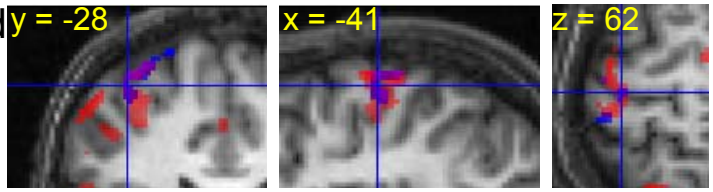

d) Mapping of Index finger movements P<0.05 uncorrected, masked by main effect movement
Displayed on axial, sagittal and coronal sections. Red - post real rTMS, Blue – post sham rTMS

6.6 e

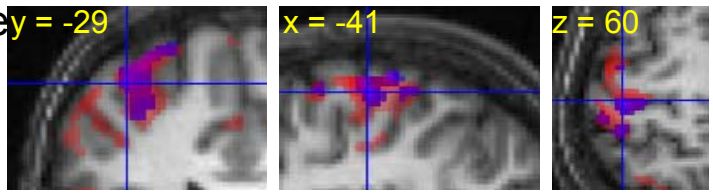

e) Mapping of Little finger movements P<0.05 uncorrected, masked by main effect movement
Displayed on axial, sagittal and coronal sections. Red - post real rTMS, Blue – post sham rTMS

Figure 6.7: Motor Mapping Subject 5

6.7 a

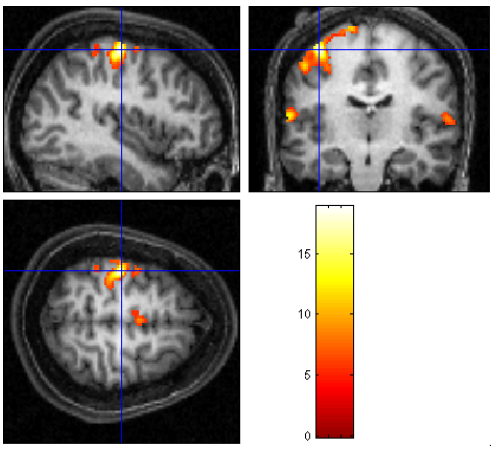

6.7 b

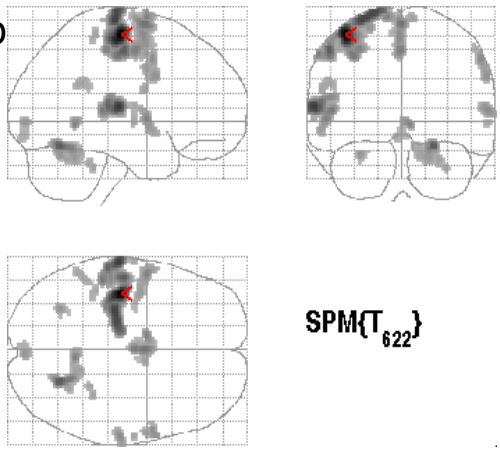

Main effect of move P<0.0000001 uncorrected.
a) Maxima of effect in primary motor cortex (-36 -24 58) displayed on subject's structural
b) Maximum intensity projection

6.7 c

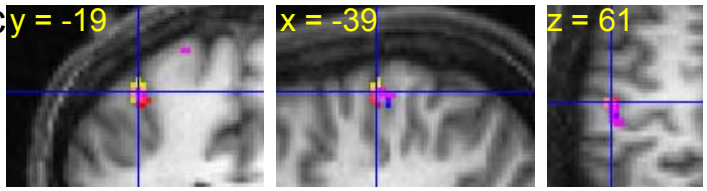

c) Mapping of individual finger movements P<0.05 uncorrected, masked by main effect movement Displayed on axial, sagittal and coronal sections. Red: index, yellow: middle, blue: ring and magenta: little finger

6.7 d

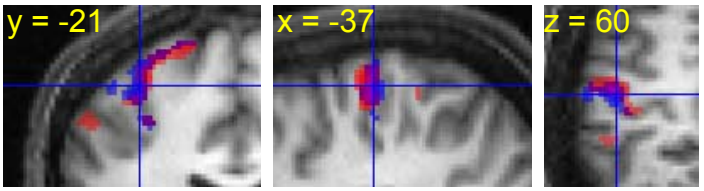

d) Mapping of Index finger movements P<0.05 uncorrected, masked by main effect movement
Displayed on axial, sagittal and coronal sections. Red - post real rTMS, Blue – post sham rTMS

6.7 e

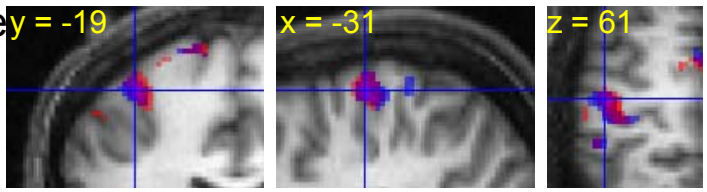

e) Mapping of Little finger movements P<0.05 uncorrected, masked by main effect movement
Displayed on axial, sagittal and coronal sections. Red - post real rTMS, Blue – post sham rTMS

Figure 6.8: Motor Mapping Subject 6

6.8 a

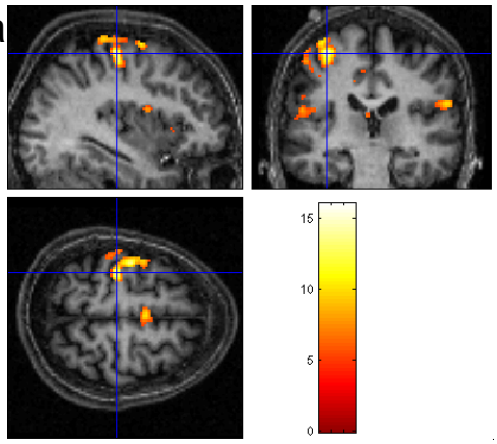

6.8 b

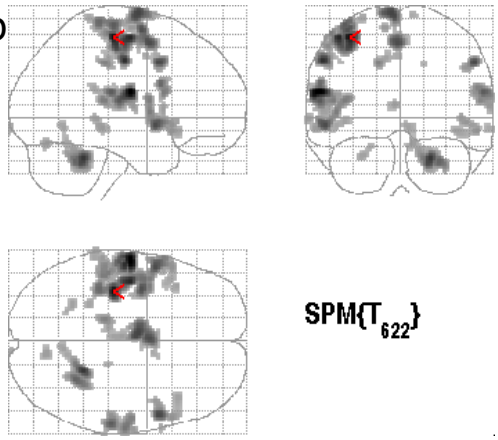

Main effect of move P<0.00001 uncorrected.
a) Maxima of effect in primary motor cortex (-36 -24 58) displayed on subject's structural
b) Maximum intensity projection

6.8 c

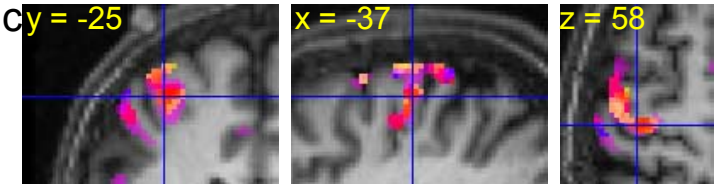

c) Mapping of individual finger movements P<0.05 uncorrected, masked by main effect movement Displayed on axial, sagittal and coronal sections. Red: index, yellow: middle, blue: ring and magenta: little finger

6.8 d

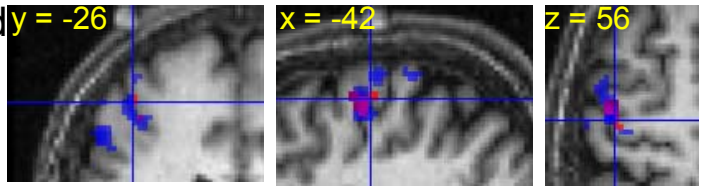

d) Mapping of Index finger movements P<0.05 uncorrected, masked by main effect movement
Displayed on axial, sagittal and coronal sections. Red - post real rTMS, Blue – post sham rTMS

6.8 e

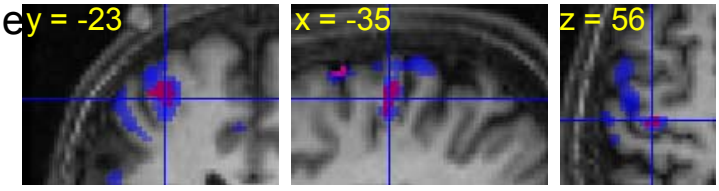

e) Mapping of Little finger movements P<0.05 uncorrected, masked by main effect movement
Displayed on axial, sagittal and coronal sections. Red - post real rTMS, Blue – post sham rTMS

6.3.2.2 Analyses of Effective Connectivity

One subject failed to show any significant interactions between rTMS and either the move or switch effects. This subject (Subject 2) was therefore excluded from further analysis.

Table 6.2: Regions of Interest for DCMs

		MNI Co-ordinates of peak activation		
		x	**y**	**z**
Subject 1	Left PMd	-30	-12	70
	Left SMA	-2	-4	62
	Right PMd	26	-14	72
	L M1 (interaction)	-36	-22	50
Subject 3	Left PMd	-34	-12	66
	Left SMA	-2	-10	54
	Right PMd	28	-20	48
	L M1 (interaction)	-30	-34	60
Subject 4	Left PMd	-34	-16	70
	Left SMA	-4	-14	54
	Right PMd	32	-8	62
	L M1 (interaction)	-38	-26	68
Subject 5	Left PMd	-26	-8	72
	Left SMA	-2	0	62
	Right PMd	32	-8	58
	L M1 (interaction)	-28	-26	62
Subject 6	Left PMd	-40	-4	64
	Left SMA	0	4	54
	Right PMd	42	0	56
	L M1 (interaction)	-36	-28	46

Table 6.2: Co-ordinates of brain regions showing a main effect of 'move' or 'switch' in L PMd and L SMA, and a switch-by-rTMS interaction in L M1 and R PMd.

The first analysis of effective connectivity examined the effect of rTMS on the efficacy of connections from the Left PMd to the Left M1 during the switch condition. Model A was constructed to test the hypothesis that rTMS modulated the strength of inputs from L PMd to L M1. The results of this DCM are shown in Figure 6.9. It can be seen that in four of the five subjects rTMS has a positive modulatory effect on the strength of connections between L PMd and L M1, whereas in Subject 3 rTMS appears to have a negative modulatory effect. Model B examined the effect of rTMS

on the inhibitory self connections in Left M1. The results, shown in Figure 6.9, show a similar pattern to those of Model A. A comparison between the two models (Table 6.3i) failed to show any advantage of either model for any of the five subjects.

The second analysis of effective connectivity examined the effect of rTMS on the efficacy of connections from Left SMA to Left M1 during the epochs of finger tapping (move). Model A was constructed to test the hypothesis that rTMS modulated the strength of inputs from L SMA to L M1. The results of this DCM are shown in Figure 6.10. It can be seen that in four of the five subjects rTMS has a positive modulatory effect on the strength of connections between L SMA and L M1, whereas in Subject 3 rTMS appears to have a negative modulatory effect. Model B examined the effect of rTMS on the Left M1 inhibitory self connections, shown in Figure 6.10. The results, shown in Figure 6.10, show a similar pattern to those of Model A. A comparison between the two models (Table 6.3ii) failed to show any advantage of either model for any of the five subjects.

The third analysis of effective connectivity used dynamic causal modelling to examine the contribution of the Right PMd following rTMS. Model A was constructed to test the hypothesis that the Right PMd modulates movement-related responses in Left M1 and that this influence increases with the strength of connections from Left to Right PMd following rTMS. Model B was constructed to test the hypothesis that the contribution of Right PMd is mediated via an increase in the strength of connections from Right to Left PMD following rTMS. The results of these two DCMs are shown in Figure 6.11. rTMS appears to have a positive modulatory effect on the connectivity of the premotor cortices in all subjects, except Subject 3. The results of the Bayesian model comparison suggest that for 4 of the 5 subjects Model B provides a markedly better explanation of the data (Table 6.3iii).

Figure 6.9: Effects of rTMS on PMd to M1 Connectivity

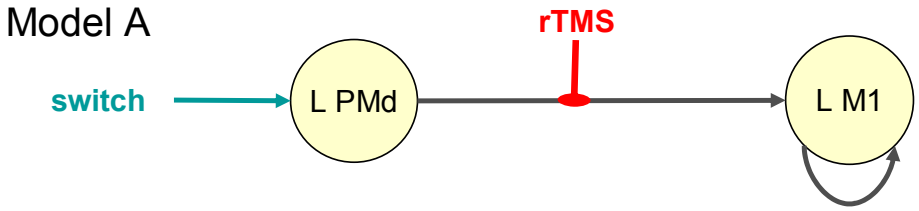

	switch	LPMd-LM1	rTMS
Subject 1	0.31 (99%)	0.99 (100%)	0.19 (79%)
Subject 3	0.20 (100%)	1.23 (100%)	-0.14 (72%)
Subject 4	0.19 (100%)	1.23 (100%)	0.39 (96%)
Subject 5	0.14 (100%)	0.97 (100%)	0.06 (59%)
Subject 6	0.11 (100%)	0.19 (100%)	0.19 (75%)

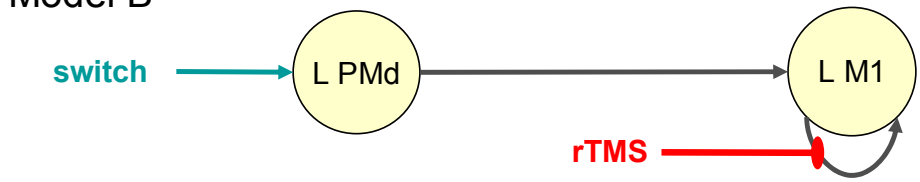

	switch	LPMd-LM1	rTMS
Subject 1	0.31 (99%)	1.0 (100%)	0.006 (51%)
Subject 3	0.20 (100%)	1.24 (100%)	-0.22 (82%)
Subject 4	0.19 (100%)	1.35 (100%)	0.30 (96%)
Subject 5	0.14 (100%)	0.95 (100%)	0.21 (77%)
Subject 6	0.11 (100%)	0.57(100%)	0.08 (59%)

Figure 6.9: Results of DCM analysis applied to the data extracted from the regions of interest described in Methods. A schematic of the architecture of Models A and B are shown, demonstrating the location of the driving input (switch) and the modulatory input (rTMS). For each model the coupling parameters for the five subjects are shown below, where blue denotes the effects of the input 'switch', black denotes the coupling from L PMd to L M1, and red denotes the modulatory effect of rTMS on the connection in indicated in the figure above. Figures in brackets are the percentage confidence that these values exceed zero.

Figure 6.10: Effects of rTMS on SMA to M1 Connectivity

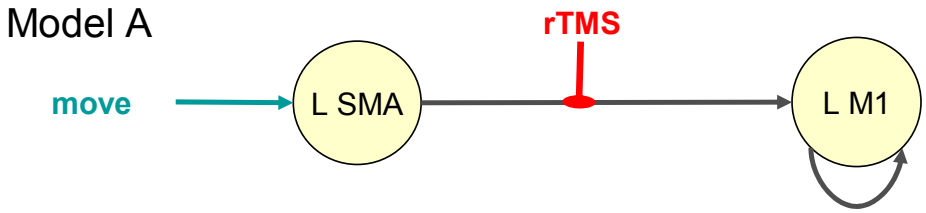

	move	LSMA-LM1	rTMS
Subject 1	0.15(100%)	1.11(100%)	0.25 (84%)
Subject 3	0.09 (100%)	1.02 (100%)	-0.25 (90%)
Subject 4	0.13 (100%)	1.28 (100%)	0.62 (99%)
Subject 5	0.08 (100%)	0.64 (100%)	0.07 (60%)
Subject 6	0.11(99%)	0.31 (99%)	0.09 (66%)

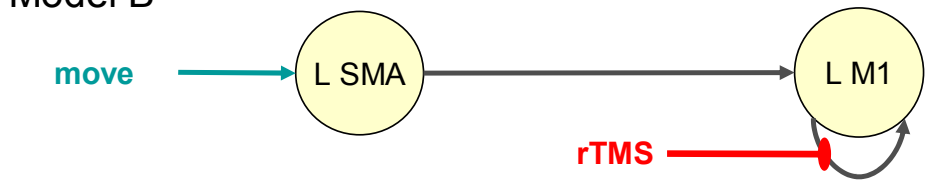

	move	LSMA-LM1	rTMS
Subject 1	0.15(100%)	1.11 (100%)	0.19 (82%)
Subject 3	0.09 (100%)	1.04 (100%)	-0.37 (94%)
Subject 4	0.13 (100%)	1.27 (100%)	0.53 (100%)
Subject 5	0.08 (100%)	0.64 (100%)	0.12 (65%)
Subject 6	0.11 (100%)	0.33 (99%)	0.06 (57%)

Figure 6.10: Results of DCM analysis applied to the data extracted from the regions of interest described in Methods. A schematic of the architecture of Models A and B are shown, demonstrating the location of the driving input (move) and the modulatory input (rTMS). For each model the coupling parameters for the five subjects are shown below, where blue denotes the effects of the input 'move', black denotes the coupling from L SMA to L M1, and red denotes the modulatory effect of rTMS on the connection in indcated in the figure above. Figures in brackets are the percentage confidence that these values exceed zero.

Figure 6.11: Effects of rTMS on PMd to PMd Connectivity

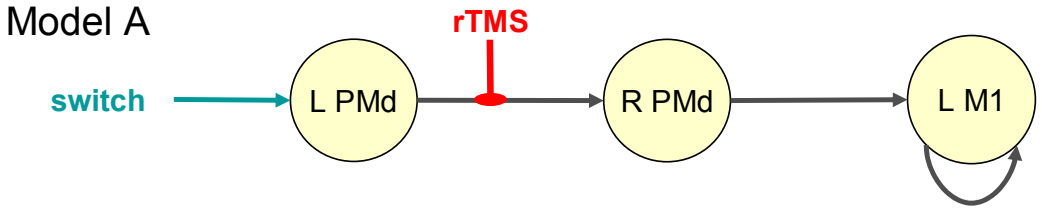

	switch	LPMd-RPMd-LM1	rTMS
Subject 1	0.40 (100%)	0.66(100%) 1.28(100%)	0.18 (89%)
Subject 3	0.26 (100%)	1.03 (100%) 1.22(100%)	-0.08 (69%)
Subject 4	0.26 (100%)	1.08 (100%) 1.45(100%)	0.26 (97%)
Subject 5	0.20 (100%)	0.61 (100%) 1.00(100%)	0.06 (62%)
Subject 6	0.12 (100%)	0.54 (100%) 0.52 (100%)	0.26 (88%)

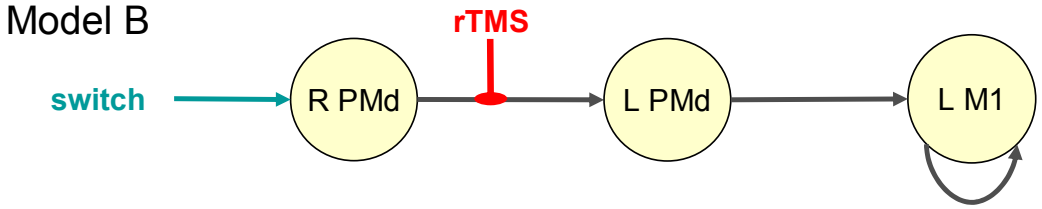

	switch	RPMd-LPMd-LM1	rTMS
Subject 1	0.26(100%)	1.36(100%) 1.08 (100%)	0.27 (91%)
Subject 3	0.25 (100%)	1.18 (100%) 1.15 (100%)	-0.06 (63%)
Subject 4	0.28 (100%)	1.04 (100%) 1.47 (100%)	0.36 (98%)
Subject 5	0.14 (100%)	1.12 (100%) 0.96 (100%)	0.06 (59%)
Subject 6	0.12 (100%)	1.13 (100%) 0.53 (100%)	0.26 (88%)

Figure 6.11: Results of DCM analysis applied to the data extracted from the regions of interest described in Methods. A schematic of the architecture of Models A and B are shown, demonstrating the location of the driving input (move) and the modulatory input (rTMS). For each model the coupling parameters for the five subjects are shown below, where blue denotes the effects of the input 'switch', black denotes the coupling from L PMd to R PMd (Model A) and R PMd to L PMd (Model B), and red denotes the modulatory effect of rTMS on the connection between R and L PMd. Figures in brackets are the percentage confidence that these values exceed zero.

Table 6.3 Model Comparison

i) Effects of rTMS on L PMd to L M1 Connectivity

	Model A Vs Model B AIC	BIC	Bayes Factor	Evidence
Subject 1	-0.4	-0.4	0	nil
Subject 3	1.42	1.42	0	nil
Subject 4	-1.28	-1.28	0	nil
Subject 5	0.33	0.33	0	nil
Subject 6	-0.17	-0.17	0	nil

ii) Effects of rTMS on L SMA to L M1 Connectivity

	Model A Vs Model B AIC	BIC	Bayes Factor	Evidence
Subject 1	-0.18	-0.18	0	nil
Subject 3	1.12	1.12	0	nil
Subject 4	1.32	1.32	0	nil
Subject 5	0.09	0.09	0	nil
Subject 6	-0.07	-0.07	0	nil

ii) Effects of rTMS on L PMd to R PMd Connectivity

	Model A Vs Model B AIC	BIC	Bayes Factor	Evidence
Subject 1	-1.61	-1.61	>3.05	A
Subject 3	2.84	2.84	>7.16	B
Subject 4	5.35	5.35	>40.73	B
Subject 5	5.66	5.66	>50.4	B
Subject 6	6.52	6.52	>92.47	B

Table 6.3: Akaike's Information Criterion (AIC) and Bayesian Information Criterion (BIC) used to compute Bayes Factors for the comparison of models described in Methods. When Bayes Factors computed from AIC and BIC are both greater than 2.7183, this is considered consistent evidence in favour of one model.

6.4 Discussion

The results of this experiment are discussed in three sections: the effects of rTMS on the somatotopic representation of individual fingers; the effects of rTMS on coupling between motor areas during the motor task and methodological considerations.

6.4.1 Somatotopic mapping in the primary motor cortex: no evidence of an effect of 1Hz rTMS on individual finger representations.

The individual subject data obtained following sham rTMS (Table 6.2, Figures 6.3-9) demonstrate that the motor paradigm used in this experiment was sufficient to resolve localised activations for individual finger movements. It was not always possible to detect separate maxima for adjacent fingers; neither was it possible to detect a consistent mediolateral pattern of organisation within subjects. This is in keeping with previous studies in humans and animals, demonstrating the presence of overlapping representations of individual digits, without clear somatomotor organisation (Sanes et al., 1995;Sanes and Schieber, 2001;Indovina and Sanes, 2001). Based on the results presented in Chapter 3, it was hypothesised that the sites of activity would shift following rTMS, from superficial primary motor cortex (Area 4a) to Area 4p located in the depth of the central sulcus (Geyer et al., 1996). It was not possible to detect a consistent effect of rTMS on the topography of maxima for individual finger movements, based on the locations of the maximally activated voxels and a visual inspection of the data. It is possible that changes occurred in the spatial extent of the motor activations that were not detected by the methods used.

The lack of significant remapping at the level of topography of individual finger representations may reflect a lack of specificity of 1Hz rTMS on the excitability of individual muscles. The use paired associated stimulation (Stefan et al., 2000), with topographically specific effects on excitability, might yield more promising results.

6.4.2 1Hz rTMS modulates the connectivity of the motor system

This study provides a replication of the effects of rTMS seen on the connections from premotor cortex and SMA to primary motor cortex (Chapter 3) using a more sophisticated analysis of effective connectivity. The first two models explore the modulation of the coupling between Left PMd or SMA and Left M1 by rTMS. This was achieved by comparing two models, where rTMS could modulate either the inputs from L PMd or L SMA to L M1, or the strength of the inhibitory self connections within L M1. In four of the five subjects rTMS appears to have a positive modulatory effect i.e. increasing the strength of inputs from Left PMd and Left SMA to Left M1. In an alternative model, rTMS also modulated the inhibitory self connections in Left M1. Both models suggest that the intrinsic excitability of the primary motor cortex is altered by rTMS. In the first model, by increasing the post synaptic response to extrinsic afferents from premotor cortex; in the second, by a disinhibition of local or intrinsic dynamics by decreasing post-synaptic responses to inhibitory interneurons (or increasing sensitivity to intrinsic excitatory inputs). Bayesian model comparison failed to show an advantage of either model in explaining the data. The aim of this experiment was to determine if dynamic causal modelling could offer additional information regarding the mechanism of rTMS effects on motor excitability. In relation to the relative role of the changes in extrinsic and intrinsic connections, there was insufficient evidence in the fMRI data to disambiguate them.

The final pair of dynamic causal models investigated the contribution of the right premotor cortex (R PMd) to movement after rTMS. The data presented in Chapters 3 and 4 implicate the right PMd (ipsilateral to the moving hand and contralateral to the site of stimulation) in maintaining of motor performance during periods of abnormal cortical excitability. There are three potential mechanisms by which R PMd could influence right handed movement: first, via cortico-cortical connections from R PMd to R M1 (and then via direct ipsilateral corticospinal connections), second, via cortico-cortical connections between the R PMd and the contralateral (left) M1 and third, indirectly, via cortico-cortical connections from R PMd to L PMd (and then from L PMd to L M1).

The models examined the second two possibilities because no movement-related responses were seen in R M1. Bayesian model comparison of the two alternatives suggests strongly that, following rTMS, the influence of the right premotor cortex is mediated via transcallosal cortical connections to the left premotor cortex, not via projections to the contralateral primary motor cortex. This is consistent with the relative strength of anatomical connections between the premotor cortices as compared to those from premotor cortex to contralateral primary motor cortices (Rouiller et al., 1994;Marconi et al., 2003).

6.4.3 Methodological considerations

In the DCM analyses, the majority of subjects (4/6) show a similar pattern of rTMS effects, but the effects in individual subjects are not particularly striking. rTMS effects show a range of variability across individuals (Maeda et al., 2000a), with a minority of subjects showing increased cortical excitability following 1Hz rTMS (Gangitano et al., 2002). It is therefore likely that a single subject approach is best suited to the analysis of rTMS data. At present DCM is designed to be used for single subject data; however, small but consistent effects over subjects may become significant, in terms of population inference, in studies of larger cohorts. One approach would be to take estimates of coupling parameters obtained at the single subject level and compare these across subjects. An alternative approach would be to use Bayesian model averaging and conditional inferences. The analyses presented in Chapter 3 disclosed a significant effect with eight subjects, it would therefore be reasonable to anticipate similar results with DCM in a similar sized group of subjects.

In order to increase the interpretability of DCM data pertaining to the inhibitory effects of 1Hz rTMS on motor excitability, it may be necessary to classify a cohort of subjects in term of their previously determined response to 1Hz rTMS.

6.5 Conclusions

This experiment fails to detect a systematic change in the topography of individual finger representations, following 1Hz rTMS to the left primary motor cortex. A less fine-grained approach, looking at changes across subjects at a coarser anatomical scale (e.g. comparing arm and hand movements) may prove to be more successful.

This experiment successfully replicates the findings presented in Chapter 3, providing evidence that it is possible to examine the effects of rTMS on the connectivity between cortical areas using dynamic causal modelling. DCM did not disambiguate extrinsic and intrinsic explanations for the increased sensitivity of motor cortex to premotor afferents, but this may reflect the limited spatio-temporal precision of fMRI data.

A combination of dynamic causal modelling and Bayesian model comparison was used to examine the changes in connectivity of the premotor cortices, to determine how increased activity in the right (non-stimulated) premotor cortex after rTMS contributes to the maintenance of motor performance. There was strong and consistent evidence that rTMS increases the transcallosal connections from right to left premotor cortex, as opposed to non-homologous connections from right premotor to left motor cortex.

Chapter 7

Discussion

The work presented in this thesis explores how rTMS changes regional excitability and how the motor system compensates for these changes.

Data from four experiments were presented. PET was used to image the effects of subthreshold 1Hz rTMS to left M1 on movement-related responses during freely selected right finger movements or during paced finger tapping with the right and left hand. fMRI was used to image the effects of subthreshold 1Hz rTMS to left M1 on randomly cued paced finger tapping with the right hand. A 'virtual lesion' approach using subthreshold 20 Hz rTMS was used to examine the contribution of the right premotor cortex to a choice reaction task before and after 1Hz rTMS to left M1.

The results of the two PET experiments (Chapters 3 and 5) demonstrate that there are significant changes in movement-related responses and coupling with the motor system following rTMS. The results of the fMRI experiment (Chapter 6) confirm that there are significant changes in movement-related responses and coupling with the motor system. The results of the behavioural experiment (Chapter 4) suggests that the increased movement-related responses in the right premotor cortex (Chapters 3 and 6) has a functional role in maintaining motor performance following 1Hz rTMS to left M1. The analyses of effective connectivity presented in Chapter 6 suggest that the influence of the right premotor cortex in maintaining motor performance after rTMS is mediated via increased transcallosal connections from right to left premotor cortex, as opposed to non-homologous connections from right premotor to left motor cortex.

The implications of these findings will be discussed in three sections: the relationship between changes in movement-related responses and motor performance, modulating the motor system with rTMS and finally, implications for future work.

7.1 The relationship between changes in movement-related activity and motor performance following rTMS

No impairment of manual motor control by 1Hz rTMS has been convincingly demonstrated during simple motor tasks e.g. paced fist clench (Pascual-Leone et al., 1998), finger tapping (Wassermann et al., 1996;Chen et al., 1997a), maintenance of tonic contraction (Strens et al., 2002) peak force and acceleration during finger pinch (Muellbacher et al., 2000). In the four experiments presented in this thesis 1Hz rTMS alone did not significantly disrupt the ability of subjects' performance during simple motor tasks. 1Hz rTMS has been shown to disrupt more demanding motor behaviour such as fastest possible finger tapping (Jancke et al., 2003) and reaction times during a 'masked prime' task (Schlaghecken et al., 2003). This suggests that the motor system may be able to compensate, to some extent, for changes in excitability induced by rTMS.

During a motor task with an element of movement selection, there were increased movement-related responses in the right PMd (contralateral to the site of stimulations) and increased coupling from the left PMd and left SMA to a site in left M1 (ipsilateral to the site of stimulation) showing significantly increased movement-related responses following rTMS (Chapters 3 and 6). During a fully cued paced finger tapping task (Chapter 5) increased movement-related responses were seen in the right cerebellum (ipsilateral to the moving hand) and increased movement-related coupling was seen within the cerebello-thalamic system. Altered movement-related activity during unaltered motor performance following 1Hz rTMS has been observed previously using EEG. Following rTMS to M1 (Strens et al., 2002) and PMd (Chen et al., 2003) increases in task-related coherence are observed between cortical motor areas ipsilateral and contralateral to the site of stimulation. Changes are also reported in the Beretischaftspotential (reflecting preparatory activity during the initiation of voluntary movement) following 1Hz rTMS to M1 (Rossi et al., 2000).

Increased activity in motor areas not normally engaged in task performance may contribute to compensatory mechanisms during altered cortical excitability. The analyses of effective connectivity presented in Chapters 3, 5 and 6 suggest an

additional or possibly complementary mechanism: after rTMS there is a re-modelling of the motor system. Operational remapping of motor networks may explain how the motor system compensates for rTMS-induced reductions in cortical excitability.

7.2 Modulating the motor system with 1Hz rTMS

Operational remapping of motor networks as a compensatory mechanism does not imply that 1Hz rTMS remodels motor networks per se, but having rendered a part of primary motor cortex less sensitive to inputs from components of the motor network engaged in the task (premotor and mesial motor areas in Chapters 3 and 6; cerebellum in Chapter 5), task performance may be maintained by increasing movement-related activity in distal components of the motor network.

For this explanation to be plausible there are four requirements. First, the adult motor cortex should contain multiple motor representations and be capable of plastic changes. Second, such changes should occur at time-scales similar to those seen in this experiment i.e. within one hour. Third, rTMS parameters should be comparable with stimulation protocols that modulate neuronal systems involved in motor cortical plasticity in animals. Fourth, the motor system should display the characteristics of degeneracy, and the anatomical basis for such features.

Recent work with fMRI has confirmed early PET findings (Colebatch et al., 1991;Grafton et al., 1991) that multiple, overlapping sensorimotor representations of distinct hand movements exist in human primary motor cortex (Sanes et al., 1995;Rao et al., 1995;Indovina and Sanes, 2001). Plasticity of motor representations in the human motor cortex occurs after stroke (Liepert et al., 2000), amputation (Cohen et al., 1991), surgery (Duffau, 2001), learning (Classen et al., 1998) and modulation of cortical excitability (Ziemann et al., 2002). It has been measured using functional imaging, transcranial and direct cortical stimulation.

Work in rat motor cortex confirms that within hours of motor nerve lesion (Donoghue et al., 1990) or repetitive intracortical microstimulation (Nudo et al., 1990), reorganisation of cortical representations can be seen. In humans reorganisation of the motor strip, assessed using intraoperative electrical stimulation, has been reported within thirty minutes following tumour resection (Duffau, 2001). The

reorganisation within primary sensorimotor cortex seen in this study is in good agreement with a study by (Ziemann et al., 2002), demonstrating a rapid remapping of body representations in the motor cortex after 0.1Hz rTMS during transient deafferentation of the contralateral forearm.

The basis for cortical reorganisation is thought to involve changes in cortical synaptic efficacy, through mechanisms such as long term potentiation (LTP) and depression (LTD) (Buonomano and Merzenich, 1998). The primary substrate for plasticity in the motor cortex is thought to be the intrinsic horizontal connections (Sanes and Donoghue, 2000). Repetitive low frequency stimulation (2Hz) induces LTD in these connections in rat motor cortex (Hess and Donoghue, 1996). This suggests it is possible to modulate the neural substrate for map reorganisation in motor cortex (intrinsic horizontal connections) using stimulation parameters similar to those used for rTMS.

As outlined in Chapter 4 degeneracy is a many-to-one structure-function mapping and, in this context, implies that more than one set of cortical structures can support the same function. The anatomy of the motor system is well suited to supporting such functionality. At the neuronal level, large areas of primary motor cortex converge onto single spinal motor neurons, while at the same time outputs from any single neuron synapse with multiple spinal neuron pools (Shinoda et al., 1981). Both primary and non-primary cortical subcortical motor areas contain multiple distributed representations of body parts (Fink et al., 1997;Indovina and Sanes, 2001). A significant proportion of corticospinal neurons originate from non-primary motor areas (Jane et al., 1967;Dum and Strick, 1991), and 10-30% of the corticospinal projections from the primary motor cortex project to ipsilateral spinal cord (Nathan et al., 1990). In addition, the motor and premotor cortices are well connected to the homologous contralateral areas (Rouiller et al., 1994;Marconi et al., 2003).

The data presented in Chapter 4 suggests that either, or both, the motor and pre-motor regions may be sufficient for performance of the choice reaction time task used and the possibility of a degenerate mapping from structure (motor and premotor regions) to function (as measured by reaction times). It has also been shown in normal subjects that short trains of subthreshold 5Hz rTMS to either contralateral or ipsilateral M1 had very limited effects performance of a precision finger tapping task; whereas stimulating both primary motor cortices simultaneously

had a marked, prolonged, detrimental effect on performance, suggesting that when one primary motor cortex is disrupted during motor performance, the other motor cortex provides functionally significant compensation (Strens et al., 2003).

7.3 Implications for future work

The work presented in this thesis establishes a number of important principles.

The identification of patterns of reorganisation in the motor system after rTMS may provide useful insights into compensatory plasticity of the human brain and may help to understand how the brain reacts in response to more permanent lesions. Based on the results of Chapters 3 and 5, it appears that the specific patterns of reorganisation may be task dependent. This has implications for neurorehabillitation, and could be tested by directly comparing patterns of activity during different tasks within one experiment.

In order to confirm that the changes in motor activity during movement after rTMS are functionally relevant it is important to combine information from functional imaging with the approach used in Chapter 4.

The possible task dependency of movement-related changes in synaptic activity suggests that the group of motor areas that constitute a degenerate network for one motor task may be specific to that task, and that different groups of areas may be necessary to provide degeneracy for other tasks. Establishing the order of degeneracy using TMS and contribution analyses of the sort presented in Chapter 4 may play a key role in rehabilitation and a mechanistic understanding of compensatory mechanisms in patients.

Having identified candidate areas that may contribute to compensatory mechanisms during periods of altered cortical excitability, a combination of dynamic causal modelling and Bayesian model comparison can be used to examine the changes in the connectivity of candidate areas in order to provide mechanistic insights into how increased task-related activity contributes to task performance during altered cortical excitability. It is anticipated that the connectivity analyses pertaining to the motor system presented in this thesis will generalise to other cognitive systems.

Reference List

Abbott LF, Varela JA, Sen K, Nelson SB (1997) Synaptic depression and cortical gain control. Science 275: 220-224.

Ackermann RF, Finch DM, Babb TL, Engel J, Jr. (1984) Increased glucose metabolism during long-duration recurrent inhibition of hippocampal pyramidal cells. J Neurosci 4: 251-264.

Aertsen A, Preissl H (1991) Dynamics of Activity and Connectivity in Physiological Neuronal Networks. New York: VCH.

Alexander GE, Crutcher MD (1990) Neural representations of the target (goal) of visually guided arm movements in three motor areas of the monkey. J Neurophysiol 64: 164-178.

Allen GI, Tsukahara N (1974) Cerebrocerebellar communication systems. Physiol Rev 54: 957-1006.

Amassian VE, Eberle L, Maccabee PJ, Cracco RQ (1992) Modelling magnetic coil excitation of human cerebral cortex with a peripheral nerve immersed in a brain-shaped volume conductor: the significance of fiber bending in excitation. Electroencephalogr Clin Neurophysiol 85: 291-301.

Amassian VE, Stewart M, Quirk GJ, Rosenthal JL (1987) Physiological basis of motor effects of a transient stimulus to cerebral cortex. Neurosurgery 20: 74-93.

Andersson JL, Hutton C, Ashburner J, Turner R, Friston K (2001) Modeling geometric deformations in EPI time series. Neuroimage 13: 903-919.

Asanuma C, Thach WR, Jones EG (1983) Anatomical evidence for segregated focal groupings of efferent cells and their terminal ramifications in the cerebellothalamic pathway of the monkey. Brain Res 286: 267-297.

Ashe J, Georgopoulos AP (1994) Movement parameters and neural activity in motor cortex and area 5. Cereb Cortex 4: 590-600.

Baraduc P, Lang N, Rothwell JC, Wolpert DM (2004) Consolidation of dynamic motor learning is not disrupted by rTMS of primary motor cortex. Curr Biol 14: 252-256.

Barker AT (1999) The history and basic principles of magnetic nerve stimulation. Electroencephalogr Clin Neurophysiol Suppl 51: 3-21.

Barker AT, Jalinous R, Freeston IL (1985) Non-invasive magnetic stimulation of human motor cortex. Lancet 1: 1106-1107.

Baumer T, Lange R, Liepert J, Weiller C, Siebner HR, Rothwell JC, Munchau A (2003) Repeated premotor rTMS leads to cumulative plastic changes of motor cortex excitability in humans. Neuroimage 20: 550-560.

Bohning DE, Shastri A, McGavin L, McConnell KA, Nahas Z, Lorberbaum JP, Roberts DR, George MS (2000) Motor cortex brain activity induced by 1-Hz transcranial magnetic stimulation is similar in location and level to that for volitional movement. Invest Radiol 35: 676-683.

Bonvento G, Sibson N, Pellerin L (2002) Does glutamate image your thoughts? Trends Neurosci 25: 359-364.

Brasil-Neto JP, McShane LM, Fuhr P, Hallett M, Cohen LG (1992) Topographic mapping of the human motor cortex with magnetic stimulation: factors affecting accuracy and reproducibility. Electroencephalogr Clin Neurophysiol 85: 9-16.

Brodmann K (1903) Beitrage zur histologischen Lokalisation der Grosshirnringe: Die Regio Rolandica. J Psychol Neurol 2: 79-132.

Buonomano DV, Merzenich MM (1998) Cortical plasticity: from synapses to maps. Annu Rev Neurosci 21: 149-186.

Butefisch CM, Khurana V, Kopylev L, Cohen LG (2004) Enhancing encoding of a motor memory in the primary motor cortex by cortical stimulation. J Neurophysiol 91: 2110-2116.

Buxton RB, Frank LR, Wong EC, Siewert B, Warach S, Edelman RR (1998) A general kinetic model for quantitative perfusion imaging with arterial spin labeling. Magn Reson Med 40: 383-396.

Caesar K, Gold L, Lauritzen M (2003) Context sensitivity of activity-dependent increases in cerebral blood flow. Proc Natl Acad Sci U S A 100: 4239-4244.

Cao Y, D'Olhaberriague L, Vikingstad EM, Levine SR, Welch KM (1998) Pilot study of functional MRI to assess cerebral activation of motor function after poststroke hemiparesis. Stroke 29: 112-122.

Carey JR, Kimberley TJ, Lewis SM, Auerbach EJ, Dorsey L, Rundquist P, Ugurbil K (2002) Analysis of fMRI and finger tracking training in subjects with chronic stroke. Brain 125: 773-788.

Chen R, Classen J, Gerloff C, Celnik P, Wassermann EM, Hallett M, Cohen LG (1997a) Depression of motor cortex excitability by low-frequency transcranial magnetic stimulation. Neurology 48: 1398-1403.

Chen R, Gerloff C, Classen J, Wassermann EM, Hallett M, Cohen LG (1997b) Safety of different inter-train intervals for repetitive transcranial magnetic stimulation and recommendations for safe ranges of stimulation parameters. Electroencephalogr Clin Neurophysiol 105: 415-421.

Chen R, Gerloff C, Hallett M, Cohen LG (1997c) Involvement of the ipsilateral motor cortex in finger movements of different complexities. Ann Neurol 41: 247-254.

Chen R, Lozano AM, Ashby P (1999) Mechanism of the silent period following transcranial magnetic stimulation. Evidence from epidural recordings. Exp Brain Res 128: 539-542.

Chen R, Tam A, Butefisch C, Corwell B, Ziemann U, Rothwell JC, Cohen LG (1998) Intracortical inhibition and facilitation in different representations of the human motor cortex. J Neurophysiol 80: 2870-2881.

Chen WH, Mima T, Siebner HR, Oga T, Hara H, Satow T, Begum T, Nagamine T, Shibasaki H (2003) Low-frequency rTMS over lateral premotor cortex induces lasting changes in regional activation and functional coupling of cortical motor areas. Clin Neurophysiol 114: 1628-1637.

Chollet F, DiPiero V, Wise RJ, Brooks DJ, Dolan RJ, Frackowiak RS (1991) The functional anatomy of motor recovery after stroke in humans: a study with positron emission tomography. Ann Neurol 29: 63-71.

Chouinard PA, Van Der Werf YD, Leonard G, Paus T (2003) Modulating neural networks with transcranial magnetic stimulation applied over the dorsal premotor and primary motor cortices. J Neurophysiol 90: 1071-1083.

Civardi C, Cantello R, Asselman P, Rothwell JC (2001) Transcranial magnetic stimulation can be used to test connections to primary motor areas from frontal and medial cortex in humans. Neuroimage 14: 1444-1453.

Classen J, Liepert J, Wise SP, Hallett M, Cohen LG (1998) Rapid plasticity of human cortical movement representation induced by practice. J Neurophysiol 79: 1117-1123.

Clower DM, Dum RP, Strick PL (2004) Basal Ganglia and Cerebellar Inputs to 'AIP'. Cereb Cortex.

Cohen LG, Bandinelli S, Findley TW, Hallett M (1991) Motor reorganization after upper limb amputation in man. A study with focal magnetic stimulation. Brain 114 (Pt 1B): 615-627.

Colebatch JG, Deiber MP, Passingham RE, Friston KJ, Frackowiak RS (1991) Regional cerebral blood flow during voluntary arm and hand movements in human subjects. J Neurophysiol 65: 1392-1401.

Cowey A, Walsh V (2001) Tickling the brain: studying visual sensation, perception and cognition by transcranial magnetic stimulation. Prog Brain Res 134: 411-425.

Cracco RQ, Amassian VE, Maccabee PJ, Cracco JB (1989) Comparison of human transcallosal responses evoked by magnetic coil and electrical stimulation. Electroencephalogr Clin Neurophysiol 74: 417-424.

Cramer SC, Nelles G, Benson RR, Kaplan JD, Parker RA, Kwong KK, Kennedy DN, Finklestein SP, Rosen BR (1997) A functional MRI study of subjects recovered from hemiparetic stroke. Stroke 28: 2518-2527.

Crossman AR (2000) Functional anatomy of movement disorders. J Anat 196 (Pt 4): 519-525.

Cuadrado ML, Egido JA, Gonzalez-Gutierrez JL, Varela-De-Seijas E (1999) Bihemispheric contribution to motor recovery after stroke: A longitudinal study with transcranial doppler ultrasonography. Cerebrovasc Dis 9: 337-344.

Day BL, Rothwell JC, Thompson PD, Maertens dN, Nakashima K, Shannon K, Marsden CD (1989) Delay in the execution of voluntary movement by electrical or magnetic brain stimulation in intact man. Evidence for the storage of motor programs in the brain. Brain 112 (Pt 3): 649-663.

Deiber MP, Honda M, Ibanez V, Sadato N, Hallett M (1999) Mesial motor areas in self-initiated versus externally triggered movements examined with fMRI: effect of movement type and rate. J Neurophysiol 81: 3065-3077.

Desmond JE, Gabrieli JD, Wagner AD, Ginier BL, Glover GH (1997) Lobular patterns of cerebellar activation in verbal working-memory and finger-tapping tasks as revealed by functional MRI. J Neurosci 17: 9675-9685.

Di Lazzaro V, Oliviero A, Profice P, Insola A, Mazzone P, Tonali P, Rothwell JC (1999a) Direct demonstration of interhemispheric inhibition of the human motor cortex produced by transcranial magnetic stimulation. Exp Brain Res 124: 520-524.

Di Lazzaro V, Restuccia D, Oliviero A, Profice P, Ferrara L, Insola A, Mazzone P, Tonali P, Rothwell JC (1998) Magnetic transcranial stimulation at intensities below active motor threshold activates intracortical inhibitory circuits. Exp Brain Res 119: 265-268.

Di Lazzaro V, Rothwell JC, Oliviero A, Profice P, Insola A, Mazzone P, Tonali P (1999b) Intracortical origin of the short latency facilitation produced by pairs of threshold magnetic stimuli applied to human motor cortex. Exp Brain Res 129: 494-499.

Dirnagl U, Lindauer U, Villringer A (1993) Role of nitric oxide in the coupling of cerebral blood flow to neuronal activation in rats. Neurosci Lett 149: 43-46.

Donoghue JP (1995) Plasticity of adult sensorimotor representations. Curr Opin Neurobiol 5: 749-754.

Donoghue JP, Hess G, Sanes JN (1996) Substrates and mechanisms for learning in the motor cortex. In: Aquisition and mechanisms for learning in motor cortex (Bloedel JR, Ebner TJ, Wise SP, eds), pp 363-386. Cambridge (MA): MIT Press.

Donoghue JP, Suner S, Sanes JN (1990) Dynamic organization of primary motor cortex output to target muscles in adult rats. II. Rapid reorganization following motor nerve lesions. Exp Brain Res 79: 492-503.

Doyon J, Penhune V, Ungerleider LG (2003) Distinct contribution of the cortico-striatal and cortico-cerebellar systems to motor skill learning. Neuropsychologia 41: 252-262.

Duffau H (2001) Acute functional reorganisation of the human motor cortex during resection of central lesions: a study using intraoperative brain mapping. J Neurol Neurosurg Psychiatry 70: 506-513.

Dum RP, Li C, Strick PL (2002) Motor and nonmotor domains in the monkey dentate. Ann N Y Acad Sci 978: 289-301.

Dum RP, Strick PL (1991) The origin of corticospinal projections from the premotor areas in the frontal lobe. J Neurosci 11: 667-689.

Dum RP, Strick PL (2003) An unfolded map of the cerebellar dentate nucleus and its projections to the cerebral cortex. J Neurophysiol 89: 634-639.

Duvernoy HM (1999) The Human Brain: Surface, Blood Supply, and Three-Dimensional Sectional Anatomy. New York: Springer-Verlag Wien.

Edelman GM, Gally JA (2001) Degeneracy and complexity in biological systems. Proc Natl Acad Sci U S A 98: 13763-13768.

Enomoto H, Ugawa Y, Hanajima R, Yuasa K, Mochizuki H, Terao Y, Shiio Y, Furubayashi T, Iwata NK, Kanazawa I (2001) Decreased sensory cortical excitability after 1 Hz rTMS over the ipsilateral primary motor cortex. Clin Neurophysiol 112: 2154-2158.

Ferbert A, Priori A, Rothwell JC, Day BL, Colebatch JG, Marsden CD (1992) Interhemispheric inhibition of the human motor cortex. J Physiol 453: 525-546.

Fink GR, Frackowiak RS, Pietrzyk U, Passingham RE (1997) Multiple nonprimary motor areas in the human cortex. J Neurophysiol 77: 2164-2174.

Fitzgerald PB, Brown TL, Daskalakis ZJ, Chen R, Kulkarni J (2002) Intensity-dependent effects of 1 Hz rTMS on human corticospinal excitability. Clin Neurophysiol 113: 1136-1141.

Fox P, Ingham R, George MS, Mayberg H, Ingham J, Roby J, Martin C, Jerabek P (1997) Imaging human intra-cerebral connectivity by PET during TMS. Neuroreport 8: 2787-2791.

Fox PT, Raichle ME, Mintun MA, Dence C (1988) Nonoxidative glucose consumption during focal physiologic neural activity. Science 241: 462-464.

Frackowiak RS, Jones T, Lenzi GL, Heather JD (1980a) Regional cerebral oxygen utilization and blood flow in normal man using oxygen-15 and positron emission tomography. Acta Neurol Scand 62: 336-344.

Frackowiak RS, Lenzi GL, Jones T, Heather JD (1980b) Quantitative measurement of regional cerebral blood flow and oxygen metabolism in man using 15O and positron emission tomography: theory, procedure, and normal values. J Comput Assist Tomogr 4: 727-736.

Fransson P, Kruger G, Merboldt KD, Frahm J (1998a) Physiologic aspects of event related paradigms in magnetic resonance functional neuroimaging. Neuroreport 9: 2001-2005.

Fransson P, Kruger G, Merboldt KD, Frahm J (1998b) Temporal characteristics of oxygenation-sensitive MRI responses to visual activation in humans. Magn Reson Med 39: 912-919.

Fridman EA, Hanakawa T, Chung M, Hummel F, Leiguarda RC, Cohen LG (2004) Reorganization of the human ipsilesional premotor cortex after stroke. Brain 127: 747-758.

Friston KJ, Ashburner J, Frith CD, Poline J-B, Heather JD, Frackowiak RS (1995a) Spatial registration and normalisation of images. Hum Brain Mapp 2: 165-189.

Friston KJ, Buechel C, Fink GR, Morris J, Rolls E, Dolan RJ (1997) Psychophysiological and modulatory interactions in neuroimaging. Neuroimage 6: 218-229.

Friston KJ, Frith CD, Frackowiak RS (1993a) Time-dependent changes in effective connectivity measured with PET. Hum Brain Mapp 1: 69-80.

Friston KJ, Frith CD, Liddle PF, Frackowiak RS (1993b) Functional connectivity: the principal-component analysis of large (PET) data sets. J Cereb Blood Flow Metab 13: 5-14.

Friston KJ, Harrison L, Penny W (2003) Dynamic causal modelling. Neuroimage 19: 1273-1302.

Friston KJ, Holmes A, Worsley KJ, Poline J-B, Frith CD, Frackowiak RS (1995b) Statistical Parametric Maps in functional imaging: a general linear approach. Hum Brain Mapp 2: 189-210.

Friston KJ, Mechelli A, Turner R, Price CJ (2000) Nonlinear responses in fMRI: the Balloon model, Volterra kernels, and other hemodynamics. Neuroimage 12: 466-477.

Frost SB, Barbay S, Friel KM, Plautz EJ, Nudo RJ (2003) Reorganization of remote cortical regions after ischemic brain injury: a potential substrate for stroke recovery. J Neurophysiol 89: 3205-3214.

Fuhr P, Cohen LG, Roth BJ, Hallett M (1991) Latency of motor evoked potentials to focal transcranial stimulation varies as a function of scalp positions stimulated. Electroencephalogr Clin Neurophysiol 81: 81-89.

Gangitano M, Valero-Cabre A, Tormos JM, Mottaghy FM, Romero JR, Pascual-Leone A (2002) Modulation of input-output curves by low and high frequency repetitive transcranial magnetic stimulation of the motor cortex. Clin Neurophysiol 113: 1249-1257.

Georgopoulos AP, Kalaska JF, Caminiti R, Massey JT (1982) On the relations between the direction of two-dimensional arm movements and cell discharge in primate motor cortex. J Neurosci 2: 1527-1537.

Georgopoulos AP, Schwartz AB, Kettner RE (1986) Neuronal population coding of movement direction. Science 233: 1416-1419.

Gerloff C, Cohen LG, Floeter MK, Chen R, Corwell B, Hallett M (1998a) Inhibitory influence of the ipsilateral motor cortex on responses to stimulation of the human cortex and pyramidal tract. J Physiol 510 (Pt 1): 249-259.

Gerloff C, Corwell B, Chen R, Hallett M, Cohen LG (1997) Stimulation over the human supplementary motor area interferes with the organization of future elements in complex motor sequences. Brain 120 (Pt 9): 1587-1602.

Gerloff C, Corwell B, Chen R, Hallett M, Cohen LG (1998b) The role of the human motor cortex in the control of complex and simple finger movement sequences. Brain 121 (Pt 9): 1695-1709.

Gerschlager W, Siebner HR, Rothwell JC (2001) Decreased corticospinal excitability after subthreshold 1 Hz rTMS over lateral premotor cortex. Neurology 57: 449-455.

Gerstein GL, Perkel DH (1969) Simultaneously recorded trains of action potentials: analysis and functional interpretation. Science 164: 828-830.

Geyer S, Ledberg A, Schleicher A, Kinomura S, Schormann T, Burgel U, Klingberg T, Larsson J, Zilles K, Roland PE (1996) Two different areas within the primary motor cortex of man. Nature 382: 805-807.

Geyer S, Matelli M, Luppino G, Zilles K (2000a) Functional neuroanatomy of the primate isocortical motor system. Anat Embryol (Berl) 202: 443-474.

Geyer S, Schleicher A, Zilles K (1999) Areas 3a, 3b, and 1 of human primary somatosensory cortex. Neuroimage 10: 63-83.

Geyer S, Schormann T, Mohlberg H, Zilles K (2000b) Areas 3a, 3b, and 1 of human primary somatosensory cortex. Part 2. Spatial normalization to standard anatomical space. Neuroimage 11: 684-696.

Ghosh S, Brinkman C, Porter R (1987) A quantitative study of the distribution of neurons projecting to the precentral motor cortex in the monkey (M. fascicularis). J Comp Neurol 259: 424-444.

Ghosh S, Porter R (1988) Morphology of pyramidal neurones in monkey motor cortex and the synaptic actions of their intracortical axon collaterals. J Physiol 400: 593-615.

Gilio F, Rizzo V, Siebner HR, Rothwell JC (2003) Effects on the right motor hand-area excitability produced by low-frequency rTMS over human contralateral homologous cortex. J Physiol 551: 563-573.

Gold L, Lauritzen M (2002) Neuronal deactivation explains decreased cerebellar blood flow in response to focal cerebral ischemia or suppressed neocortical function. Proc Natl Acad Sci U S A 99: 7699-7704.

Grafton ST, Woods RP, Mazziotta JC, Phelps ME (1991) Somatotopic mapping of the primary motor cortex in humans: activation studies with cerebral blood flow and positron emission tomography. J Neurophysiol 66: 735-743.

Grefkes C, Geyer S, Schormann T, Roland P, Zilles K (2001) Human somatosensory area 2: observer-independent cytoarchitectonic mapping, interindividual variability, and population map. Neuroimage 14: 617-631.

Grezes J, Decety J (2001) Functional anatomy of execution, mental simulation, observation, and verb generation of actions: a meta-analysis. Hum Brain Mapp 12: 1-19.

Hallett M, Chen R, Ziemann U, Cohen LG (1999) Reorganization in motor cortex in amputees and in normal volunteers after ischemic limb deafferentation. Electroencephalogr Clin Neurophysiol Suppl 51: 183-187.

Hanajima R, Ugawa Y, Machii K, Mochizuki H, Terao Y, Enomoto H, Furubayashi T, Shiio Y, Uesugi H, Kanazawa I (2001) Interhemispheric facilitation of the hand motor area in humans. J Physiol 531: 849-859.

Hebb DO (1949) The Organisation of Behaviour. New York: Wiley.

Hess G, Aizenman CD, Donoghue JP (1996) Conditions for the induction of long-term potentiation in layer II/III horizontal connections of the rat motor cortex. J Neurophysiol 75: 1765-1778.

Hess G, Donoghue JP (1994) Long-term potentiation of horizontal connections provides a mechanism to reorganize cortical motor maps. J Neurophysiol 71: 2543-2547.

Hess G, Donoghue JP (1996) Long-term depression of horizontal connections in rat motor cortex. Eur J Neurosci 8: 658-665.

Hess G, Jacobs KM, Donoghue JP (1994) N-methyl-D-aspartate receptor mediated component of field potentials evoked in horizontal pathways of rat motor cortex. Neuroscience 61: 225-235.

Hilgetag CC, Theoret H, Pascual-Leone A (2001) Enhanced visual spatial attention ipsilateral to rTMS-induced 'virtual lesions' of human parietal cortex. Nat Neurosci 4: 953-957.

Holsapple JW, Preston JB, Strick PL (1991) The origin of thalamic inputs to the "hand" representation in the primary motor cortex. J Neurosci 11: 2644-2654.

Huntley GW (1997) Correlation between patterns of horizontal connectivity and the extend of short-term representational plasticity in rat motor cortex. Cereb Cortex 7: 143-156.

Huntley GW, Jones EG (1991) Relationship of intrinsic connections to forelimb movement representations in monkey motor cortex: a correlative anatomic and physiological study. J Neurophysiol 66: 390-413.

Hyder F, Rothman DL, Mason GF, Rangarajan A, Behar KL, Shulman RG (1997) Oxidative glucose metabolism in rat brain during single forepaw stimulation: a spatially localized 1H[13C] nuclear magnetic resonance study. J Cereb Blood Flow Metab 17: 1040-1047.

Ilmoniemi RJ, Virtanen J, Ruohonen J, Karhu J, Aronen HJ, Naatanen R, Katila T (1997) Neuronal responses to magnetic stimulation reveal cortical reactivity and connectivity. Neuroreport 8: 3537-3540.

Indovina I, Sanes JN (2001) On somatotopic representation centers for finger movements in human primary motor cortex and supplementary motor area. Neuroimage 13: 1027-1034.

Jacobs KM, Donoghue JP (1991) Reshaping the cortical motor map by unmasking latent intracortical connections. Science 251: 944-947.

Jalinous R (1991) Technical and practical aspects of magnetic nerve stimulation. J Clin Neurophysiol 8: 10-25.

Jancke L, Steinmetz H, Benilow S, Ziemann U (2003) Slowing fastest finger movements of the dominant hand with low-frequency rTMS of the hand area of the primary motor cortex. Exp Brain Res.

Jane JA, Yashon D, DeMyer W, Bucy PC (1967) The contribution of the precentral gyrus to the pyramidal tract of man. J Neurosurg 26: 244-248.

Jenkins IH, Brooks DJ, Nixon PD, Frackowiak RS, Passingham RE (1994) Motor sequence learning: a study with positron emission tomography. J Neurosci 14: 3775-3790.

Johansen-Berg H, Dawes H, Guy C, Smith SM, Wade DT, Matthews PM (2002a) Correlation between motor improvements and altered fMRI activity after rehabilitative therapy. Brain 125: 2731-2742.

Johansen-Berg H, Rushworth MF, Bogdanovic MD, Kischka U, Wimalaratna S, Matthews PM (2002b) The role of ipsilateral premotor cortex in hand movement after stroke. Proc Natl Acad Sci U S A 99: 14518-14523.

Jones EG (1983) The nature of the afferent pathways conveying short-latency inputs to primate motor cortex. Adv Neurol 39: 263-285.

Jones EG (1987) Ascending inputs to, and internal organization of, cortical motor areas. Ciba Found Symp 132: 21-39.

Jones EG, Coulter JD, Burton H, Porter R (1977) Cells of origin and terminal distribution of corticostriatal fibers arising in the sensory-motor cortex of monkeys. J Comp Neurol 173: 53-80.

Jueptner M, Stephan KM, Frith CD, Brooks DJ, Frackowiak RS, Passingham RE (1997) Anatomy of motor learning. I. Frontal cortex and attention to action. J Neurophysiol 77: 1313-1324.

Kakei S, Hoffman DS, Strick PL (1999) Muscle and movement representations in the primary motor cortex. Science 285: 2136-2139.

Kelly RM, Strick PL (2003) Cerebellar loops with motor cortex and prefrontal cortex of a nonhuman primate. J Neurosci 23: 8432-8444.

Kiers L, Cros D, Chiappa KH, Fang J (1993) Variability of motor potentials evoked by transcranial magnetic stimulation. Electroencephalogr Clin Neurophysiol 89: 415-423.

Knecht S, Ellger T, Breitenstein C, Bernd RE, Henningsen H (2003) Changing cortical excitability with low-frequency transcranial magnetic stimulation can induce sustained disruption of tactile perception. Biol Psychiatry 53: 175-179.

Knecht S, Floel A, Drager B, Breitenstein C, Sommer J, Henningsen H, Ringelstein EB, Pascual-Leone A (2002) Degree of language lateralization determines susceptibility to unilateral brain lesions. Nat Neurosci 5: 695-699.

Kobayashi M, Hutchinson S, Theoret H, Schlaug G, Pascual-Leone A (2004) Repetitive TMS of the motor cortex improves ipsilateral sequential simple finger movements. Neurology 62: 91-98.

Kosslyn SM, Pascual-Leone A, Felician O, Camposano S, Keenan JP, Thompson WL, Ganis G, Sukel KE, Alpert NM (1999) The role of area 17 in visual imagery: convergent evidence from PET and rTMS. Science 284: 167-170.

Kujirai T, Caramia MD, Rothwell JC, Day BL, Thompson PD, Ferbert A, Wroe S, Asselman P, Marsden CD (1993) Corticocortical inhibition in human motor cortex. J Physiol 471: 501-519.

Kuschinsky W, Wahl M (1978) Local chemical and neurogenic regulation of cerebral vascular resistance. Physiol Rev 58: 656-689.

Lauritzen M, Gold L (2003) Brain function and neurophysiological correlates of signals used in functional neuroimaging. J Neurosci 23: 3972-3980.

Lemon RN, van der Burg J (1979) Short-latency peripheral inputs to thalamic neurones projecting to the motor cortex in the monkey. Exp Brain Res 36: 445-462.

Liebetanz D, Fauser S, Michaelis T, Czeh B, Watanabe T, Paulus W, Frahm J, Fuchs E (2003) Safety aspects of chronic low-frequency transcranial magnetic stimulation based on localized proton magnetic resonance spectroscopy and histology of the rat brain. J Psychiatr Res 37: 277-286.

Liepert J, Bauder H, Wolfgang HR, Miltner WH, Taub E, Weiller C (2000) Treatment-induced cortical reorganization after stroke in humans. Stroke 31: 1210-1216.

Liepert J, Schwenkreis P, Tegenthoff M, Malin JP (1997) The glutamate antagonist riluzole suppresses intracortical facilitation. J Neural Transm 104: 1207-1214.

Liu Y, Rouiller EM (1999) Mechanisms of recovery of dexterity following unilateral lesion of the sensorimotor cortex in adult monkeys. Exp Brain Res 128: 149-159.

Logothetis NK, Pauls J, Augath M, Trinath T, Oeltermann A (2001) Neurophysiological investigation of the basis of the fMRI signal. Nature 412: 150-157.

Maccabee PJ, Amassian VE, Eberle LP, Cracco RQ (1993) Magnetic coil stimulation of straight and bent amphibian and mammalian peripheral nerve in vitro: locus of excitation. J Physiol 460: 201-219.

Maeda F, Keenan JP, Tormos JM, Topka H, Pascual-Leone A (2000a) Interindividual variability of the modulatory effects of repetitive transcranial magnetic stimulation on cortical excitability. Exp Brain Res 133: 425-430.

Maeda F, Keenan JP, Tormos JM, Topka H, Pascual-Leone A (2000b) Modulation of corticospinal excitability by repetitive transcranial magnetic stimulation. Clin Neurophysiol 111: 800-805.

Magistretti PJ, Pellerin L (1999) Cellular mechanisms of brain energy metabolism and their relevance to functional brain imaging. Philos Trans R Soc Lond B Biol Sci 354: 1155-1163.

Marconi B, Genovesio A, Giannetti S, Molinari M, Caminiti R (2003) Callosal connections of dorso-lateral premotor cortex. Eur J Neurosci 18: 775-788.

Marshall RS, Perera GM, Lazar RM, Krakauer JW, Constantine RC, DeLaPaz RL (2000) Evolution of cortical activation during recovery from corticospinal tract infarction. Stroke 31: 656-661.

Matelli M, Luppino G (1996) Thalamic input to mesial and superior area 6 in the macaque monkey. J Comp Neurol 372: 59-87.

Matelli M, Luppino G, Fogassi L, Rizzolatti G (1989) Thalamic input to inferior area 6 and area 4 in the macaque monkey. J Comp Neurol 280: 468-488.

Mathiesen C, Caesar K, Akgoren N, Lauritzen M (1998) Modification of activity-dependent increases of cerebral blood flow by excitatory synaptic activity and spikes in rat cerebellar cortex. J Physiol 512 (Pt 2): 555-566.

Mazzocchio R, Rothwell JC, Day BL, Thompson PD (1994) Effect of tonic voluntary activity on the excitability of human motor cortex. J Physiol 474: 261-267.

Mechelli A, Price CJ, Friston KJ (2001) Nonlinear coupling between evoked rCBF and BOLD signals: a simulation study of hemodynamic responses. Neuroimage 14: 862-872.

Meyer BU, Roricht S, Grafin vE, Kruggel F, Weindl A (1995) Inhibitory and excitatory interhemispheric transfers between motor cortical areas in normal humans and patients with abnormalities of the corpus callosum. Brain 118 (Pt 2): 429-440.

Meyer BU, Roricht S, Woiciechowsky C (1998) Topography of fibers in the human corpus callosum mediating interhemispheric inhibition between the motor cortices. Ann Neurol 43: 360-369.

Meyer BU, Voss M (2000) Delay of the execution of rapid finger movement by magnetic stimulation of the ipsilateral hand-associated motor cortex. Exp Brain Res 134: 477-482.

Meyer G (1987) Forms and spatial arrangement of neurons in the primary motor cortex of man. J Comp Neurol 262: 402-428.

Mills KR, Boniface SJ, Schubert M (1992) Magnetic brain stimulation with a double coil: the importance of coil orientation. Electroencephalogr Clin Neurophysiol 85: 17-21.

Mochizuki H, Terao Y, Okabe S, Furubayashi T, Arai N, Iwata NK, Hanajima R, Kamakura K, Motoyoshi K, Ugawa Y (2004) Effects of motor cortical stimulation on the excitability of contralateral motor and sensory cortices. Exp Brain Res.

Mottaghy FM, Gangitano M, Horkan C, Chen Y, Pascual-Leone A, Schlaug G (2003) Repetitive TMS temporarily alters brain diffusion. Neurology 60: 1539-1541.

Muakkassa KF, Strick PL (1979) Frontal lobe inputs to primate motor cortex: evidence for four somatotopically organized 'premotor' areas. Brain Res 177: 176-182.

Muellbacher W, Ziemann U, Boroojerdi B, Hallett M (2000) Effects of low-frequency transcranial magnetic stimulation on motor excitability and basic motor behavior. Clin Neurophysiol 111: 1002-1007.

Muellbacher W, Ziemann U, Wissel J, Dang N, Kofler M, Facchini S, Boroojerdi B, Poewe W, Hallett M (2002) Early consolidation in human primary motor cortex. Nature 415: 640-644.

Muir RB, Lemon RN (1983) Corticospinal neurons with a special role in precision grip. Brain Res 261: 312-316.

Munchau A, Bloem BR, Irlbacher K, Trimble MR, Rothwell JC (2002) Functional connectivity of human premotor and motor cortex explored with repetitive transcranial magnetic stimulation. J Neurosci 22: 554-561.

Nakamura H, Kitagawa H, Kawaguchi Y, Tsuji H (1997) Intracortical facilitation and inhibition after transcranial magnetic stimulation in conscious humans. J Physiol 498 (Pt 3): 817-823.

Nathan PW, Smith MC, Deacon P (1990) The corticospinal tracts in man. Course and location of fibres at different segmental levels. Brain 113 (Pt 2): 303-324.

Norup-Nielsen A., Lauritzen M (2001) Coupling and uncoupling of activity-dependent increases of neuronal activity and blood flow in rat somatosensory cortex. J Physiol 533: 773-785.

Nudo RJ, Jenkins WM, Merzenich MM (1990) Repetitive microstimulation alters the cortical representation of movements in adult rats. Somatosens Mot Res 7: 463-483.

Nudo RJ, Masterton RB (1986) Stimulation-induced [14C]2-deoxyglucose labeling of synaptic activity in the central auditory system. J Comp Neurol 245: 553-565.

Ogawa S, Lee TM, Kay AR, Tank DW (1990) Brain magnetic resonance imaging with contrast dependent on blood oxygenation. Proc Natl Acad Sci U S A 87: 9868-9872.

Okabe S, Hanajima R, Ohnishi T, Nishikawa M, Imabayashi E, Takano H, Kawachi T, Matsuda H, Shiio Y, Iwata NK, Furubayashi T, Terao Y, Ugawa Y (2003) Functional connectivity revealed by single-photon emission computed tomography (SPECT) during repetitive transcranial magnetic stimulation (rTMS) of the motor cortex. Clin Neurophysiol 114: 450-457.

Parent A, Hazrati LN (1995a) Functional anatomy of the basal ganglia. I. The cortico-basal ganglia-thalamo-cortical loop. Brain Res Brain Res Rev 20: 91-127.

Parent A, Hazrati LN (1995b) Functional anatomy of the basal ganglia. II. The place of subthalamic nucleus and external pallidum in basal ganglia circuitry. Brain Res Brain Res Rev 20: 128-154.

Pascual-Leone A, Grafman J, Hallett M (1994a) Modulation of cortical motor output maps during development of implicit and explicit knowledge. Science 263: 1287-1289.

Pascual-Leone A, Tormos JM, Keenan J, Tarazona F, Canete C, Catala MD (1998) Study and modulation of human cortical excitability with transcranial magnetic stimulation. J Clin Neurophysiol 15: 333-343.

Pascual-Leone A, Valls-Sole J, Wassermann EM, Hallett M (1994b) Responses to rapid-rate transcranial magnetic stimulation of the human motor cortex. Brain 117 (Pt 4): 847-858.

Passingham R (1997) Functional organisation of the motor system. In: Human Brain Function (Frackowiak R, Friston K, Frith CD, Dolan RJ, Mazziotta JC, eds), pp 243-274. San Diego: Academic Press.

Passingham RE (1996) Functional specialization of the supplementary motor area in monkeys and humans. Adv Neurol 70: 105-116.

Patton HD, Amassian VE (1954) Single and multiple-unit analysis of cortical stage of pyramidal tract activation. J Neurophysiol 17: 345-363.

Paus T, Petrides M, Evans AC, Meyer E (1993) Role of the human anterior cingulate cortex in the control of oculomotor, manual, and speech responses: a positron emission tomography study. J Neurophysiol 70: 453-469.

Penfield W, Rasmussen T (1950) The Cerebral Cortex of Man. pp 78-79. New York: MacMillan.

Penny WD, Stephan KE, Mechelli A, Friston KJ (2004) Comparing dynamic causal models. Neuroimage 22: 1157-1172.

Picard N, Strick PL (1996) Motor areas of the medial wall: a review of their location and functional activation. Cereb Cortex 6: 342-353.

Picard N, Strick PL (2001) Imaging the premotor areas. Curr Opin Neurobiol 11: 663-672.

Plewnia C, Lotze M, Gerloff C (2003) Disinhibition of the contralateral motor cortex by low-frequency rTMS. Neuroreport 14: 609-612.

Price CJ, Friston KJ (2002) Degeneracy and cognitive anatomy. Trends Cogn Sci 6: 416-421.

Raichle ME (1998) Behind the scenes of functional brain imaging: a historical and physiological perspective. Proc Natl Acad Sci U S A 95: 765-772.

Rao SM, Binder JR, Hammeke TA, Bandettini PA, Bobholz JA, Frost JA, Myklebust BM, Jacobson RD, Hyde JS (1995) Somatotopic mapping of the human primary motor cortex with functional magnetic resonance imaging. Neurology 45: 919-924.

Raymond JL, Lisberger SG, Mauk MD (1996) The cerebellum: a neuronal learning machine? Science 272: 1126-1131.

Ridding MC, Taylor JL, Rothwell JC (1995) The effect of voluntary contraction on cortico-cortical inhibition in human motor cortex. J Physiol 487 (Pt 2): 541-548.

Rizzolatti G, Luppino G, Matelli M (1998) The organization of the cortical motor system: new concepts. Electroencephalogr Clin Neurophysiol 106: 283-296.

Roland PE, Zilles K (1996) Functions and structures of the motor cortices in humans. Curr Opin Neurobiol 6: 773-781.

Romero JR, Anschel D, Sparing R, Gangitano M, Pascual-Leone A (2002) Subthreshold low frequency repetitive transcranial magnetic stimulation selectively decreases facilitation in the motor cortex. Clin Neurophysiol 113: 101-107.

Rossi S, Pasqualetti P, Rossini PM, Feige B, Ulivelli M, Glocker FX, Battistini N, Lucking CH, Kristeva-Feige R (2000) Effects of repetitive transcranial magnetic stimulation on movement-related cortical activity in humans. Cereb Cortex 10: 802-808.

Roth BJ, Saypol JM, Hallett M, Cohen LG (1991) A theoretical calculation of the electric field induced in the cortex during magnetic stimulation. Electroencephalogr Clin Neurophysiol 81: 47-56.

Rothwell JC (1997) Techniques and mechanisms of action of transcranial stimulation of the human motor cortex. J Neurosci Methods 74: 113-122.

Rothwell JC, Hallett M, Berardelli A, Eisen A, Rossini P, Paulus W (1999) Magnetic stimulation: motor evoked potentials. The International Federation of Clinical Neurophysiology. Electroencephalogr Clin Neurophysiol Suppl 52: 97-103.

Rouiller EM, Babalian A, Kazennikov O, Moret V, Yu XH, Wiesendanger M (1994) Transcallosal connections of the distal forelimb representations of the primary and supplementary motor cortical areas in macaque monkeys. Exp Brain Res 102: 227-243.

Sanes JN, Donoghue JP (2000) Plasticity and primary motor cortex. Annu Rev Neurosci 23: 393-415.

Sanes JN, Donoghue JP, Thangaraj V, Edelman RR, Warach S (1995) Shared neural substrates controlling hand movements in human motor cortex. Science 268: 1775-1777.

Sanes JN, Schieber MH (2001) Orderly somatotopy in primary motor cortex: does it exist? Neuroimage 13: 968-974.

Satow T, Mima T, Yamamoto J, Oga T, Begum T, Aso T, Hashimoto N, Rothwell JC, Shibasaki H (2003) Short-lasting impairment of tactile perception by 0.9Hz-rTMS of the sensorimotor cortex. Neurology 60: 1045-1047.

Schambra HM, Sawaki L, Cohen LG (2003) Modulation of excitability of human motor cortex (M1) by 1 Hz transcranial magnetic stimulation of the contralateral M1. Clin Neurophysiol 114: 130-133.

Schlaghecken F, Munchau A, Bloem BR, Rothwell J, Eimer M (2003) Slow frequency repetitive transcranial magnetic stimulation affects reaction times, but not priming effects, in a masked prime task. Clin Neurophysiol 114: 1272-1277.

Schluter ND, Rushworth MF, Passingham RE, Mills KR (1998) Temporary interference in human lateral premotor cortex suggests dominance for the selection of movements. A study using transcranial magnetic stimulation. Brain 121 (Pt 5): 785-799.

Schmahmann JD, Doyon J, Toga AW, Petrides M, Evans AC (2000) MRI Atlas of the Human Cerebellum. San Diego: Academic Press.

Seitz RJ, Hoflich P, Binkofski F, Tellmann L, Herzog H, Freund HJ (1998) Role of the premotor cortex in recovery from middle cerebral artery infarction. Arch Neurol 55: 1081-1088.

Shadmehr R, Mussa-Ivaldi FA (1994) Adaptive representation of dynamics during learning of a motor task. J Neurosci 14: 3208-3224.

Sherman SM, Guillery RW (2002) The role of the thalamus in the flow of information to the cortex. Philos Trans R Soc Lond B Biol Sci 357: 1695-1708.

Shinoda Y, Yokota J, Futami T (1981) Divergent projection of individual corticospinal axons to motoneurons of multiple muscles in the monkey. Neurosci Lett 23: 7-12.

Siebner HR, Filipovic SR, Rowe JB, Cordivari C, Gerschlager W, Rothwell JC, Frackowiak RS, Bhatia KP (2003) Patients with focal arm dystonia have increased sensitivity to slow-frequency repetitive TMS of the dorsal premotor cortex. Brain.

Siebner HR, Peller M, Willoch F, Minoshima S, Boecker H, Auer C, Drzezga A, Conrad B, Bartenstein P (2000) Lasting cortical activation after repetitive TMS of the motor cortex: a glucose metabolic study. Neurology 54: 956-963.

Siebner HR, Rothwell J (2003) Transcranial magnetic stimulation: new insights into representational cortical plasticity. Exp Brain Res 148: 1-16.

Siebner HR, Takano B, Peinemann A, Schwaiger M, Conrad B, Drzezga A (2001) Continuous transcranial magnetic stimulation during positron emission tomography: a suitable tool for imaging regional excitability of the human cortex. Neuroimage 14: 883-890.

Simpson EH (1949) Measurement of Diversity. Nature 163: 688.

Sloper JJ, Powell TP (1979) An experimental electron microscopic study of afferent connections to the primate motor and somatic sensory cortices. Philos Trans R Soc Lond B Biol Sci 285: 199-226.

Speer AM, Willis MW, Herscovitch P, Daube-Witherspoon M, Shelton JR, Benson BE, Post RM, Wassermann EM (2003) Intensity-dependent regional cerebral blood flow during 1-Hz repetitive transcranial magnetic stimulation (rTMS) in healthy volunteers studied with H215O positron emission tomography: I. Effects of primary motor cortex rTMS. Biol Psychiatry 54: 818-825.

Stefan K, Kunesch E, Cohen LG, Benecke R, Classen J (2000) Induction of plasticity in the human motor cortex by paired associative stimulation. Brain 123 Pt 3: 572-584.

Strafella AP, Paus T (2001) Cerebral blood-flow changes induced by paired-pulse transcranial magnetic stimulation of the primary motor cortex. J Neurophysiol 85: 2624-2629.

Strafella AP, Paus T, Barrett J, Dagher A (2001) Repetitive transcranial magnetic stimulation of the human prefrontal cortex induces dopamine release in the caudate nucleus. J Neurosci 21: RC157.

Strens LH, Fogelson N, Shanahan P, Rothwell JC, Brown P (2003) The ipsilateral human motor cortex can functionally compensate for acute contralateral motor cortex dysfunction. Curr Biol 13: 1201-1205.

Strens LH, Oliviero A, Bloem BR, Gerschlager W, Rothwell JC, Brown P (2002) The effects of subthreshold 1 Hz repetitive TMS on cortico-cortical and interhemispheric coherence. Clin Neurophysiol 113: 1279-1285.

Takano, B., Drzezga, A., Peller, M., Sax, I., Schwaiger, M., Lee, L., and Siebner, H. R. Modulation of regional excitability and synaptic activity in human motor cortex following high-frequency transcranial magnetic stimulation: a TMS-PET study. Neuroimage. 2004.
Ref Type: In Press

Talairach P, Tournoux J (1988) A stereotactic coplanar atlas of the human brain. Stuttgart Thieme.

Terao Y, Ugawa Y (2002) Basic mechanisms of TMS. J Clin Neurophysiol 19: 322-343.

Terao Y, Ugawa Y, Hanajima R, Machii K, Furubayashi T, Mochizuki H, Enomoto H, Shiio Y, Uesugi H, Iwata NK, Kanazawa I (2000) Predominant activation of I1-waves from the leg motor area by transcranial magnetic stimulation. Brain Res 859: 137-146.

Tofts PS (1990) The distribution of induced currents in magnetic stimulation of the nervous system. Phys Med Biol 35: 1119-1128.

Tokuno H, Tanji J (1993) Input organization of distal and proximal forelimb areas in the monkey primary motor cortex: a retrograde double labeling study. J Comp Neurol 333: 199-209.

Tononi G, Sporns O, Edelman GM (1999) Measures of degeneracy and redundancy in biological networks. Proc Natl Acad Sci U S A 96: 3257-3262.

Touge T, Gerschlager W, Brown P, Rothwell JC (2001) Are the after-effects of low-frequency rTMS on motor cortex excitability due to changes in the efficacy of cortical synapses? Clin Neurophysiol 112: 2138-2145.

Tsuji T, Rothwell JC (2002) Long lasting effects of rTMS and associated peripheral sensory input on MEPs, SEPs and transcortical reflex excitability in humans. J Physiol 540: 367-376.

Turner R, Le Bihan D, Moonen CT, Despres D, Frank J (1991) Echo-planar time course MRI of cat brain oxygenation changes. Magn Reson Med 22: 159-166.

Ugawa Y, Hanajima R, Kanazawa I (1993) Interhemispheric facilitation of the hand area of the human motor cortex. Neurosci Lett 160: 153-155.

Voogd J, Glickstein M (1998) The anatomy of the cerebellum. Trends Neurosci 21: 370-375.

Vorobiev V, Govoni P, Rizzolatti G, Matelli M, Luppino G (1998) Parcellation of human mesial area 6: cytoarchitectonic evidence for three separate areas. Eur J Neurosci 10: 2199-2203.

Walsh V, Rushworth M (1999) A primer of magnetic stimulation as a tool for neuropsychology. Neuropsychologia 37: 125-135.

Ward NS, Brown MM, Thompson AJ, Frackowiak RS (2003a) Neural correlates of motor recovery after stroke: a longitudinal fMRI study. Brain 126: 2476-2496.

Ward NS, Brown MM, Thompson AJ, Frackowiak RS (2003b) Neural correlates of outcome after stroke: a cross-sectional fMRI study. Brain 126: 1430-1448.

Wassermann EM (1998) Risk and safety of repetitive transcranial magnetic stimulation: report and suggested guidelines from the International Workshop on the Safety of Repetitive Transcranial Magnetic Stimulation, June 5-7, 1996. Electroencephalogr Clin Neurophysiol 108: 1-16.

Wassermann EM, Grafman J, Berry C, Hollnagel C, Wild K, Clark K, Hallett M (1996) Use and safety of a new repetitive transcranial magnetic stimulator. Electroencephalogr Clin Neurophysiol 101: 412-417.

Wassermann EM, McShane LM, Hallett M, Cohen LG (1992) Noninvasive mapping of muscle representations in human motor cortex. Electroencephalogr Clin Neurophysiol 85: 1-8.

Wassermann EM, Wedegaertner FR, Ziemann U, George MS, Chen R (1998) Crossed reduction of human motor cortex excitability by 1-Hz transcranial magnetic stimulation. Neurosci Lett 250: 141-144.

Weiller C, Chollet F, Friston KJ, Wise RJ, Frackowiak RS (1992) Functional reorganization of the brain in recovery from striatocapsular infarction in man. Ann Neurol 31: 463-472.

Werhahn KJ, Conforto AB, Kadom N, Hallett M, Cohen LG (2003) Contribution of the ipsilateral motor cortex to recovery after chronic stroke. Ann Neurol 54: 464-472.

Wise SP, di Pellegrino G, Boussaoud D (1996) The premotor cortex and nonstandard sensorimotor mapping. Can J Physiol Pharmacol 74: 469-482.

Worsley KJ, Evans AC, Marrett S, Neelin P (1992) A three-dimensional statistical analysis for CBF activation studies in human brain. J Cereb Blood Flow Metab 12: 900-918.

Worsley KJ, Marrett S, Neelin P, Vandal A, Friston KJ, Evans AC (1996) A unified statistical approach for determining significant signals in images of cerebral activation. Hum Brain Mapp 4: 58-73.

Ziemann U, Corwell B, Cohen LG (1998a) Modulation of plasticity in human motor cortex after forearm ischemic nerve block. J Neurosci 18: 1115-1123.

Ziemann U, Hallett M, Cohen LG (1998b) Mechanisms of deafferentation-induced plasticity in human motor cortex. J Neurosci 18: 7000-7007.

Ziemann U, Lonnecker S, Steinhoff BJ, Paulus W (1996) Effects of antiepileptic drugs on motor cortex excitability in humans: a transcranial magnetic stimulation study. Ann Neurol 40: 367-378.

Ziemann U, Tergau F, Netz J, Homberg V (1997) Delay in simple reaction time after focal transcranial magnetic stimulation of the human brain occurs at the final motor output stage. Brain Res 744: 32-40.

Ziemann U, Tergau F, Wischer S, Hildebrandt J, Paulus W (1998c) Pharmacological control of facilitatory I-wave interaction in the human motor cortex. A paired transcranial magnetic stimulation study. Electroencephalogr Clin Neurophysiol 109: 321-330.

Ziemann U, Wittenberg GF, Cohen LG (2002) Stimulation-induced within-representation and across-representation plasticity in human motor cortex. J Neurosci 22: 5563-5571.

Zilles K, Schlaug G, Matelli M, Luppino G, Schleicher A, Qu M, Dabringhaus A, Seitz R, Roland PE (1995) Mapping of human and macaque sensorimotor areas by integrating architectonic, transmitter receptor, MRI and PET data. J Anat 187 (Pt 3): 515-537.